atmosphere

MDPI

Article

Analyses of Climate Variations at Four Meteorological Stations on Remote Islands in the Croatian Part of the Adriatic Sea

Ognjen Bonacci [1], Matko Patekar [2,*], Marco Pola [2] and Tanja Roje-Bonacci [1]

[1] Architecture and Geodesy, Faculty of Civil Engineering, University of Split, Matice Hrvatske 15, 21000 Split, Croatia; obonacci@gradst.hr (O.B.); tanja.roje-bonacci@gradst.hr (T.R.-B.)

[2] Department of Hydrogeology and Engineering Geology, Croatian Geological Survey, Sachsova 2, 10000 Zagreb, Croatia; mpola@hgi-cgs.hr

* Correspondence: mpatekar@hgi-cgs.hr; Tel.: +385-98-904-26-99

Received: 1 September 2020; Accepted: 29 September 2020; Published: 30 September 2020

Abstract: The Mediterranean region is one of the regions in the world that is most vulnerable to the impact of imminent climate change. In particular, climate change has an adverse effect on both the ecosystem and socioeconomic system, influencing water availability for both human and environmental purposes. The most endangered water resources are along the coasts and on islands since they have relatively small volumes and are intensively exploited. We analyzed the time series of air temperature and precipitation measured at four meteorological stations (Komiža, Palagruža, Lastovo, and Biševo) located on small islands in the Croatian part of the Adriatic Sea in this study. The investigated time series extend from the 1950s to the present, being contemporaneous for approximately 50 years. Despite possessing discontinuity, they can be considered as representative for assessing climate change and variability in the scattered environment of the Croatian islands. The results showed increasing trends in the annual air temperature, while the annual cumulative precipitation did not show significant variations. In addition, the analyses of the monthly air temperature showed that statistically significant increasing trends occurred from April to August, suggesting a more severe impact during these months. These results are in accordance with regional and local studies and climate models. Although the climate variability during the analyzed period can be considered as moderate, the impact on water resources could be severe due to the combined effect of the increase in air temperature during warm periods and the intensive exploitation for tourism purposes.

Keywords: air temperature; precipitation; global warming; Mediterranean; Adriatic Sea

1. Introduction

Climate change continues to draw attention in the scientific community and the general public. The air temperature increase is the most common effect of global warming and this causes negative effects on local and regional economies and the social system, as well as environmental issues. Climate variability is a natural feature of a climate system and it is a consequence of the inherent variabilities of both the atmosphere and the oceans [1–3]. Human activities could add to this natural variability leading to climate change. The investigation of the climate and its modifications in a specific region require detailed local-scale analyses since the forces driving these modifications and their magnitudes could change during the year and at nearby locations. The results of these investigations can be used by stakeholders to implement appropriate, site-specific measures that could mitigate the impact of climate change on both natural and socioeconomic systems. Modifications of the climate can be

considered as climate change when significant variations in the statistical distribution of climate parameters occur over a relatively long period (a standard reference period generally longer than 30 years). Among climate parameters, air temperature and precipitation are used to analyze variations and changes in climate [2,4] since they are generally measured over a dense network of monitoring stations for a long time.

With more than 5000 islands of various sizes, the Mediterranean region is considered as one of the most diverse regions in the world from the geographical, geological, and biological points of view [5,6]. The population of this area is approximately 480 million, with one-third living along the coasts and approximately 10 million people on islands [7]. The Mediterranean region is recognized as one of the hotspots of climate change [8]. Rađa et al. [9] estimated that 20% of the Mediterranean population lives under permanent water stress. This peculiar condition is both natural, due to the water scarcity and the high intrinsic vulnerability of the water resources, and anthropogenic, due to the high population density and the sudden increases in water demand during the peaks of the touristic season. The most important source of fresh water is represented by groundwater, and precipitation is generally the sole source of recharge [10]. Islands of the Mediterranean region have limited fresh water resources that are more and more affected by droughts as a consequence of an increase in air temperature and changes in precipitation.

The Croatian coast comprises 79 islands, 525 islets, and 642 rocks and reefs [11,12]. Merely a few Croatian islands have favorable hydrological or hydrogeological conditions for a sufficient local water supply [11]. Numerous archaeological sites have been discovered in this area testifying to its important position and historical role [13,14]. Climate change will severely affect the Croatian coastal region during the 21st century. Climate models [2,15,16] predict an increase of the mean air temperature up to 5.5 °C and a slight decrease of precipitation but also the occurrence of more and more frequent extreme events, such as flash floods and droughts. These modifications of climate conditions could represent a serious threat to the population of Croatian islands that is highly scattered and relies on local fresh water resources.

This study aims to assess the occurrence of climate variability and change in remote islands with scarce fresh water resources. Time series of the annual and monthly air temperature and precipitation measured at four meteorological stations on remote islands of the Croatian coast are analyzed. First, we will describe the study area and the temperature and precipitation datasets. The results of the exploratory statistical analysis will be shown, and the annual and monthly trends will be described. The results will be used to assess the possible occurrence of climate change in this scattered part of the Adriatic coast providing an effective tool for more efficient water management of the local water resources through the rising challenge of climate change.

2. Study Area

The study area is located in the central part of the Adriatic Sea to the west of the southern Croatian mainland (Figure 1). This part of the Croatian coast is characterized by several islands with different sizes showing a predominant W–E or WSW–ENE direction. The analyzed meteorological stations are situated on small and very small islands (Vis, Biševo, Lastovo, and Palagruža) that are 43 to 54 km away from the mainland (Figure 1).

Figure 1. Map of the study area showing the locations of the four meteorological stations whose data were analyzed in this work.

The study area is part of the Outer Dinaric range, an area characterized by very deep and irregular karstification [9]. The investigated islands are mostly composed of Mesozoic carbonate rocks that are intensely fractured and karstified. Karst aquifers have a heterogeneous distribution of the hydrogeological properties influenced by the regional and local fracture networks and karstic conduits. Due to their peculiar hydrogeological settings, the groundwater resources in karst aquifers are irregularly distributed and highly vulnerable to seawater intrusion.

According to the Köppen climate classification, the study area is characterized by the Csa climate type [17]. It is a semiarid variety of Mediterranean climate, sometimes referred to as the "olive" climate, characterized by mild, humid, and rainy winters with dry and hot summers. Although temperature extremes (i.e., summer heating and winter frosty days) are mitigated, extreme precipitation events alternated with long periods of drought are common. Alpert et al. [18] demonstrated the paradoxical behavior of precipitation in the Mediterranean region showing both a decrease of the total rainfall but an increase in the extreme daily rainfall.

Vis Island is located 43 km from the mainland. The meteorological station on Vis is in the city of Komiža, in the western part of the island (Figure 1). As a result of favorable geological and hydrogeological conditions, Vis has a water supply from its own karst aquifer. Due to its distance from other islands as well as from the mainland, Vis and its archipelago are exposed to stronger winds than other islands in southern Croatia. Biševo Island is part of the Vis archipelago, and Biševo is located 5 km SW from Vis. The Biševo meteorological station is in the northern part of the island. On Biševo Island, the fresh water is obtained from rainwater harvesting.

The Lastovo archipelago is composed of 44 islands, islets, and rocky reefs covering 53 and 143 km^2 of land and sea surface area, respectively. The meteorological station is located in the town of Lastovo, in the northern part of the island. Lastovo has a distance from the mainland similar to Vis (Table 1). Part of the drinking water on Lastovo is obtained by desalination of brackish water from wells [11] and part is delivered through a regional water supply network from the mainland.

Table 1. Characteristics of the investigated islands and their meteorological stations.

	Lastovo	Komiža	Biševo	Palagruža
Type of Station	**AMS and MMS**	**AMS and MMS**	**PS**	**AMS**
A (km^2)	40.81	90.03	5.91	0.3
L (km)	48.5	43.5	53.69	51.69 (IT) 113.96 (HR)
H_{max} (m a.s.l.)	417	587	239	103
Latitude	42°46′06″	43°02′55″	42°59′13″	42°23′33″
Longitude	16°54′00″	16°05′13″	16°00′30″	16°15′20″
$H_{station}$ (m a.s.l.)	186	20	65	98

Note: AMS—automatic meteorological station; MMS—main meteorological station; PS—precipitation station; A—area of the island; L—minimum distance of the island from the mainland; H_{max}—maximum altitude of the island.

The Palagruža meteorological station, located on Velika Palagruža Island, is situated in the vicinity of the largest lighthouse in the Adriatic Sea, built in 1875. The Palagruža archipelago lies 51 km NE from the Italian coast and 113 km from the Croatian mainland. The archipelago consists of several very small islands and a dozen islets and rocky reefs [19–22]. The relatively low relief and exposure to the open sea result in the lowest amount of precipitation of the Dalmatian coast. The local meteorological conditions on Palagruža have been thoroughly investigated [23–25]. Fresh water is delivered to Palagruža with water carrier ships.

Vis and Lastovo islands are covered with dense Mediterranean vegetation. Biševo was covered with dense pine forest before it was devastated by fire in 1936. Although the vegetation recovered, it was again devastated by fire in 1994 and 2003. Palagruža is barren. The vegetation cover likely influences the climate variations, primarily air temperature, at stations analyzed within this study.

The main geographical characteristics of the investigated islands and the meteorological stations used in this study are summarized in Table 1.

3. Materials and Methods

3.1. Data Collection and Quality of Data

The temperature and precipitation data used in this study were provided by the Croatian Meteorological and Hydrological Service (DHMZ). Meteorological data were collected at main meteorological stations (MMS, Table 1) and on the precipitation station (PS). At MMS, the temperature data is measured hourly, while the precipitation is measured once a day at 7 h (also at PS). MMS are equipped with minimum and maximum thermometers, and the absolute minimum and maximum temperature are measured once a day. In addition, most of the analyzed stations are equipped with automatic monitoring and recording systems (AMS). Due to the complexity of the automatic measurements of meteorological phenomena and gradual modernization of the meteorological network, many AMS still have human operators. At AMS, the time resolution of measurements is 10 min. The mean daily air temperature is given as:

$$t_{mean,daily} = \frac{t_7 + t_{14} + 2t_{21}}{4} \quad (1)$$

where t_7, t_{14}, and t_{21} are the air temperature values measured at 7, 14, and 21 h (local time), respectively [26]. The daily air temperature data (i.e., minimum, mean, and maximum values) are usually processed by DHMZ to obtain the monthly statistics (i.e., the minimum, mean, and maximum values of daily temperature during a month, hereafter referred to as the minimum, mean, and maximum monthly air temperature, respectively). The monthly data were processed in the scope of this work to calculate the annual statistics (i.e., the minimum, mean, and maximum values during a year, hereafter referred to as the minimum, mean, and maximum annual air temperature). Similarly to the temperature, monthly cumulative precipitation data were provided by DHMZ, while annual values were calculated.

Table 2 shows the time series recorded by the meteorological stations. The time series shows several interruptions, and the only station with continuous measurements was Lastovo. Missing data were excluded from the statistical analyses in this study. The temperature time series were considered as contemporaneous from 1958 to 2018 (missing 1964–1965, 1975, 1982–1985, 1993–1997, and 2011), while the precipitation time series were considered as contemporaneous from 1963 to 2018 (missing 1971, 1982–1986, 1990–1998, 2000–2001, and 2006). During the investigated period, external influences or modifications in the data collection (i.e., relocation of the station, change of sensors, and changes in observation rules) did not occur.

Table 2. Available time series of data used within this study.

		Minimum Temperature	Mean Temperature	Maximum Temperature	Precipitation
Lastovo	*Investigated period*	1/1949–12/2018	1/1948–12/2018	1/1948–12/2018	1/1949–12/2018
	Missing data	-	-	-	-
Komiža	*Investigated period*	1/1956–12/2018	1/1956–12/2018	2/1956–12/2018	1/1956–12/2018
	Missing data	3/1957–8/1957; 6/1982–2/1983; 7/1983–6/1984; 7/1985	3/1957–8/1957; 6/1982–2/1983; 7/1985	3/1957–8/1957; 6/1982–2/1983; 7/1985	3/1957–8/1957; 6/1982–2/1983; 7/1985
Biševo	*Investigated period*	-	-	-	2/1955–12/2018
	Missing data	-	-	-	3/1956–7/1957; 1/1991–2/1991
Palagruža	*Investigated period*	7/1949–12/2018	1/1950–12/2018.	2/1949–12/2018	1/1949–12/2018
	Missing data	11/1949; 9/1950–10/1950; 7/1954; 5/1956–6/1956; 1/1964–8/1964; 2/1965–8/1965; 1/1992; 3/1993–8/1995; 10/1995–2/1996; 5/1996–8/1996; 10/1996; 12/2011	9/1950–10/1950; 7/1954; 5/1956–6/1956; 8/1975–12/1975; 1/1993–8/1995; 5/1996–1/1997	11/1949; 9/1950–10/1950; 7/1954; 5/1955–6/1955; 10/1959–6/1960; 1/1992; 3/1993–7/1996	11/1949; 10/1950–11/1950; 1/1971–4/1971; 2/1982–3/1982; 7/1982–12/1982; 1/1983–4/1983; 6/1984–8/1985; 1/1986; 5/1992–7/1992; 10/1992; 12/1992; 3/1993–7/1994; 10/1994–9/1996; 12/1997–1/1998; 11/1998; 1/2000; 1/2001; 1/2006

3.2. Methods

The annual and monthly air temperature and precipitation were investigated in this study to assess their variations from the 1950s to the present and to highlight the modifications of their distributions within the different years. We employed different statistical methods. First, exploratory data analysis was performed to summarize the main statistical characteristics of the dataset. Afterward, regression analyses were used to detect the trends in the variables (air temperature or precipitation, respectively). Both linear and quadratic regressions were performed, and the correlation coefficients r and R for the linear and quadratic regressions, respectively, were calculated. When the coefficients were comparable, the linear regression was preferred. To validate the observed trends and to assess their statistical significance, the Spearman Rank Order Correlation (SROC) nonparametric test was used.

This test evaluates the monotonic relationship between two variables, thus providing a more general assessment of their correlation than the linear correlation coefficient. This approach was profitably used to investigate the existence of long-term trends in a hydrological time series [27]. Additionally, a significance test for assessing the statistical significance of the SROC coefficient was performed. The null hypothesis was that there was no monotonic association between the two variables.

The trend variations within the times series were also analyzed using the Rescaled Adjusted Partial Sums method (RAPS) [28–30]. This method can be applied to continuous time series detecting (i) subperiods with similar characteristics, (ii) a larger number of trends, (iii) sudden peaks or declines in values, (iv) irregular fluctuations, and (v) periodicity. RAPS is defined as:

$$RAPS_k = \sum_{t=1}^{k} \frac{Y_t - \overline{Y}}{S_y} \quad (2)$$

where Y_t = the value of the observed parameter at time t; $\overline{Y}$ = the mean value of the observed time series; S_y = the standard deviation of the observed time series and k = the number of observations. The visualization of the RAPS results over time allows the overcoming of small systematic changes in the records and the variability of data values [29,30].

In addition to their trends, the correlations among the time series were investigated. The differences of their statistical parameters were evaluated using the F-test and the *t*-test, while their correlations were assessed by calculating their linear correlation coefficient. In particular, the F-test of equality of variances was used to compare the variances of two populations, and its null hypothesis was that two normal populations have the same variance. The *t*-test was used to determine if there was a significant difference between the means of two groups, and its null hypothesis was that two normal populations have the same mean value.

4. Results

4.1. Exploratory Analysis of the Data

Table 3 shows a summary of the statistical analysis performed on the annual air temperature and the annual cumulative precipitation values at the analyzed stations, while the results of the analysis for the monthly data are reported in Tables S1 and S2 of the Supplementary Materials for the monthly temperature and precipitation, respectively. In addition, the *p*-values of the F-test and the *t*-test for comparing the populations of the time series are reported in Tables S3 and S4 of the Supplementary Materials for the annual air temperature and the annual precipitation, respectively.

Table 3. Statistics (minimum, average, and maximum) of the annual minimum, mean, and maximum air temperature and of the annual cumulative precipitation at the analyzed stations. The range of the annual air temperature was calculated subtracting the minimum annual temperature from the maximum annual temperature. The total dataset includes all available data. The contemporaneous temperature dataset spans from 1958 to 2018 (missing 1964–1965, 1975, 1982–1985, 1993–1997, and 2011), while the contemporaneous precipitation dataset spans from 1963 to 2018 (missing 1971, 1982–1986, 1990–1998, 2000–2001, and 2006).

		Annual Temperature (°C)				**Precipitation**
		Minimum	***Mean***	***Maximum***	***Range***	**(mm)**
Lastovo; Total Dataset	*Minimum*	−6.80	14.66	31.70	29.80	368.00
	Average	−1.30	15.80	34.78	36.08	666.48
	Maximum	4.00	17.41	38.30	42.70	1088.60

Table 3. *Cont.*

		Annual Temperature (°C)				Precipitation
		Minimum	***Mean***	***Maximum***	***Range***	**(mm)**
Lastovo; Contemporaneous Dataset	*Minimum*	−6.80	14.66	31.70	30.00	376.90
	Average	−1.18	15.89	34.94	36.12	690.31
	Maximum	4.00	17.41	38.30	42.70	1008.30
Komiža; Total Dataset	*Minimum*	−4.50	15.50	32.10	29.50	426.00
	Average	−1.12	16.71	35.01	36.03	792.00
	Maximum	3.00	18.00	38.80	43.20	1269.00
Komiža; Contemporaneous Dataset	*Minimum*	−4.50	15.50	32.50	30.90	426.00
	Average	−1.09	16.71	35.09	36.17	836.09
	Maximum	3.00	17.90	38.80	43.20	1269.00
Biševo; Total Dataset	*Minimum*	-	-	-	-	255.10
	Average	-	-	-	-	617.01
	Maximum	-	-	-	-	1045.30
Biševo; Contemporaneous Dataset	*Minimum*	-	-	-	-	374.00
	Average	-	-	-	-	640.34
	Maximum	-	-	-	-	1045.30
Palagruža; Total Dataset	*Minimum*	−4.30	15.60	30.00	25.50	109.90
	Average	1.06	16.57	32.64	31.56	314.92
	Maximum	5.60	18.00	36.40	37.80	541.10
Palagruža; Contemporaneous Dataset	*Minimum*	−2.60	15.60	30.00	26.20	109.90
	Average	1.04	16.61	32.75	31.71	326.34
	Maximum	5.60	18.00	36.40	37.80	541.10

4.2. Analyses of Annual Air Temperature Time Series

Figure 2 shows the time series of all available minimum, mean, and maximum annual air temperature measured at the stations Komiža, Lastovo, and Palagruža.

The minimum temperature ranged from −6.8 °C to 4 °C at Lastovo, from −4.5 °C to 3 °C at Komiža, and from −4.3 °C to 5.6 °C at Palagruža (Table 3). The statistical analyses evidenced (i) similar ranges (Table 3) and variances reflecting the failure to reject the null hypothesis of F-tests (i.e., high *p*-values; Table S3); and (ii) a higher average value in Palagruža than those in Komiža and Lastovo (Table 3) with the rejection of the null hypothesis of the *t*-test for Palagruža versus Komiža and Lastovo (i.e., low *p*-values; Table S3). These differences were corroborated by the linear regression results. All three stations showed an increase in the minimum temperature values, but this was not statistically significant (SROC $p > 0.05$).

The values of the mean annual air temperature were similar for all the stations ranging from approximately 15 °C to 18 °C. The statistical analyses evidenced (i) similar ranges and variances (Table 3) failing to reject the null hypothesis of the F-tests (Table S3); and (ii) similar average values for Komiža and Palagruža and higher than the average values of Lastovo (Table 3) resulting in both the failure to reject the null hypothesis of the *t*-tests for Palagruža versus Komiža and the rejection of the null hypothesis of the *t*-test for the other analyses (Table S3). The linear regressions evidenced increasing trends for all of the time series (Figure 2), which were corroborated by the results of the SROC tests showing statistically significant increasing trends ($p < 0.01$). The quadratic regressions were also tested, obtaining slightly higher R values than the linear correlation coefficient *r* (Figure 2). These regressions evidenced stability or a slight decrease in the mean annual air temperature until the 1970s followed by a gradual increase in the 1980s and a rapid increase from the 1990s.

The maximum annual air temperature was up to 38.3, 38.8, and 36.4 °C at Lastovo, Komiža, and Palagruža, respectively. The statistical analyses evidenced (i) similar ranges (Table 3) and variances and the failure to reject the null hypothesis of the F-tests (Table S3); and (ii) similar average values for

Komiža and Lastovo being 2.4 °C higher than the average value of Lastovo (Table 3) and the failure to reject the null hypothesis of the *t*-tests for Komiža versus Lastovo (Table S3). We performed both linear and quadratic regressions. All three stations showed increasing trends in the maximum annual air temperature, and the SROC test corroborated these results ($p < 0.01$) while quadratic regressions evidenced an increase from the 1980s (Figure 2).

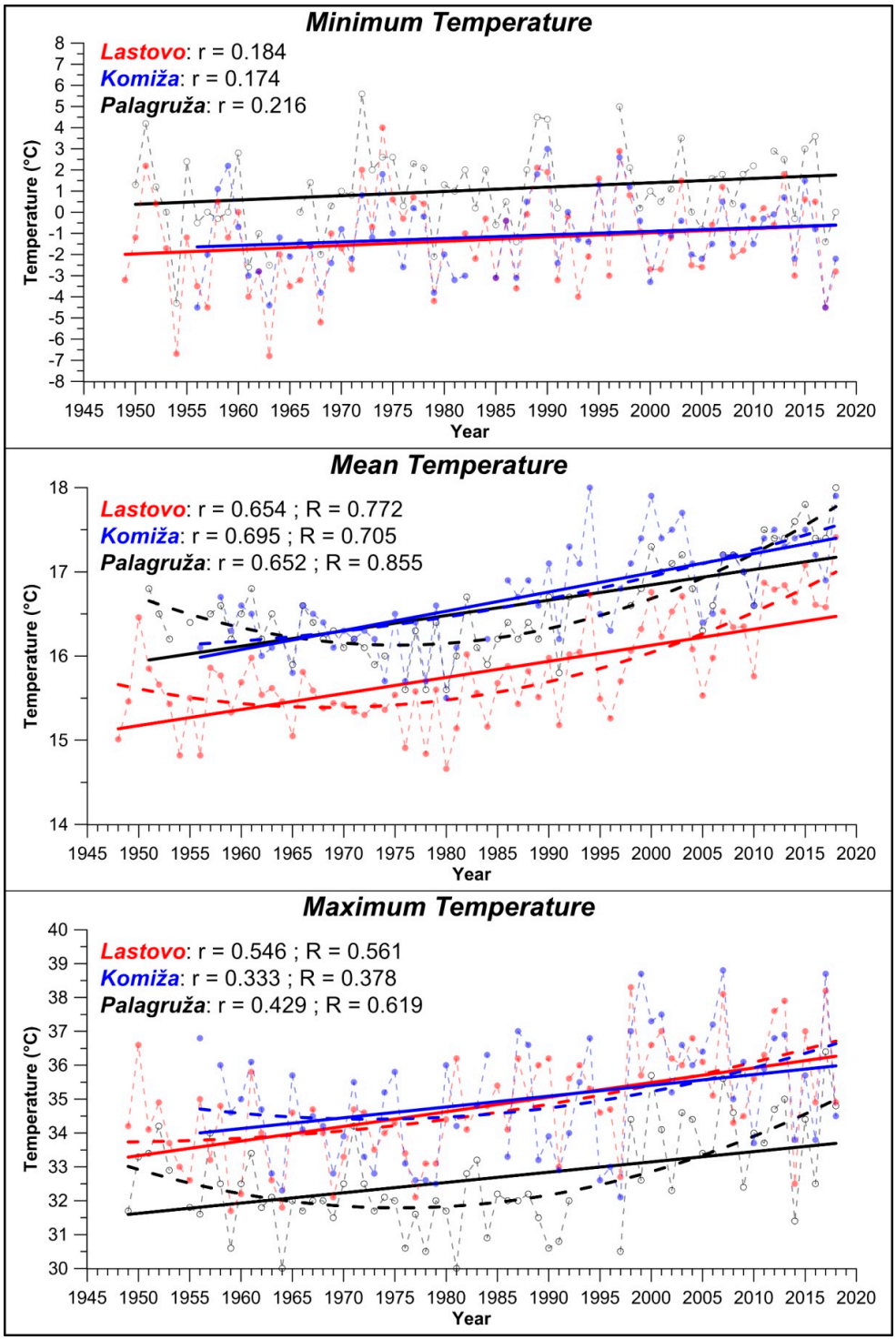

Figure 2. Time series of the minimum, mean, and maximum annual air temperature measured at the Komiža, Lastovo, and Palagruža stations. The *r* and R represent the correlation coefficients of the linear and quadratic regressions, respectively.

The annual air temperature ranges (i.e., the maximum annual temperature minus the minimum annual temperature) were investigated (Figure 3; Table 3). They were comparable at Komiža and Lastovo with average values of 36 °C, and these were approximately 4.5 °C higher than at Palagruža. The time series showed slightly increasing values, although the low values of the linear correlation coefficient r and the results of the SROC test pointed to a low significance of the observed variations (SROC $p > 0.05$).

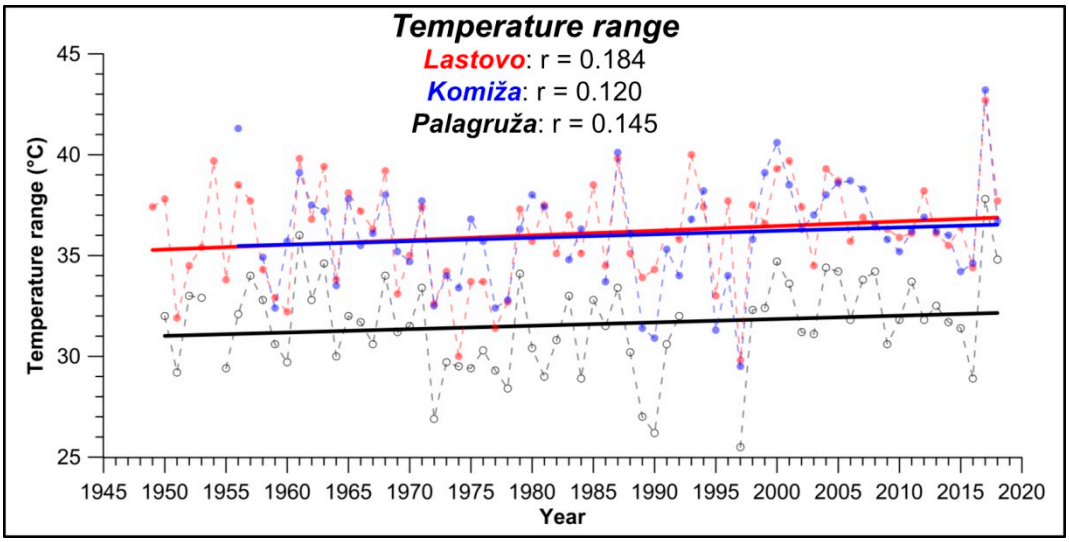

Figure 3. Annual air temperature ranges at Komiža, Lastovo, and Palagruža. The range was calculated subtracting the minimum annual temperature from the maximum annual temperature. r is the linear correlation coefficient.

The RAPS method has been used on the time series of annual air temperature measured at Lastovo (Figure 4) as it was the only station showing a continuous recording (Table 2).

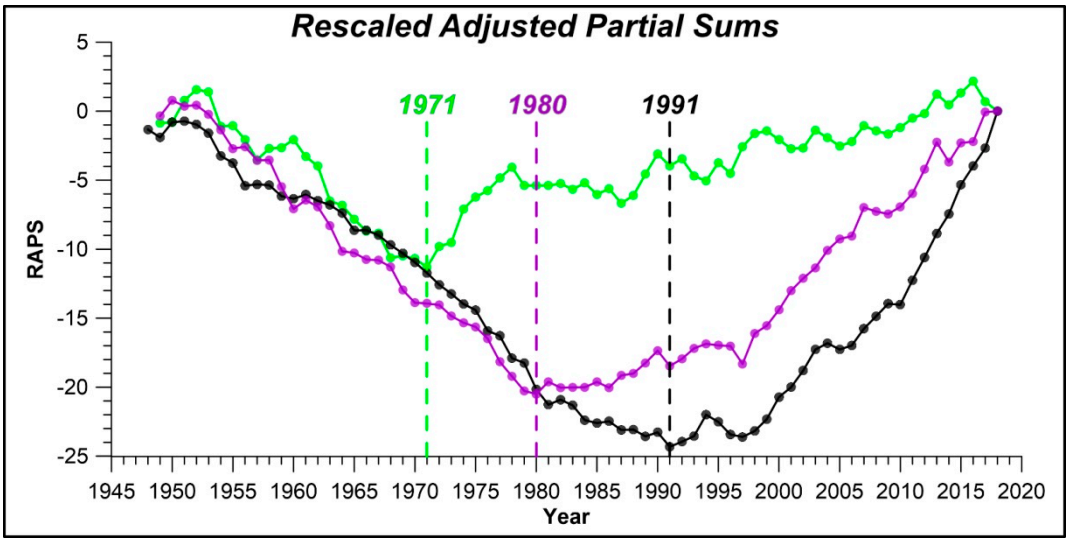

Figure 4. Rescaled Adjusted Partial Sums (RAPS) values for the minimum (green), mean (black), and maximum (purple) annual air temperature measured at the Lastovo station.

The results indicated two different trends in RAPS values. The RAPS of the minimum annual air temperature (green line in Figure 4) showed a sharp decrease until 1971 followed by an initially sharp and subsequently moderate increase. The RAPS of the mean annual air temperature (black line in Figure 4) showed a sharp decrease from the 1950s to the 1970s and a moderate decrease in the 1980s. A moderate increase started in 1992 followed by a sharp increase from the end of the 1990s. The RAPS of the maximum annual air temperature (purple line in Figure 4) showed a sharp decrease until the 1970s followed by a gradual increase in the 1980s–1990s and a sharp increase from the end of the 1990s.

4.3. Analyses of the Characteristic Monthly Air Temperature Time Series

The exploratory data analysis of the minimum, mean, and maximum monthly air temperature measured at the analyzed stations is reported in Table S1 of the Supplementary Materials. Table 4 shows the linear correlation coefficients r calculated for the monthly time series. The results of the SROC test were used to highlight the statistically significant correlations.

Table 4. The linear correlation coefficient r calculated from the contemporaneous dataset of the minimum, mean, and maximum monthly air temperature. The values in red correspond to the months that showed statistically significant results of the SROC test ($p < 0.01$).

Month	Minimum			Mean			Maximum		
	Komiža	Lastovo	Palagruža	Komiža	Lastovo	Palagruža	Komiža	Lastovo	Palagruža
1	0.165	0.185	0.203	0.272	0.164	0.241	0.075	0.01	−0.057
2	0.166	0.15	0.13	0.132	0.142	0.102	0.224	0.039	0.026
3	0.256	0.245	0.247	0.301	0.307	0.3	0.25	0.291	0.137
4	0.283	0.132	0.212	0.394	0.351	0.361	0.286	0.289	0.224
5	0.534	0.277	0.453	0.354	0.406	0.385	0.261	0.386	0.32
6	0.471	0.298	0.276	0.583	0.513	0.491	0.494	0.521	0.47
7	0.559	0.364	0.225	0.591	0.577	0.518	0.317	0.459	0.429
8	0.415	0.371	0.367	0.454	0.494	0.481	0.33	0.394	0.35
9	0.276	0.033	0.082	0.18	0.144	0.187	0.216	0.156	0.302
10	0.32	0.166	0.206	0.235	0.247	0.279	0.014	0.218	0.01
11	0.311	0.149	0.247	0.208	0.23	0.219	0.22	0.273	0.133
12	0.144	0.02	0.03	0.144	−0.003	0.004	0.135	0.061	0.003

Statistically significant increasing trends for all analyzed variables (high r values; Table 4) were generally observed in the warmer periods of the year (April–August), while the temperature variations were moderate (low positive or negative r values; Table 4) during the colder part of the year (September–March).

The mean monthly air temperature shown in Figure 5 can be considered as representative of the behavior of all monthly variables. For each month, the mean air temperature values calculated for each year of the investigated period (Table 2) are plotted. The spring and summer months showed a moderate to the rapid increase of the air temperature, while random fluctuations with unsystematic spikes were observed during the autumn and winter months. In particular, the most rapidly increasing trends at all analyzed stations occurred in July, as corroborated by the highest r values of the time series for this month (Table 4).

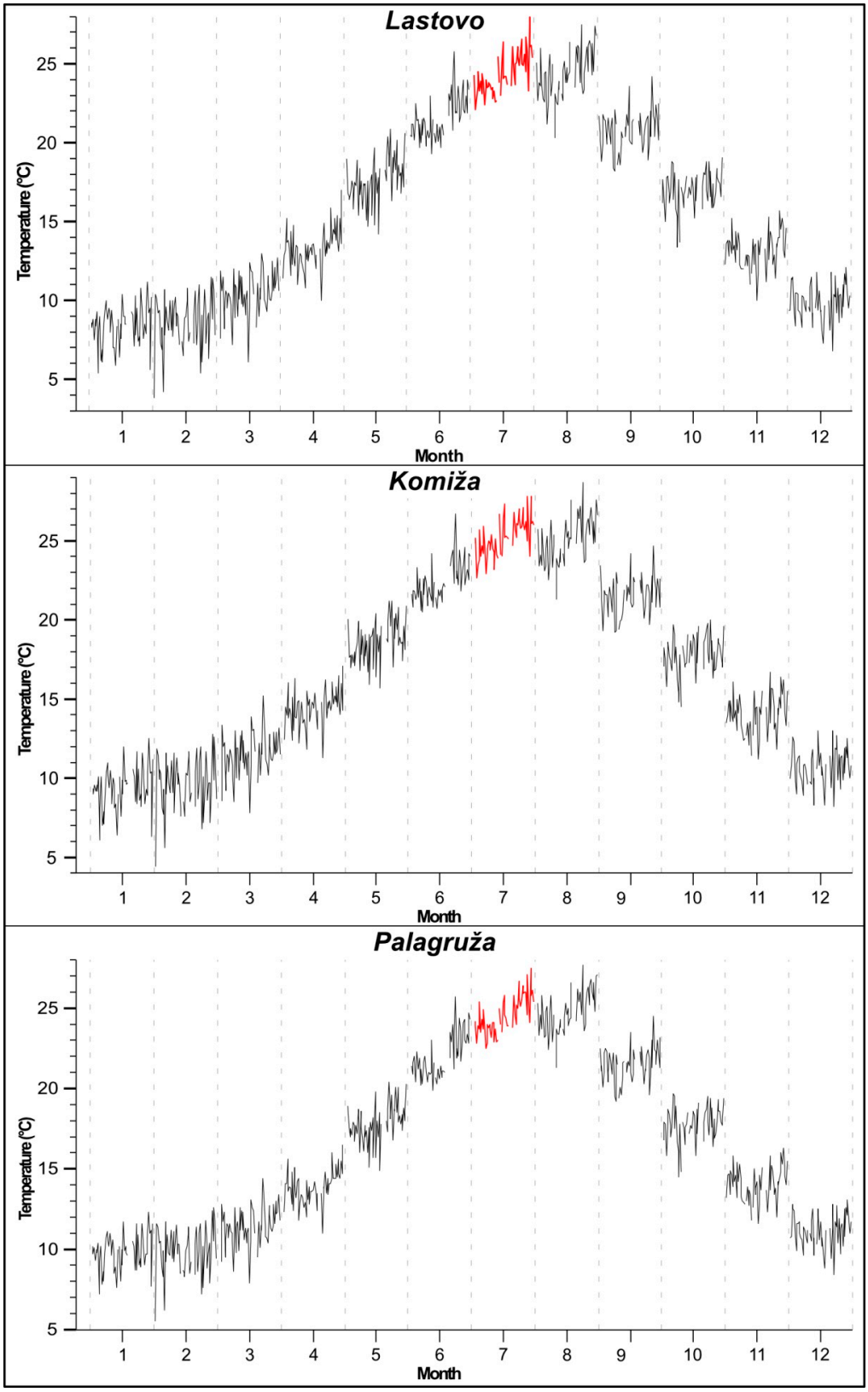

Figure 5. Monthly subseries plot of the mean air temperature at the Lastovo, Komiža, and Palagruža stations. Within a month, the mean monthly values were plotted in chronological order over the period 1958–2018 (Table 2). The time series of July (in red) shows the most prominent increasing trends as suggested by the highest linear correlation coefficient *r* values (Table 4).

Figure 6 shows the temperature differences of the average monthly minimum, mean, and maximum air temperature between the analyzed stations demonstrating the differences in their temperature regimes. The average monthly minimum air temperature at Palagruža was always higher than at Komiža and Lastovo. Their differences fluctuated throughout the year and were the highest in January, February, and October and the lowest during July.

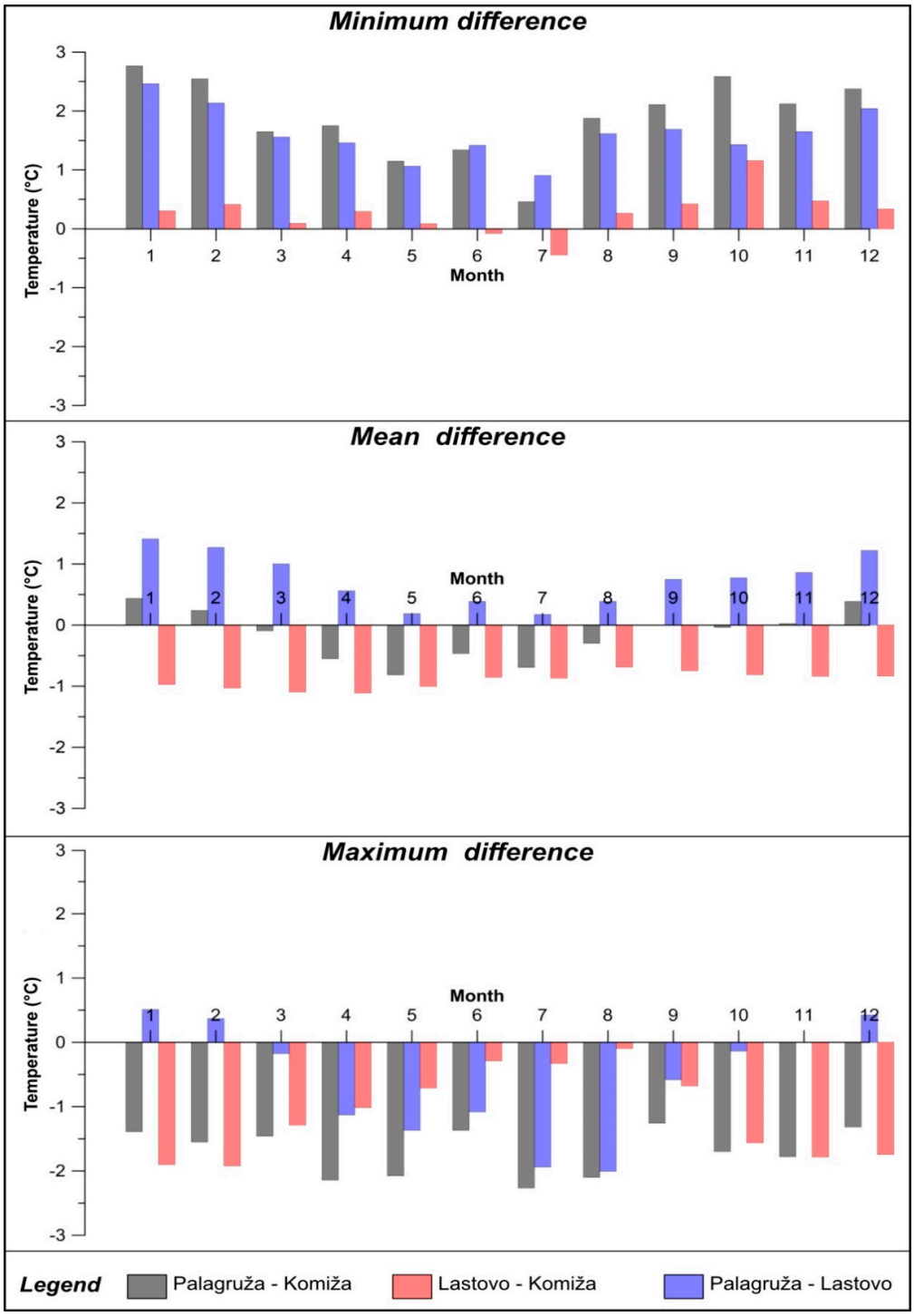

Figure 6. The minimum, mean, and maximum monthly air temperature differences between stations. The differences were calculated based on contemporaneous datasets. Palagruža and Komiža stations (shown in gray), $\Delta T_{P\text{-}K} = {}_{av}T_P - {}_{av}T_K$; Lastovo and Komiža (shown in red), $\Delta T_{L\text{-}K} = {}_{av}T_L - {}_{av}T_K$; and Palagruža and Lastovo (shown in blue), $\Delta T_{P\text{-}L} = {}_{av}T_P - {}_{av}T_L$.

The average monthly mean air temperature at Palagruža was slightly higher than at Komiža during January, February, and December and nearly equal during March, September, October, and November (Figure 6). Palagruža had a higher mean monthly air temperature than Lastovo, and their differences ranged from 0.2 °C to 1.4 °C. The monthly mean air temperature at Lastovo was always lower than at Komiža with a fairly constant difference throughout the year.

The average monthly maximum air temperature at Palagruža was lower than at Komiža in each month and lower than at Lastovo except during the winter period. The maximum temperature at Komiža was always higher than at Lastovo, and their differences ranged from 0.01 °C in August to 1.9 °C in February.

4.4. Analyses of Annual Precipitation Time Series

The annual precipitation was analyzed at four measuring stations (Table 2). During the investigated period, it ranged from 376 to 1008 mm at Lastovo, 426 to 1269 mm at Komiža, 374 to 1045 mm at Biševo, and 109 to 541 mm at Palagruža (Table 3). The statistical analyses evidenced (i) similar ranges and variances for Lastovo, Komiža, and Biševo reflecting the failure to reject the null hypothesis of the F-tests (i.e., high *p*-values; Table S4), (ii) the lower average value at Palagruža than at Komiža, Lastovo, and Biševo (i.e., low *p*-values) with the rejection of the null hypothesis of the *t*-test for Palagruža versus Lastovo, Komiža, and Biševo. (i.e., low *p*-values; Table S4); and (iii) similar values of cumulative precipitation at Lastovo and Biševo (i.e., high *p*-values; Table S4). The linear correlation coefficients *r* close to 0 indicated the lack of a correlation between the precipitation and the time. Random fluctuations around the average values were observed, and systematically lower precipitation only occurred at the beginning of the 1990s and 2000s. The mean value of the cumulative annual precipitation was the highest at Komiža with 836 mm and the lowest at Palagruža with only 326 mm of precipitation (Figure 7). These results suggest that the amount of precipitation decreases with the distance from the mainland (Table 1), but an effect of the station's altitudes cannot be excluded.

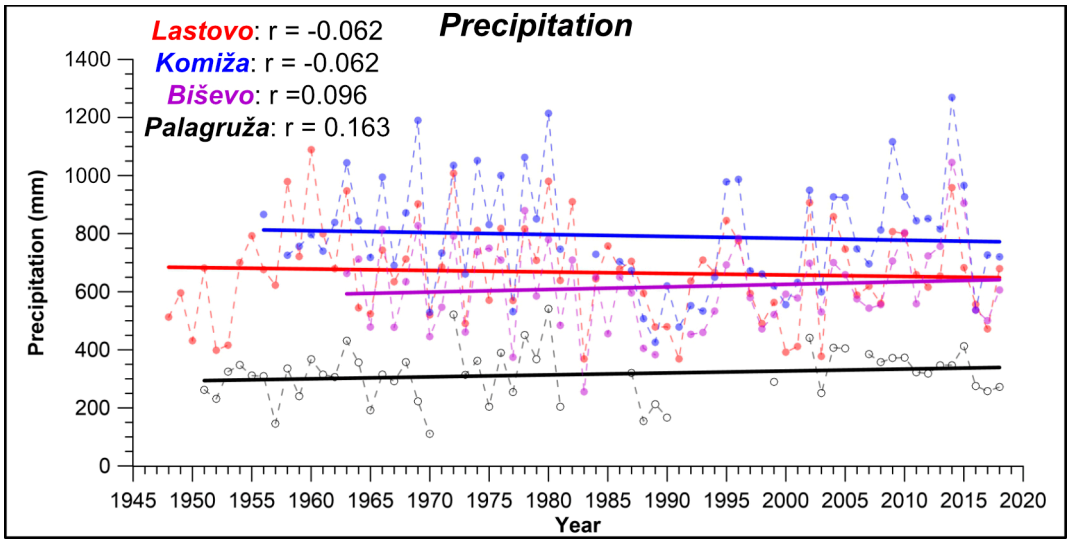

Figure 7. Annual precipitation time series. The linear correlation coefficient *r* was calculated from the total datasets.

4.5. Analyses of Monthly Precipitation Time Series

The distribution of precipitation through the months of the year is an essential factor that affects all environmental processes. The mean and maximum values of the monthly precipitation were analyzed at four measuring stations (Figure 8).

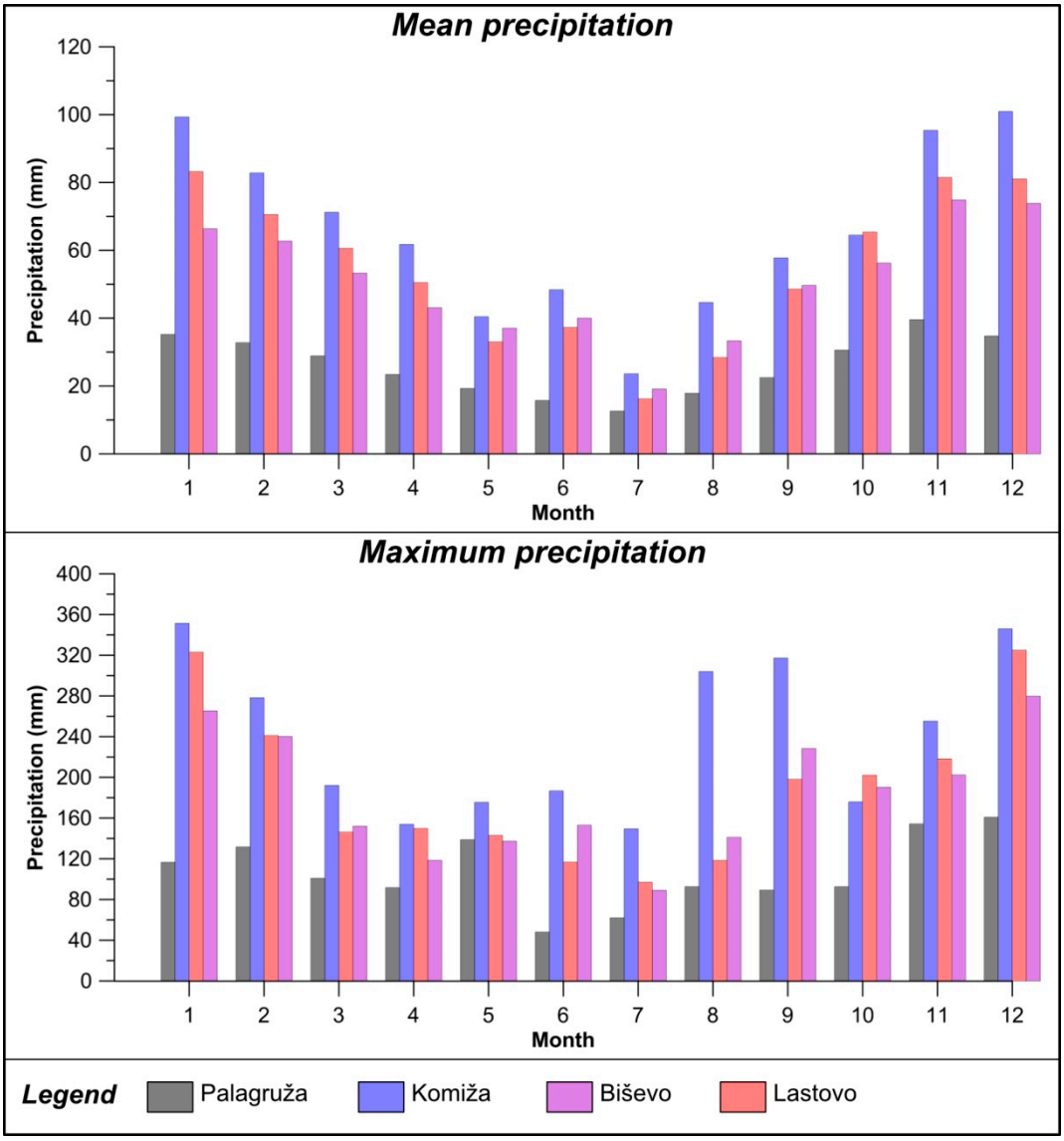

Figure 8. Histograms of the mean and maximum values of the monthly precipitation at the analyzed stations.

The mean values of monthly precipitation ranged from 12 to 39 mm at Palagruža, 23 to 100 mm at Komiža, 19 to 75 mm at Biševo, and 16 to 83 mm at Lastovo (Figure 8). These different ranges reflect the distance of the stations from the mainland as shown by their mean annual values (Tables 1 and 3). The distribution over one year was similar at all stations. The highest precipitation occurred during January, November, and December and the lowest during July and August.

The maximum values of monthly precipitation occurred during January and December at the Komiža, Biševo, and Lastovo stations while, at Palagruža, the maximum precipitation occurred during November and December. The highest monthly precipitation of 351.4 mm was measured at Komiža in January 1978 (Figure 8). During August and October, Komiža had significantly higher values of maximum precipitation than the other stations. The maximum value of monthly precipitation at the Palagruža station was significantly lower than at other stations with only 160 mm in December 2002.

5. Discussion and Conclusions

The annual and monthly air temperature and precipitation data were analyzed from four meteorological stations located on remote islands in the Adriatic Sea (Vis, Biševo, Lastovo, and

Palagruža; Figure 1). Statistical analyses, significance tests, and correlation analyses (i.e., linear and quadratic regressions, Spearman Rank Order Correlation) were performed to investigate the trends of the time series and their relationships. Different trends, as well as trend variations within a time series, were observed. Due to the heterogeneous behavior of the variables, the linear correlation represents the most consistent approach for a comprehensive and homogeneous comparison of the analyzed time series.

Increasing trends in the annual air temperature were observed (Figure 2). During the investigated period, the mean temperature increased by 0.034, 0.029, and 0.018 °C/y at Lastovo, Komiža, and Palagruža, respectively. The mean annual air temperature increased rapidly from the 1990s while the maximum annual air temperature rapidly increased from the 1980s (Figure 2). The RAPS results from the Lastovo time series corroborated these results (Figure 4). In particular, the increases in the mean annual air temperature at Lastovo were 0.004 and 0.053 °C/y from 1948 to 1991 and from 1992 to present, respectively. These results are in accordance with findings in several stations of Croatia and the western Balkan region, where warming started between 1987 and 1997 [29–31]. In particular, the rapid warming started in 1992 at the nearby meteorological stations of Hvar, Korčula, and Split (Figure 1) was in accordance with the RAPS results of Lastovo [30]. These results fit with the acceleration in warming from 1975 observed at a global scale [32]. However, numerous authors reported that the increasing trends in the Mediterranean area were higher than the global values, e.g., [16,32–34]. Increasing trends at Lastovo, Komiža, and Palagruža were consistent with increasing trends in the Adriatic region of 0.07–0.22 for 1951–2010, as well as with 0.29–0.71 °C/decade for 1981–2010 [16]. In addition, a comparison to the Berkeley Earth datasets [34] regarding the mean rate of air temperature change (°C/century) showed similar warming rates of 2.94 ± 0.26, 3.54 ± 0.33, and 3.35 ± 0.40 °C/century for Europe, Croatia, and Split, respectively.

Statistically significant increasing trends in the monthly air temperature occurred only in the warmer periods of the year, from April to August (Table 4). The most prominent increasing trends in the mean air temperature were observed in July at all analyzed stations (Figure 5). Hence, we concluded that the effects of global warming on increasing air temperature were higher in the warmer periods of the year at the analyzed stations. Pronounced warming in the summer season was previously reported by several authors, e.g., [16,29].

The lower warming intensity during the colder periods of the year is most likely a result of the influence of the sea temperature. The study area is located along the Palagruža sill and between the Mid and the South Adriatic pits, the deepest areas of the Adriatic Sea [35]. In the proximity of these pits, the highest annual mean air temperature at sea level is observed [36] and the sea acts as a temperature buffer resulting in milder summer and warmer autumn and winter. The microclimatic conditions at all stations strongly reflect the maritime influence, which, compared to stations located on the mainland, is apparent through (i) lower summer air temperature, (ii) lower amplitudes of the annual air temperature, (iii) lesser cloud cover, (iv) lesser precipitation, and (v) higher relative humidity.

The distribution of precipitation through the months of the year is an essential factor that affects all environmental processes. Annual precipitation time series showed neither increasing nor decreasing trends at the analyzed stations (Figure 7). The highest value of the cumulative annual precipitation was 1269 mm at Komiža while the lowest was only 109 mm at Palagruža (Table 3). The amount of precipitation decreased with distance from the mainland, but could be also affected by the altitude and the position of the measuring station.

The annual precipitation trends reflect monthly trends in terms of Komiža receiving the highest precipitation and Palagruža the lowest. The highest monthly precipitation occurred during January, November, and December and the lowest during July and August. Statistical analyses of the monthly precipitation trends were performed for Lastovo, as the only station with continuous records from 1948 to 2018. Statistically significant increasing or decreasing trends cannot be seen in the months of the year. Global and regional precipitation patterns showed a mix of increasing and decreasing trends, and most were statistically insignificant, e.g., [16,33,37].

The similarity between the climate regimes in the study area was corroborated by the relation between the island distances and the correlation coefficients of their mean annual air temperature and precipitation (Figure 9). The values of the linear correlation coefficients of air temperature were very high and ranged from at the lowest, $r = 0.894$, for the furthest stations at Komiža and Palagruža, to the highest, $r = 0.977$, for the closest stations at Palagruža and Lastovo. As anticipated, the highest linear correlation coefficient of precipitation, $r = 0.863$, occurred between Komiža and Biševo, as their distance is 9.3 km. Other pairs of stations, having similar distances from each other, ranging from 63.5 to 76.3 km, showed varying linear correlation coefficients from $r = 0.582$ to $r = 0.732$.

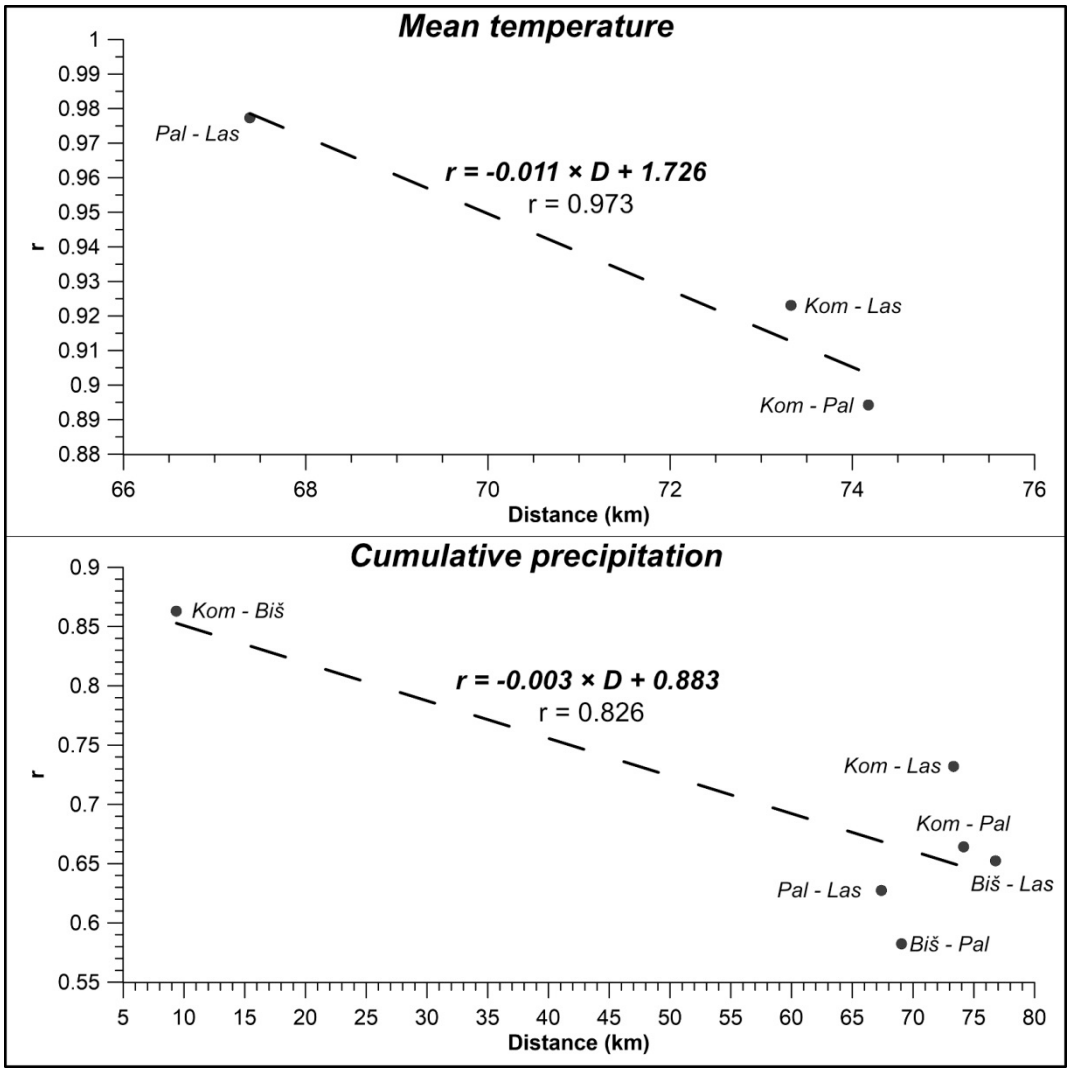

Figure 9. The ratio of the linear correlation coefficient *r* of the mean annual air temperature (up) and precipitation (down) against the distance between stations, L.

Air temperature is an important factor for explaining and addressing past events and for foreseeing future significant climate modification ascribable to global warming processes [38]. Therefore, it is essential to continue detailed monitoring and predict future trends in air temperature at different locations. Climate models for the Mediterranean region predict a gradual decrease in precipitation and an increase in variability, with a negative influence on the water balance [39]. The main conclusions of this study, namely an increase in air temperature, corroborate the results based on climate models. An increasing trend in air temperature could have a negative effect on the water balance through higher evapotranspiration and decreased recharge.

However, there are insufficient meteorological stations in the investigated area. Another drawback is the lack of data from investigated stations due to the cease of work. Precipitation can significantly differ between nearby locations, especially on remote islands with dynamic topography. Therefore, it is necessary to improve meteorological measurements that would allow for a more detailed investigation of precipitation regimes. Detailed monitoring and investigation of storm events could reveal how the duration, frequency, and intensity of storm events are linked to global warming.

The authors hope that this study initiates more detailed interdisciplinary research regarding the changes in air temperature and precipitation on the islands and coastal zones. Such research will foster better preparation for future climatic uncertainty. Hence, intensive interdisciplinary cooperation based on a detailed and carefully planned network of new meteorological stations will enable this crucial task to be fulfilled.

Supplementary Materials: The following are available online at http://www.mdpi.com/2073-4433/11/10/1044/s1. Table S1: Statistics (minimum, average, and maximum) of the monthly minimum, mean, and maximum air temperature at the stations of Lastovo, Komiža, and Palagruža. Table S2: Statistics (minimum, average, and maximum) of the monthly precipitation at the stations of Lastovo, Komiža, Biševo, and Palagruža. Table S3: *p*-values of the F-test and *t*-test for the minimum, mean, and maximum annual air temperature. Table S4: *p*-values of the F-test and *t*-test for the annual precipitation.

Author Contributions: Conceptualization, investigation, and writing of original draft, O.B.; data curation and validation, review and editing, M.P. (Matko Patekar); supervision, writing and editing, and validation, M.P. (Marco Pola); investigation, visualization, and data curation, T.R.-B. All authors have read and agreed to the published version of the manuscript.

Funding: This research was supported by the Croatian Geological Survey, Department of Hydrogeology and Engineering Geology.

Acknowledgments: Data used in this study was provided by courtesy of the Croatian Meteorological and Hydrological Service, for which we thank them. Terms of use, data availability, and contact can be found at: https://klima.hr/razno/katalog_i_cjenikDHMZ.pdf. We also thank the Editor and the Reviewers for fruitful suggestions and improvements to our manuscript.

Conflicts of Interest: The authors declare no conflict of interest.

References

1. Meehl, G.A.; Arblaster, J.M.; Branstator, G. Mechanisms contributing to the warming hole and the consequent U.S. east-west differential of heat extremes. *JCLI* **2012**, *25*, 6394–6408. [CrossRef]
2. IPCC. Summary for Policymakers. In *Climate Change 2013: The Physical Science Basis. Contribution of Working Group 1 to the 5th Assessment Report of the Intergovernmental Panel on Climate Change*; Stocker, T.F., Qin, D., Plattner, G.-K., Tignor, M., Allen, M., Boschung, J., Nauels, A., Xia, Y., Bex, V., Midgley, P.M., Eds.; Cambridge University Press: Cambridge, UK; New York, NY, USA, 2013.
3. Washington, R. Quantifying chaos in the atmosphere. *Prog. Phys. Geog.* **2000**, *24*, 499–514. [CrossRef]
4. Wood, S.J.; Jones, D.A.; Moore, R.J. Accuracy for rainfall measurement for scales of hydrological interest. *Hydrol. Earth Syst. Sci.* **2000**, *4*, 531–543. [CrossRef]
5. Médail, F.; Quézel, P. Hot-Spots Analysis for conservation of Plant Biodiversity in the Mediterranean Basin. *Ann. Mo. Bot.* **1997**, *84*, 112–127. [CrossRef]
6. Davis, S.D.; Heywood, V.H.; Hamilton, A.C. *Centres of Plant Diversity: A Guide and Strategy for Their Conservation*; Europe, Africa, South West Asia and the Middle East; World Wide Fund for Nature (WWF) and ICUN: Cambridge, UK, 1994; Volume 1.
7. European Environmental Agency. Fund & World Conservation Union, Cambridge, UK. Mediterranean Sea Region Briefing—The European Environment—State and Outlook. 2015. Available online: https://www.eea.europa.eu/soer/2015/countries/mediterranean (accessed on 4 June 2020).
8. Ahlonsou, E.; Ding, Y.; Schimel, D. The Climate System: An Overview. In *Climate Change 2001: The Scientific Basis*; Houghton, J.T., Ding, Y., Griggs, D.J., Noguer, M., van der Linden, P.J., Dai, X., Maskell, K., Johnson, C.A., Eds.; Cambridge University Press: Cambridge, UK, 2001; pp. 99–183.
9. Rađa, B.; Bonacci, O.; Rađa, T.; Šantić, M. The water and biology on a small Karstic island: The Island of Brač (Croatia) as one example. *Environ. Earth Sci.* **2020**, *79*, 116. [CrossRef]

10. Falkland, A. *Hydrology and Water Resources of Small Islands: A Practical Guide*; UNESCO: Paris, France, 1991; p. 275.
11. Borović, S.; Terzić, J.; Pola, M. Groundwater Quality on the Adriatic Karst Island of Mljet (Croatia) and its Implications on Water Supply. *Geofluids* **2019**, *2019*, 14. [CrossRef]
12. Duplančić Leder, T.; Ujević, T.; Čala, M. Coastline lengths and areas of islands in the Croatian part of the Adriatic Sea determined from the topographic maps at the scale 1:25,000. *Geoadria* **2004**, *9*, 5–32.
13. Jurica, M. *Lastovo Kroz Stoljeća*; Matica Hrvatska: Lastovo, Croatia, 2001; 595p.
14. Della Casa, P.; Bas, B.; Katunarić, K.; Kirigin, B.; Radić, D. An overview of prehistoric and early historic settlement, topography, and maritime connections on Lastovo Island, Croatia. In *Maritime Interaction in Adriatic Prehistory*; Forenbaher, S., Ed.; Archaeopress: Oxford, UK, 2009; pp. 113–136.
15. ENSEMBLES Project. European Centre for Medium-Range Weather Forecasts. Available online: https://www.ecmwf.int/ (accessed on 30 July 2020).
16. Branković, Č.; Güttler, I.; Gajić-Čapka, M. Evaluating climate change at the Croatian Adriatic from observations and regional climate models' simulations. *Clim. Dyn.* **2013**, *41*, 9–10, 2353–2373. [CrossRef]
17. Gajić-Čapka, M.; Zaninović, K. Climate of Croatia. In *Climate Atlas of Croatia 1961–1990, 1971–2000*; Zaninović, K., Gajić-Čapka, M., Perčec Tadić, M., Vučetić, M., Milković, J., Bajić, A., Cindric, K., Cvitan, L., Katušin, Z., Kaučić, D., et al., Eds.; Croatian Meteorological and Hydrological Service: Zagreb, Croatia, 2008; pp. 15–17.
18. Alpert, P.; Ben-Gai, T.; Baharad, A.; Benjamini, Y.; Yekutieli, D.; Colacino, M.; Diodato, L.; Ramis, C.; Homar, V.; Romero, R.; et al. The paradoxical increase of Mediterranean extreme daily rainfall in spite of decrease in total values. *Geophys. Res. Lett.* **2002**, *29*, 311–314. [CrossRef]
19. Bognar, A. Geomorfološke značajke arhipelaga Palagruže. In *Zbornik Radova Simpozija Palagruža Jadranski Dragulj*; Hodžić, M., Ed.; Matica Hrvatska: Kaštela, Croatia, 1996; pp. 87–95.
20. Špoljarić, D.; Kranjec, M.; Medak, F.; Šoštar, K. Suvremena topografska izmjera i geovizualizacija palagruškog arhipelaga za potrebe interdisciplinarnih istraživanja. *Geod. List* **2010**, *2*, 87–106.
21. Bonacci, O. Značaj meteoroloških podataka sakupljenih na Palagruži za bilancu voda Jadranskog mora. In *Zbornik Radova Simpozija Palagruža Jadranski Dragulj*; Hodžić, M., Ed.; Matica Hrvatska: Kaštela, Croatia, 1996; pp. 287–291.
22. Lukšić, I. Kakvoća i raspoloživost klimatoloških podataka Palagruže. In *Zbornik Radova Simpozija Palagruža Jadranski Dragulj*; Hodžić, M., Ed.; Matica Hrvatska: Kaštela, Croatia, 1996; pp. 307–313.
23. Milković, J. Palagruža—Oborinski podaci. In *Zbornik Radova Simpozija Palagruža Jadranski Dragulj*; Hodžić, M., Ed.; Matica Hrvatska: Kaštela, Croatia, 1996; pp. 223–239.
24. Pandžić, K.; Sijerković, M. Dosadašnja istraživanja klime Palagruže. In *Zbornik Radova Simpozija Palagruža Jadranski Dragulj*; Hodžić, M., Ed.; Matica Hrvatska: Kaštela, Croatia, 1996; pp. 299–306.
25. Bonacci, O.; Željković, I. Differences between true mean temperatures and means calculated with four different approaches: A case study from three Croatian stations. *Theor. Appl. Climatol.* **2008**, *131*, 733–743. [CrossRef]
26. Adeloye, A.J.; Montaseri, M. Preliminary streamflow data analyses prior to water resources planning study. *Hydrolog. Sci. J.* **2002**, *47*, 679–692. [CrossRef]
27. Garbrecht, J.; Fernandez, G.P. Visualization of trends and fluctuations in climatic records. *Water Resour. Bull.* **1994**, *30*, 297–306. [CrossRef]
28. Bonacci, O. Analiza nizova srednjih godišnjih temperature zraka u Hrvatskoj. *Građevinar* **2010**, *62*, 781–791.
29. Bonacci, O. Increase of mean annual surface air temperature in the Western Balkans during last 30 years. *Vodoprivreda* **2012**, *44*, 75–89.
30. Levi, B.G. Trends in the hydrology of the Western US Bear the imprint of manmade change. *Phys. Today* **2008**, *61*, 16–18. [CrossRef]
31. Le Treut, H.; Somerville, R.; Cubasch, U.; Ding, Y.; Mauritzen, C.; Mokssit, A.; Peterson, T.; Prather, M. Historical Overview of Climate Change. In *Climate Change 2007: The Physical Science Basis*; Solomon, S., Qin, D., Manning, M., Chen, Z., Marquis, M., Averyt, K.B., Tignor, M., Miller, H.L., Eds.; Cambridge University Press: Cambridge, UK; New York, NY, USA, 2007.

32. Hartmann, D.L.; Tank, A.M.; Rusticucci, M.; Alexander, L.V.; Brönnimann, S.; Charabi, Y.A.; Dentener, F.J.; Dlugokencky, E.J.; Easterling, D.R.; Kaplan, A.; et al. Observations: Atmosphere and Surface. In *Climate Change 2013: The Physical Science Basis*; Stocker, T.F., Qin, D., Plattner, G.-K., Tignor, M., Allen, S.K., Boschung, J., Nauels, A., Xia, Y., Bex, V., Midgley, P.M., Eds.; Cambridge University Press: Cambridge, UK; New York, NY, USA, 2013.
33. The Berkeley Earth Surface Temperature Study. Available online: http://berkeleyearth.org/ (accessed on 10 August 2020).
34. Cushman-Roisin, B.; Gačić, M.; Poulain, P.M.; Artegiani, A. *Physical oceanography of the Adriatic Sea: Past, Present and Future*; Springer Science & Business Media: Dordrecht, The Netherlands, 2001.
35. Penzar, B.; Penzar, I.; Orlić, M. *Vrijeme i Klima Hrvatskog Jadrana; Weather and Climate of the Croatian Adriatics*, 1st ed.; Dr. Frletar: Zagreb, Croatia, 2001.
36. Luterbacher, J.; Xoplaki, E.; Casty, C.; Wanner, H.; Pauling, A.; Küttel, M.; Brönnimann, S.; Fischer, E.; Fleitmann, D.; Gonzalez-Rouco, F.J.; et al. Mediterranean climate variability over the last centuries: A review. In *Mediterranean*; Developments in Earth and Environmental Sciences; Lionello, P., Malanotte-Rizzoli, P., Boscolo, R., Eds.; Elsevier: Amsterdam, The Netherlands, 2006; Volume 4, pp. 8–15.
37. Tadić, L.; Bonacci, O.; Brleković, T. An example of principal component analysis application on climate change assessment. *Theor. Appl. Climatol.* **2019**, *138*, 1049–1062. [CrossRef]
38. Aguilera, H.; Murillo, J.M. The effect of possible climate change on natural groundwater recharge based on a simple model: A study of four karstic aquifers in SE Spain. *Environ. Geol.* **2008**, *57*, 963–974. [CrossRef]
39. Touhami, I.; Chirino, E.; Andreu, J.M.; Sánchez, J.R.; Moutahir, H.; Bellot, J. Assessment of climate change impacts on soil water balance and aquifer recharge in a semiarid region in south east Spain. *J. Hydrol.* **2015**, *527*, 619–629. [CrossRef]

water

MDPI

Article

Hydrogeological Assessment and Modified Conceptual Model of a Dinaric Karst Island Aquifer

Josip Terzić, Tihomir Frangen, Staša Borović, Jasmina Lukač Reberski and Matko Patekar *

Department of Hydrogeology and Engineering Geology, Croatian Geological Survey, 10000 Zagreb, Croatia; jterzic@hgi-cgs.hr (J.T.); tfrangen@hgi-cgs.hr (T.F.); sborovic@hgi-cgs.hr (S.B.); jlukac@hgi-cgs.hr (J.L.R.)
* Correspondence: mpatekar@hgi-cgs.hr; Tel.: +385-98-904-26-99

Abstract: Vis Island is situated in southern Croatia. The island is mostly composed of karstified carbonate rocks and belongs to the Dinaric karst region, which is a locus typicus of karst landforms. Located far from the mainland, Vis island has maintained a successful water supply from its own karst aquifer for decades. Hydrogeological research has been undertaken to protect this excellent karst aquifer by establishing sanitary protection zones and to explore the possibility of increasing the pumping yield. New groundwater velocity data obtained via a tracer test were in accordance with the rock mass hydraulic conductivity calculated from previous pumping tests. The hydrochemical interpretation indicated several different phenomena, from carbonate and sulfate rock dissolution to seawater mixing with groundwater. A conceptual model of the island's aquifer was improved, and two main catchments were delineated according to tracer test results, and connected with the geological setting, hydrochemical data, and new climatological insights. Such an approach is applicable for similar karst aquifers, in which topographic and hydrogeological divides usually do not coincide.

Keywords: karst; island; hydrogeology; tracer test; hydrochemistry; sea/freshwater relations

Citation: Terzić, J.; Frangen, T.; Borović, S.; Reberski, J.L.; Patekar, M. Hydrogeological Assessment and Modified Conceptual Model of a Dinaric Karst Island Aquifer. *Water* **2022**, *14*, 404. https://doi.org/10.3390/w14030404

Academic Editor: Jean Denis Taupin

Received: 2 December 2021
Accepted: 27 January 2022
Published: 28 January 2022

1. Introduction

Karst rocks are among the most important aquifer formations in the world [1–4]. Approximately half of the Croatian territory is part of the Dinaric karst region, which is characterized by very deep karstification that is predefined by tectonics and a differentiated dissolution of carbonate rocks [5]. It is difficult to represent this type of karst terrain in numerical models; hence, other methods should be employed, the combination of which can increase the quality of the interpretation. The coastal and island aquifers involve further complexity due to the possibility of seawater intrusions [6]. As a consequence of Holocene changes in the global seawater level, the base of karstification in the Adriatic islands was much lower than it would have been according to the present sea level [7,8]. This means that aquifers can exist in much deeper zones, but it also enables seawater intrusion into the karst underground via much deeper karst conduits and joints within the rock mass.

Hydrogeological research into coastal aquifers all over the Mediterranean region show a wide variety of geological settings and hydrogeological issues [9]. Additionally, due to climate changes, overexploitation, and pollution, they are being explored in several studies [10–14].

The main problem concerning water supply from karst aquifers on islands is the high possibility of seawater intrusion, and only a few Croatian islands have secured a water supply from their own sources [15]. Importantly, the majority of populated Croatian islands have a public water supply. Some have water pipelines connected to the mainland that serve either as the only source of public water supply or as a backup solution in the event of aquifer salinization. However, Vis Island is not connected to the mainland due to its remote position (Figure 1), and instead relies exclusively on its own water resources. In

fact, Vis is fortunate in having probably one of the best water supplies originating from an island aquifer.

Figure 1. Location of the research area in Croatia and the Adriatic Sea.

The main goals of the present research of Vis Island are to: (1) determine the discharge from wells and springs and hence the groundwater dynamics; (2) to delineate sanitary protection zones (SPZ); and (3) to suggest possible locations for drilling additional observation and extraction wells in the future.

2. Physical Setting (Geography, Morphology, Geology, and Hydrogeology)

Vis Island is situated in the central part of the Croatian Adriatic coast (Figure 1).

Its distance from the city of Split on the mainland is 55 km. The largest settlements on the island are Vis and Komiža, which are connected to the public water supply along with all other populated settlements. The water supply system includes drilled wells in Korita and a coastal karst spring Pizdica. A borehole has also been drilled near Komiža (well K-1) and is being prepared for inclusion in the water supply system. Other analyzed features were either small springs (Kamenice), boreholes (Velo žalo, VP-1, VP-2, DP-1) with a low yield, or pit (dug) wells (Dragevode, Gusarica). The intake structure of the spring extraction site in Pizdica was excavated into carbonate rock by mining in the 1950s (Figure 2) in order to supply water (minimum capacity of 3.3 L/s) to the army/navy in case of nuclear warfare.

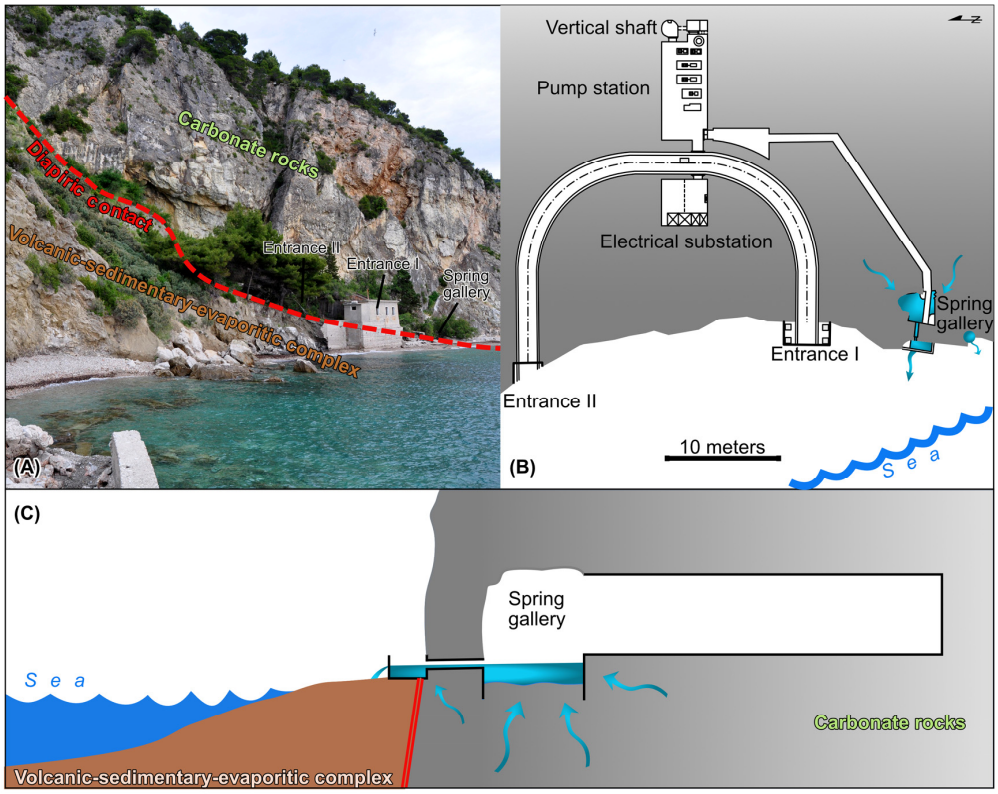

Figure 2. Pizdica karst spring. (**A**) Contact of the volcanic–sedimentary–evaporitic complex with carbonate rocks and the sea (the spring is located behind the building). (**B**) Scheme of the extraction site constructed in the carbonate rock by mining for the purpose of nuclear wartime water supply in the 1950s, which is still in use. (**C**) Illustrative cross-section.

The Korita pumping site includes a total of six wells, five of which are in use. The total designed pumping yield was 27 L/s, which was increased to 40 L/s after research and optimization. Water has been supplied from these wells since the late 1960s, when the first wells were drilled after bulk investigations that involved geological, hydrogeological, and geophysical (geoelectrical sounding) research, as well as test drilling, pumping tests, and hydrochemical interpretations (Figure 3). Terzić [16] lists the numerous unpublished technical reports, which exist from that time.

The current pumping rates for public water supply approach their limit (approximately 40 L/s) during the summer, when there is practically no groundwater recharge and water demand is at its maximum due to tourism and agriculture. To further develop the touristic potential of the island, new water sources should be ensured. An increase in available irrigation water for agricultural land could also be of significant use, especially for famous vineyards and olive groves. With the exception of the mentioned supply sites, there are some smaller springs and *vruljas* (submerged springs) on the island. The most important of these are a few springs in Komiža Bay and one strong periodical *vrulja* zone in Kut, which is part of the Vis settlement (Figure 4). There are also a few boreholes in karst poljes (large flat plains in karst, usually covered by Quaternary sediment); however, due to a relatively low yield, these have never been put to public water supply use.

The features described above make the island of Vis an extraordinary terrain for research regarding (i) the seawater–freshwater relationship in the karstified underground, and (ii) sustainable karst island aquifer management.

With an area of 89.7 km^2 and a coast length of 84.9 km, Vis is the ninth largest Adriatic island [17]. The topographic relief is comprised of three hilly chains separated by two valleys. The northern valley is relatively narrow and tectonically predisposed, and is the location of the island's most important water supply source: the Korita pumping site. The

southern valley is wider and consists of well-developed karst poljes, where the maximum thickness of Quaternary sediments has been determined to be at least 45 m [18]. The highest peak on the island is Hum (587 m above sea level (a.s.l.)), which is close to Komiža in the western part of the island. The geological structures and relief strike in a west–east direction (the so-called Hvar strike), which differs from that of the majority of the Dinaric karst, as these usually strike in a northwest–southeast direction (termed the Dinaric strike) (Figure 4).

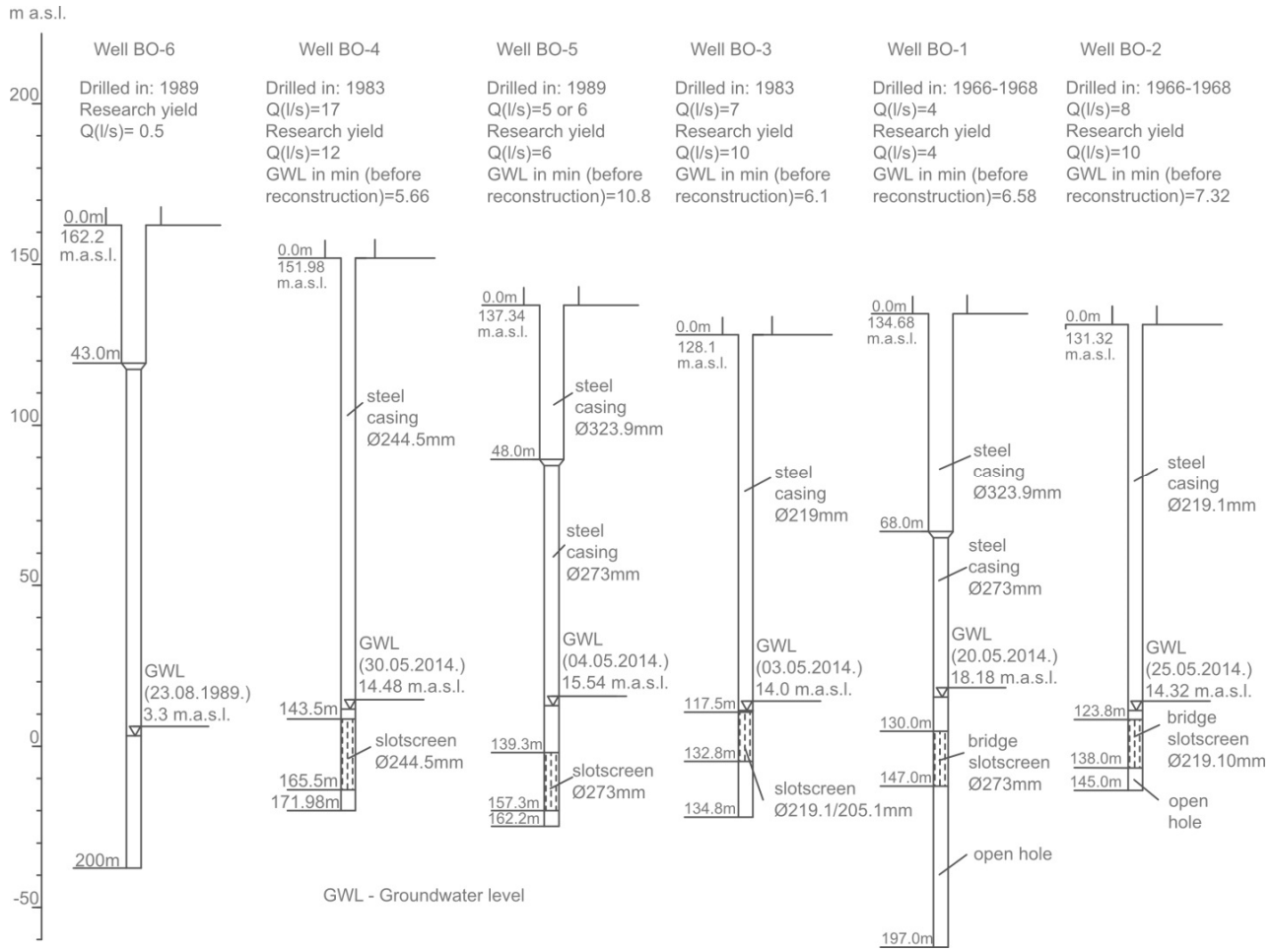

Figure 3. Profiles of the Korita wells based on a reconstruction using available data for basic parameters.

The climate of the research area can be classified as: (i) group: temperate/mesothermal (C), (ii) type: Mediterranean climate (Cs), and (iii) subtype: Mediterranean climate with dry and hot summers (i.e., an olive climate, Csa) [20]. The annual precipitation is relatively low, with a highly seasonal distribution, whereby the majority of rainfall occurs during the cold part of the year. Many climatologists, therefore, tend to consider this climate to be sub-humid when taking into account the ratio between the amount of water required for potential evapotranspiration and the water available from precipitation [20,21]. The average annual precipitation is 600–700 mm in the coastal areas, 700–800 mm in the inner island area, and 800–900 mm in the highest hills in the western part of the island. The average annual air temperature varies between 16 and 17 °C in the coastal area, 14 and 16 °C in the inner island area, and between 13 and 14 °C in the highest hills in the western part of the island. Air temperatures are highest during July and August and lowest in January [22]. In a newer study [23], there was a bulk analysis of climate variations on Komiža station, which is representative of the island of Vis (neglecting differences within the island, as no other stations were analyzed). The absolute minimum and maximum annual air temperatures were −1.12 °C and 35.01 °C, respectively, and the mean annual

air temperature was 16.71 °C, while the average annual precipitation for the station was 792 mm.

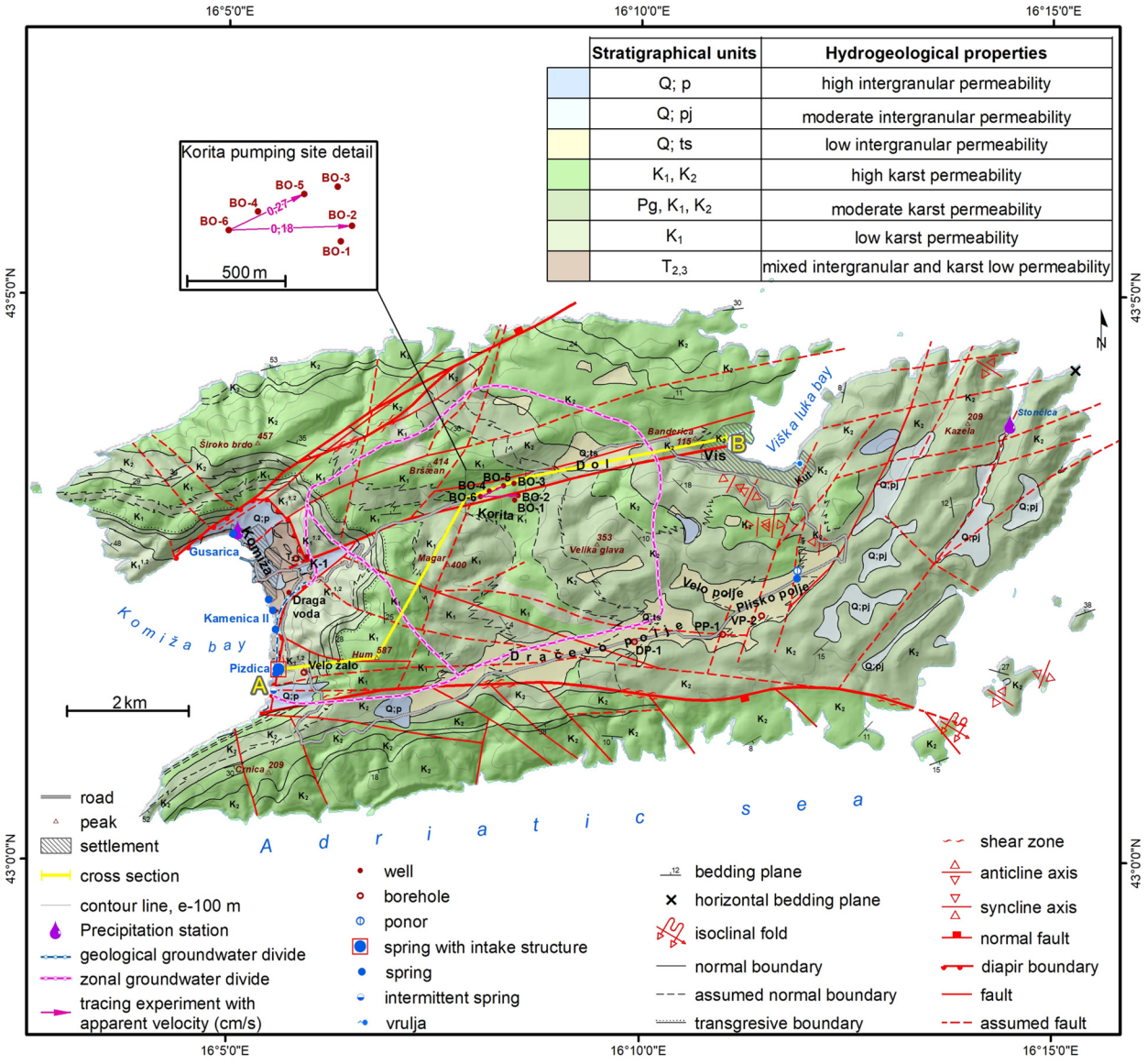

Figure 4. Hydrogeological map of Vis Island (based on the geological map by Korbar et al. [19]).

The geological framework of the Croatian Dinaric karst region has been described in numerous published papers; however, the geological evolution of the region is still a matter of debate and fundamental research [24–28]. The lithological composition of the rocks on Vis Island is summarized in the new geological map of the island [19]. Karst poljes were added from older geological maps [18,29,30], as well as some other features that are important for the local hydrogeological map (Figure 4). The rocks on the island have been grouped into five hydrogeological members [16]:

- Almost impervious rocks are those of the volcanic–sedimentary–evaporitic (VSE) complex of Komiža Bay (known as Komiža diapir), which is dated as Middle to Late Triassic (T_2^2 to T_3^1) according to recent research [19,31,32]. Several lithostratigraphic formations and members were schematized together to develop a hydrogeological map. The lithological compositions of single formations within this complex vary, and contain andesites, siltites, tuffites, marls, dolomites, gypsum, dolomitic-gypsum breccia (Figure 5c), and volcanic agglomerates (Figure 5d). Collectively, they function as a hydrogeological barrier; hence, only a small amount of groundwater flows towards

the coastal springs in the beach regions of Komiža Bay via highly fractured and superficially weathered zones.

- Low permeability carbonate rocks are mostly well-bedded dolomites of the Lower Cretaceous period (K_1). These rocks are spatially connected to the VSE complex as a narrow zone and mostly reinforce their barrier function. Still, these dolomites are fractured and even karstified to a certain extent, and groundwater can flow through significant fracture and fault zones; for example, the Pizdica spring occurs at one of these (Figure 4). The contact with the VSE complex is diapiric (practically a fault).
- Moderate permeability carbonate rocks are the most important hydrogeological unit, as they are permeable enough to allow groundwater infiltration, accumulation, and flow, but are not too permeable to allow the excessive penetration of seawater into the island's aquifer. Due to the presence of dolomitic and dolomitized rock mass, and its characteristic weathering into sand-like sediment, this material fills in most of the karst and fracture voids within this rock mass [16], thereby reducing its permeability. This hydrogeological member consists of several formations and members. Lithologically, these are laminated and bedded limestones with dolomitic beds/interbeds, bedded dolomites, and even some dolomitic breccias in some places. Stratigraphically, they are of the Cretaceous age (K_1, K_2; from Barremian to Cenomanian).
- High permeability carbonate rocks are highly karstified (mostly Upper) Cretaceous limestones (K_1, K_2) situated in two coastal belts: one in the north and one in the south of the island, although some exist in a few belts in the central part of the island. The high permeability and wide spatial distribution of the coastal belts make them completely worthless from the perspective of fresh groundwater. Their position next to the sea results in the over-salinization of groundwater that either flows from the central part of the island or infiltrates directly into them. High permeability limestone rocks in the central part of the island (Figure 5a,b) form the most important part of its aquifer, which is perfectly situated and protected from significant seawater intrusion, either by the VSE barrier or the surrounding dolomitic rocks. The lithological composition varies from thin- to thick-bedded limestones that are rarely laminated.
- Quaternary deposits encompass several types of rocks and soils that have variable hydrogeological roles. Terra rossa (ts) is spread all over the island as a thin and discontinuous cover, and as a thicker layer mixed with rock fragments in karst poljes (Figure 5e). These deposits decrease infiltration, and in the thickest parts in the poljes, they act as a local hydrogeological barrier. Aeolian sands (pj) are present in a few eastern karst poljes and colluvial sediments (p) in Komiža Bay. These deposits do not have hydrogeological importance in the context of water supply.

Aside from the diapiric structure, there are three main fault zones on the island [19], which basically run subparallel to the structural axis of the island. They are probably secondary faults connected to the so-called Vis fault, which is situated off the island's southern shore [25]. The Korita pumping site is located in the Komiža–Vis fault zone; karst poljes have developed as a belt along the southern fault zone, and even the Pizdica spring occurs exactly at the intersection of the latter fault zone and the diapiric structure (Figures 2A and 4). Within the rock mass and between the main fault zones, there are several lower-order faults, as well as joints and fractures of the local structural setting. All of these tectonic features enable the infiltration of rainwater and the gradual karstification of the rock mass.

Except for one strong *vrulja* in the town of Vis (in the locality of Kut) and a few springs in Komiža Bay, there are no notable springs or *vruljas* along the majority of the coastline. Most of the groundwater discharge is diffuse and occurs through a network of joints and cracks in highly karstified limestones of the Upper Cretaceous, which comprise the northern and southern coasts. The groundwater outflow in these regions is therefore mostly hidden from observation. These limestones are highly permeable, and seawater penetration in their zone is practically complete, such that fresh groundwater mixes with seawater in the two narrow coastal belts. A simple water balance calculation was performed by Terzić [16], but

included the following issues: (1) there are unknown boundary conditions in the mixing zone; (2) it was impossible to observe the outflow in the major part of the coastline, except in concentrated zones, including wells, springs, and *vruljas*; (3) the average annual infiltration (all over the island) was estimated to be 40% of the precipitation, based on similar karst regions and rock types, and was calculated using the simple Turc's expression [33]. The outflow was calculated for known sources, such as the Korita wells and Pizdica spring, and was estimated for observable springs and *vruljas*. After half a century of pumping, this situation is considered to be "natural" and balanced over the longer term, such that the outflow and inflow should be equal on average. Even though the precipitation on Vis Island is quite low, Terzić [16] concluded that >99% of infiltrated water flows out at diffuse discharge zones along the coastline, whereas <1% is extracted for water supply.

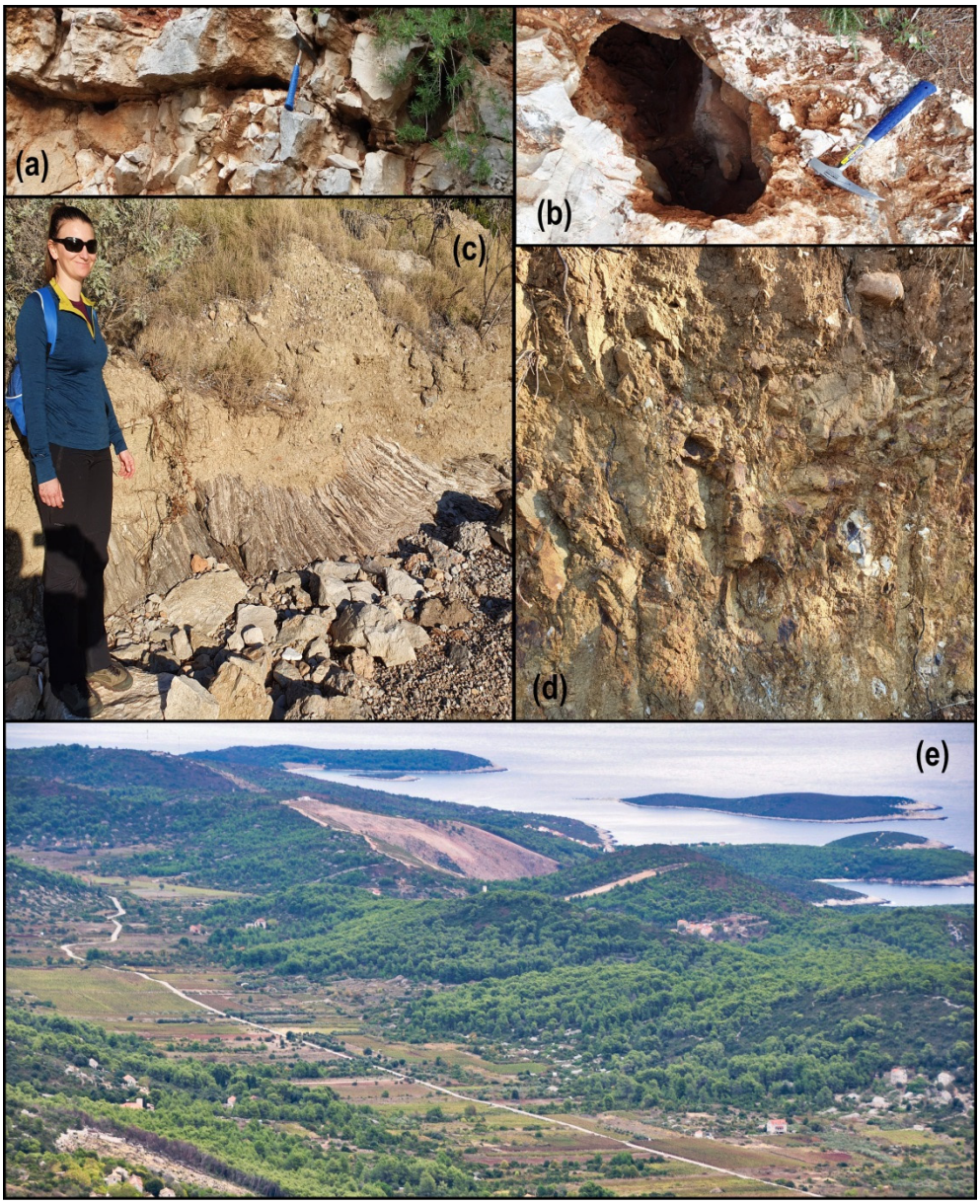

Figure 5. Specific features on Vis Island: (**a**) typical appearance of limestone rock mass in the central part; (**b**) karst conduit in the immediate vicinity of the Korita pumping site; (**c**) gypsum and anhydrite in the VSE complex near the Pizdica spring; (**d**) weathered volcanic agglomerate in the VSE complex near the Kamenice spring; (**e**) panoramic view of karst poljes in the southern tectonic valley.

The seasonal variation of the groundwater level (GWL) (minimum in August and September, maximum in January) in operational wells (by neglecting the effects of pumping as the natural state can no longer be established) is a little over 4 m. Aquifer recharge usually starts in October after the lowest annual levels, and continues mostly until March. In the receding limbs of GWL curves, there are some outlier peaks in reaction to rapid recharge after heavy rainfall [16]. Infiltration in the close vicinity of operational wells is very fast, especially through highly permeable limestones. Hydrochemical analyses of groundwater samples taken from the wells in Korita have proven that these wells extract water from the same karst aquifer. This aquifer is very heterogeneous, and consists of voids of different scales that are interconnected by fractures, cracks, and even karst conduits (Figure 5a,b). Similar examples have been recorded in comparable environments [34–48].

3. Materials and Methods

In addition to the methods described in detail below, the following general geological and hydrogeological methods were also used in this research: (1) the reinterpretations of existing small-scale maps (1:50,000 and 1:100,000), with special attention given to aerial image interpretations in order to delineate karst poljes; (2) analyzing large scale (1:5000) geological and hydrogeological maps of the immediate hinterlands of wells and springs; (3) interpretation of existing GWL data (provided by the water supply company); (4) common interpretation of all results, including GIS (geographic information system) visualization. In combination with geological mapping at different scales, hydraulic parameters were calculated using the relatively simple Thiem's equation [49], while the tracer test provided a better insight into groundwater velocities and dynamics, and hydrochemical data were a very useful tool for determining groundwater facies and tracking the extent/direction of salinization.

Due to the high, locally extreme heterogeneity and anisotropy of Dinaric karst aquifers, numerical modeling *sensu stricto* is hardly applicable. Still, hydraulic conductivity can be calculated, with a clear notation of the limitations. The method for this calculation depends primarily on the scale of the research [50,51]. For this study, at a local to sublocal scale, pumping test data interpretation using Thiem's expression [49] was chosen. However, the achieved hydraulic conductivity value should be considered to be within an order of magnitude (higher precision would not be appropriate for this parameter). Some hydraulic laws should be applied in karstic terrains, whereby many experiences from different karst regions have yielded similar results [2,35,36,41,42,51–53]. The methods for calculations should be chosen with respect to local terrain characteristics and, more importantly, the scale of research. For the karst aquifer on Vis Island, hydraulic conductivity values were calculated for the successive set of stationary states. Thiem's equation was applied based on data from pumping tests undertaken in the 1960s, 1970s, and 1980s, when the wells were being constructed [16].

A tracer test was performed with two basic purposes: (1) to obtain accurate data of the groundwater velocity in order to delineate SPZs, and (2) to delineate the groundwater divide between the Korita and Pizdica catchment areas. As no appropriate natural landform for dye injection exists in the research area, a borehole in Korita was used (well BO-6), which is situated westwards from the other wells and has never been operational. Sodium–fluorescein was used as a tracer (Figure 6a), which was monitored in situ at two sites (Pizdica and well BO-2) using GGUN-FL loggers (detection limit 0.025 µg/L). From these sites and two other locations (well BO-5 and Kamenice spring), samples were collected for laboratory analyses of tracer concentrations, which used a spectrofluorometer LS-55 (PerkinElmer) (detection limit 0.002 µg/L). The tracer test is the most commonly used tool for the delineation of catchment areas in karst terrains [51,54–56] because topographic and hydrogeological groundwater divides rarely correspond.

Figure 6. Activities performed in the scope of research: (**a**) tracer test (dye injection); (**b**) water sampling at Kamenice spring.

After collecting blank samples, the tracer test commenced by injecting a dye (0.4 kg of Na–fluorescein) on 22 May 2012, with 10 m^3 of water added to wash out the injection point and ensure that dye reached the aquifer. The general idea was to imitate the natural flow conditions as much as possible. There was considerable rainfall on the day of the tracer test. This ensured a slightly higher groundwater gradient and the imitation of natural conditions after heavy rainfall, which was, in fact, helpful for delineating the SPZs.

Groundwater and spring water samples for hydrochemical analyses were collected during two campaigns by previous researchers (Figure 6b): (1) during winter 1999 and (2) during summer 2000 [16,38]. From each location, one sample was taken at the hydrological minimum (in 2000) with respect to GWL, and one close to the maximum (in 1999). The electrical conductivity (EC), pH, and temperature (T) were measured in situ using a HACH probe (CO 150 Conductivity meter). The concentrations of chloride, sulfate, and bicarbonate anions were measured in the Croatian Geological Survey's laboratory with a spectrophotometer DL/2010 (HACH). Cations and metals were analyzed using ion chromatography plasma–mass spectrometry (ICP–MS) using laser ablation at high resolution at ACTLABS in Ancaster, ON, Canada. For the period 2010–2012, chloride concentration data were obtained from the water supply company, and the analyses were performed by the Croatian Institute of Public Health in Split.

Hydrochemical facies were determined based on the results of two water sampling campaigns using a Piper diagram [57,58]. Basic ion composition, and especially the EC value and chloride anion concentrations, are important tools for mixing zone estimations in such aquifers [59] (although not the only one, e.g., ^{18}O or trace elements could be used as well). The seawater percentage (f_{sea}) was calculated based on the conservative mixing method described in detail in Appelo and Postma [60]. The basic formula of the calculation is given by Equation (1), and finally in Equation (2):

$$m_{i,mix} = f_{sea} \times m_{i,sea} + (1 - f_{sea}) \times m_{i,fresh} \quad (1)$$

where m_i is the concentration of ion "*i*" in mmol/L, f_{sea} is the seawater percentage in the mixture, and subscripts "*mix*", "*sea*", and "*fresh*" represent mixture, seawater, and freshwater, respectively.

After including known values and simplifications, the final formula for calculating the seawater percentage is [16,60]:

$$f_{sea} = \frac{m_{Cl^-,sample}}{602}, \quad (2)$$

where f_{sea} is the seawater percentage and $m_{Cl^-,sample}$ is the concentration of Cl^- ion in the sample.

It is important to note that a Cl^-_{sea} of 602 mmol/L represents the value for average seawater salinity of 38‰. The simplification also presumes that, in rainfall, the concentration of Cl^- can be considered to be zero. The resulting f_{sea}, or the seawater fraction, comprises both the underground penetration of the seawater wedge, and the amount of previously sprayed particles all over the island's surface, which are washed out during the infiltration of the rainwater. Both values originate from seawater, and no other sources were found, or could be presumed, for this aquifer. These values are considered to be close to reality, although resulting from several presumptions, and are therefore taken as rough estimations.

4. Results

4.1. Groundwater Flow: Hydraulic Conductivity and Tracer Test

The results of the hydraulic conductivity calculations obtained by Terzić [16] (Table 1) agreed with the existing values cited in eminent publications for limestones and dolomites [57]. Since the pumping tests were carried out from the 1960s to 1980s, without the calculation of hydraulic parameters, only these values could be calculated using Thiem's equation (Equation (3)):

$$s^* = \frac{Q}{2\pi T} ln \frac{R_o}{r_z} \quad (3)$$

where s^* represents the equivalent drawdown (as an approximation, it can be considered to be a total drawdown in phreatic karst aquifers), Q is the pumping rate, T is the transmissivity, and R_o and r_z are the assumed radius of the well influence and the radial distance from the pumping well, respectively. Since these last two values are within the logarithm, they can be approximated, because the error is limited to an order of magnitude in the result.

Table 1. Calculated Values of Transmissivity (T) and Hydraulic Conductivity (K) on Vis Island.

Parameter	Karst Poljes Rock Mass under Quaternary Sediments Infilled with Secondary Material			Dolomites and Dolomitic Limestones	Highly Karstified Limestones
	Velo Polje VP-2	Plisko Polje PP-1	Dračevo Polje DP-1	K-1	BO-5
T (m^2/s)	$(3.5–4.5) \times 10^{-5}$	6×10^{-5}–1.2×10^{-4}	$(2.6–3.1) \times 10^{-5}$	$(3.0–4.6) \times 10^{-4}$	9×10^{-4}–2.3×10^{-3}
K (m/s)	9.5×10^{-7}–1.2×10^{-6}	$(1.5–3.5) \times 10^{-6}$	$(1.0–1.5) \times 10^{-6}$	$(1.0–1.2) \times 10^{-5}$	$(2.3–4.9) \times 10^{-5}$

Note: Taken from Terzić [16].

Measured daily rainfall in the vicinity of the dye injection point was 88 mm, which is extremely high for the research area and was significantly higher than that at the Komiža and Stončica meteorological stations (4.4 mm and 10 mm, respectively) managed by the Croatian Meteorological and Hydrological Service. Therefore, the groundwater gradients in the Korita catchment were higher than usual, representing naturally high GWL conditions, which was a favorable situation for obtaining good data for determining groundwater velocities. Ordinarily, groundwater gradients on the island are very low, and it would have taken much longer to record the arrival, peak, and disappearance of the tracer.

The dye was recorded in two observed wells in Korita (BO-2 and BO-5; Table 2). Wells BO-1 and BO-2 were pumped during the first ten days of the test, and BO-5 was pumped only shortly during the groundwater sampling. At the Pizdica and Kamenice springs, no tracer was detected within two months of sampling.

The dye tracer results from the in situ measurements and those from the laboratory analyses were in complete accordance with well BO-2 during the time that the field logger was in place (i.e., the first few days of sampling). Figure 7 presents curves based on the laboratory analyses for the entire sampling period for both of the monitored wells at the Korita pumping site. Precipitation data taken from two climatological stations are also

plotted. As mentioned, no dye was identified during the entire monitoring period at other monitored localities (Pizdica and Kamenice springs).

Table 2. Main Parameters Related to Dye Occurrence in Two Wells in Korita.

Well	Distance from BO-6 (m)	Time, First Occurrence (Hours)	Apparent Velocity (cm/s)	Maximum Concentration (μg/L)	Time of Maximum Concentration (Hours)	Apparent Velocity for Maximum Concentration (cm/s)
BO-2	626	96.6	0.18	0.056	193.66	0.09
BO-5	426	43.92	0.27	5.766	199.08	0.06

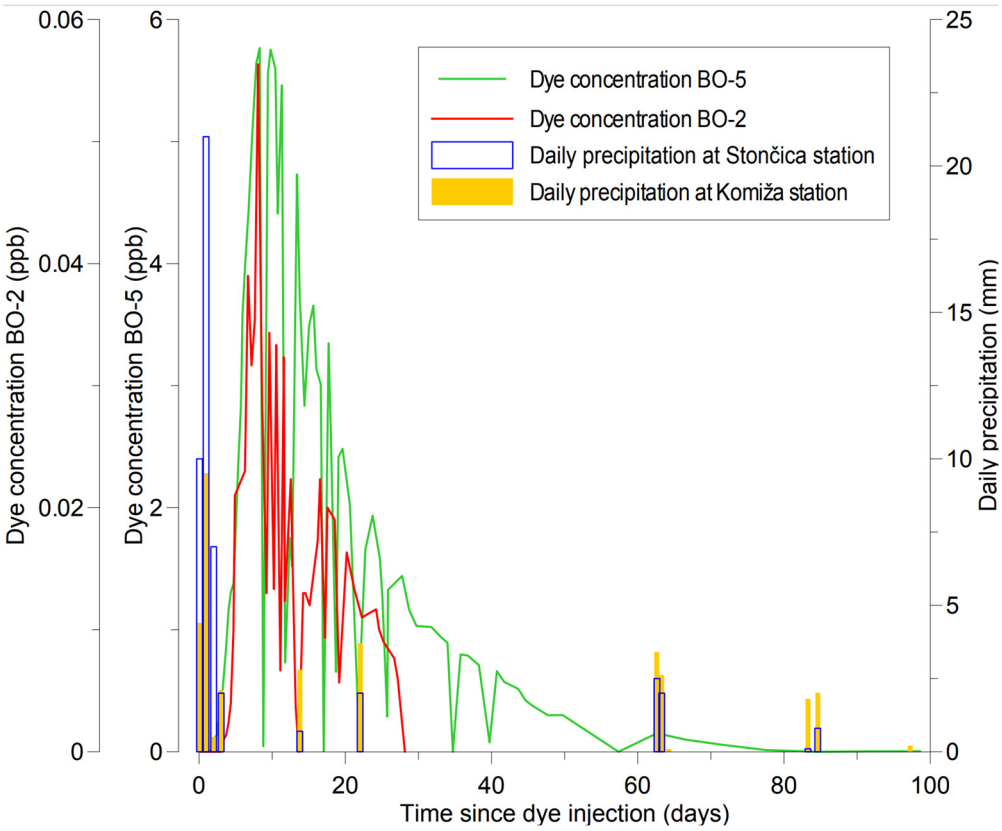

Figure 7. Dye curve for wells BO-2 and BO-5 in Korita and daily precipitation during the test.

Heavy rain at the beginning of the tracer test raised the hydraulic gradient, which increased the tracer velocity through the aquifer. The main tracer direction was towards well BO-5, which had a maximum tracer concentration of two magnitudes greater than the well BO-2. The pumping of the wells was constant only during the first ten days of the tracer test. After that, wells were pumped periodically according to the water supply needs, so the tracer concentration curves reflect that. Despite these disturbances, the tracer concentration curves exhibit a typical shape for karstic aquifers, but with an atypically long duration. The tracer was still present in well BO-5, distanced only 426 m from the injection site, after nearly 100 days.

4.2. Hydrochemical Properties

The two sampling campaigns in 1999 and 2000 provided a good insight into the hydrochemical properties of the aquifer (Table 3). The corresponding Piper diagram (Figure 8) illustrates the hydrochemical facies of the analyzed water samples. The data on GWLs during these campaigns were measured manually and represented monthly average levels during pumping. For other features, levels were not being measured at that time, while for some they were estimated.

Table 3. Basic ion composition of the spring and wells on Vis Island.

	Location	GWL (m a.s.l.) m = measured e = estimated	EC (µS/cm)	T (°C)	pH	HCO_3^- (mg/L)	Cl^- (mg/L)	SO_4^{2-} (mg/L)	NO_3^- (mg/L)	Na^+ (mg/L)	K^+ (mg/L)	Ca^{2+} (mg/L)	Mg^{2+} (mg/L)
June 2000	BO-2, Korita	4.45 (m)	1192	16.6	7.09	320	92	20	0.5	38	1.39	91	27
June 2000	BO-3, Korita	4.40 (m)	1343	16.9	7.11	361	104	23	0.6	39	1.34	109	29
June 2000	K-1	no data	1024	18.2	7.22	331	50	34	0.2	33	2.5	76	30
June 2000	Dragevode	no data	876	18.1	7.2	210	42	71	0.2	18	0.97	55	33
June 2000	Velo Žalo	no data	1286	16.9	7.6	199	214	28	0.1	127	5.7	35	34
June 2000	Gusarica	0.50 (e)	1406	21.9	7.84	245	84	290	2.2	38	2.36	168	32
June 2000	Kamenice	1.50 (e)	1818	21.2	7.87	331	82	240	7.5	50	1.7	146	51
June 2000	Pizdica	1.00 ()	2488	17.1	8.2	298	418	140	0.2	241	9.66	90	47
December 1999	BO-2, Korita	5.22 (m)	866	15.2	7.02	214	82	20	0.3	36	1.3	45	28
December 1999	BO-3, Korita	5.30 (m)	860	16.5	7.04	188	98	24	0.6	37	1.2	50	26
December 1999	K-1	no data	954	17	7.2	288	40	25	0.1	22	2.59	70	24
December 1999	Dragevode	no data	740	13.7	7.04	164	44	72	0.3	20	0.91	35	34
December 1999	Velo Žalo	no data	1552	16.6	7.88	156	290	24	0.2	153	5.14	49	34
December 1999	Gusarica	0.50 (e)	1086	17.3	7.92	145	76	170	2.6	34	1.83	83	30
December 1999	Kamenice	1.50 (e)	1084	17.5	7.98	332	112	160	7.1	49	1.87	53	47
December 1999	Pizdica	1.00 (e)	2148	16.4	8.21	92	530	90	0.4	245	9.31	61	46

Note: Data from Terzić [16].

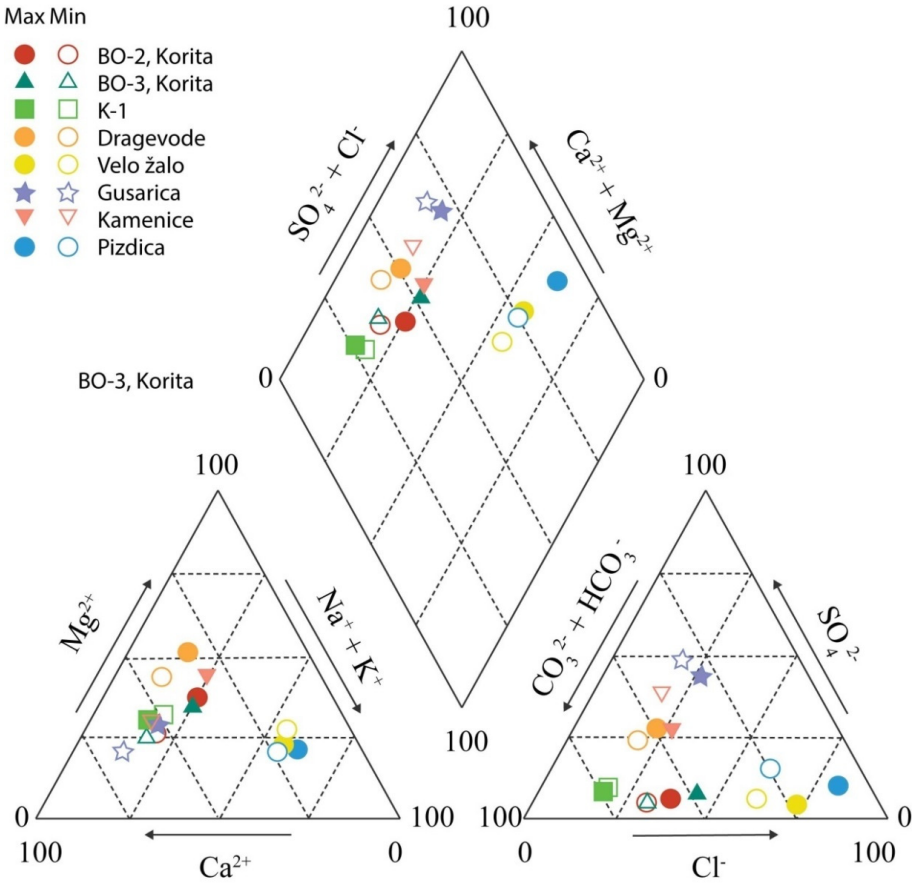

Figure 8. Piper diagram of groundwater samples from Vis Island. "Min" and "Max" represent the low GWL in June 2000 and the high GWL in December 1999, respectively.

For the majority of water samples, no dominant type could be determined in either season. This is congruent with the composite structural fabric of the island, which comprises different rock types and structures that cause variable seawater intrusion into the island's

aquifer. Moreover, seasonal effects can cause a differentiated dissolution of carbonate, sulfate, and silicate rock minerals, thus leading to slight changes in hydrochemical facies.

The hydrochemical situation was unequivocal at two sampling locations. Water from the Pizdica coastal spring belonged to the Na–Cl facies in both hydrological seasons due to its proximity to the sea. The spring water at Pizdica is part of a mixing (transition) zone between fresh groundwater and seawater, and is similar to that at the Velo žalo borehole, which is situated in the immediate hinterland of the spring. Although this is clearly a discharge zone, it is also a region where the mixing zone is moved further inland due to the narrow extent of the VSE barrier of the Komiža diapir (Figure 4).

Apart from these two cases, there were only three more instances for which the dominant hydrochemical facies could be defined: (i) at borehole K-1, which showed a clear Ca–HCO_3-type water during both hydrological conditions, and (ii) at boreholes BO-2 and BO-3 during the minimum GWL. The coastal spring at Gusarica, which is located in the part of Komiža where the VSE complex is wider, displayed Ca-mixed-type water in both seasons, but with a tendency towards a Ca–SO_4 type due to the dissolution of gypsum and anhydrite. The effect was more pronounced during the hydrological minimum, when it could also be observed, to a lesser extent, at the Kamenice spring. Higher concentrations of sulfate ions in the water of the springs at Pizdica, and much more at Gusarica and Kamenice, suggest the high influence of sulfate rocks from VSE complex dissolution. As stated, only gypsum and anhydrite rocks are present in the evaporitic sequence, and no halite was ever recorded. It means that chloride anions originate from seawater, either as a result of underground penetration, or as particles sprayed by wind and accumulated on the island's surface during the dry season, and washed out by rain.

Newer data for chloride concentrations, from occasional measurements at the Korita wells during 2010–2012, were slightly higher than those during 1999–2000 (Figure 9). Although the measured concentrations were still significantly below the maximum allowed concentration for drinking water, the trend is definitely negative from the water supply perspective. It is also indicative that, during the higher GWLs, chloride concentrations were lower, and vice versa. However, it should be emphasized that the pumping rates in the Korita wells increased by ~30–40% between 1999–2000 and 2010–2012, and that both datasets are far too short to draw any general conclusions.

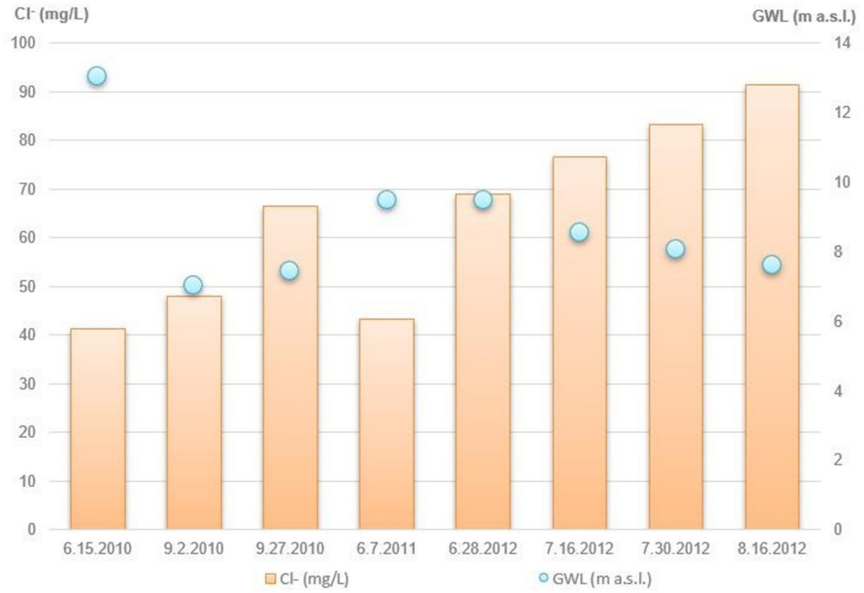

Figure 9. Chloride concentration and GWL data for boreholes at Korita from 2010 to 2012.

The f_{sea} was calculated using the chloride anion as a conservative (nonreactive) constituent of the mixture, as described in Section 3. The results are presented in Table 4.

Table 4. Seawater percentage in spring and groundwater samples from Vis Island.

Locations	December 1999		June/July 2000	
	m_{Cl} (mmol/L)	f_{sea} (%)	m_{Cl} (mmol/L)	f_{sea} (%)
BO-2, Korita	2.31	0.38	2.60	0.43
BO-3, Korita	2.76	0.46	2.93	0.49
K-1	1.13	0.19	1.41	0.23
Dragevode	1.24	0.20	1.18	0.20
Velo žalo	8.18	1.36	6.04	1.00
Gusarica	2.14	0.35	2.37	0.39
Kamenice	3.16	0.52	2.31	0.38
Pizdica	14.95	2.48	11.79	1.95

Note: Data from Terzić [16]; m_{Cl} is the concentration of chloride ion in mmol/L, and f_{sea} is the seawater percentage in the mixture.

5. Discussion

The establishment of SPZs for the protection of karst catchments differs from one case study to another [61]. The Dinaric karst differs from region to region and can be distinguished into many sub-types [62]. Island aquifers definitely differ from the aquifers in continental Dinaric mountainous areas; hence, the research approach in this study was adjusted accordingly. In Croatian karst terrains, four protection zones can be defined [63–65] based on two criteria: (1) the groundwater apparent velocity, and (2) the time required for water to reach the extraction site from the infiltration point. The first zone is the water extraction site itself, which must be fenced. The second zone is connected via the main drainage and preferential flow paths. The third zone covers the area surrounding the preferential flow paths, as well as highly karstified and permeable rock mass with an established connection to these zones. The fourth zone spreads to peripheral parts of the catchment and terrain formed by a low permeable rock mass. In most cases in Dinaric karst, the fourth zone covers an entire catchment area, as is the case in the present study. This model of karst groundwater protection was established in the 1990s [63,66]. Due to these adopted principles, groundwater tracer tests represent the most important method for delineating SPZs in Dinaric karst areas where the apparent groundwater velocity data are very important. If there are no karst features suitable for tracer tests (e.g., ponors, open discontinuities, caves, or pits) within the boundaries of the investigated terrain, then boreholes should be used, as was the case for this study.

On a regional scale, the carbonate aquifer on Vis Island can be considered to be a more or less continuous medium, with a gradual transition between several hydraulically different types of rock mass (Table 1). Therefore, even though this is a karst aquifer, the hydrogeological rules described by Darcy's law can be assumed to obtain an approximation (within an order of magnitude). In areas with poorly developed Quaternary deposits (outside of the karst poljes), the calculated mean hydraulic conductivity (K) varied from 1.1×10^{-5} m/s near borehole K-1 (Komiža) to 3.6×10^{-5} m/s in Korita (i.e., the range was within the same order of magnitude). In the karstic rock mass beneath karst poljes, karst features and tectonic joints are infilled by secondary material, which causes a decrease in the mean K to 5×10^{-6} m/s (Table 1). This corroborates the existence of the presumed barrier and groundwater divide in this area, where K values are an order of magnitude lower than those near Korita, and GWLs are the highest.

The reinterpretation of old pumping test data suggested that an impermeable layer can be presumed to be at the depth of a few tens of meters below sea level (b.s.l). Even though karstification occurred below the current seawater level, and even below what would be presumed to be the seawater level below the island's GWL according to the Ghyben–Herzberg law [67,68], the interpretation indicated that the permeability and K decrease with depth would become almost negligible a few tens of meters below sea level. Although there are karst features below this zone, such as stagnant conditions or a very slow groundwater flux, and the presence of dolomitic or dolomitized rocks, both

resulted in the infilling of karstic and tectonic voids following the weathering of dolomite to the sandy–fine-grained material [16]. This process was noted in all areas, but to the greatest extent in the karstified rock mass below karst poljes, where terra rossa provides additional fine-grained material for infilling. All interpretations pointed to the fact that in this aquifer, flow through the rock mass prevails, which is atypical of karst conduit flow. The pumping test results allowed the differentiation of three different rock mass types (Table 1): (1) highly "infilled" rock mass below karst poljes, (2) mostly dolomitic zones, and (3) karstified limestones, i.e., karst aquifer sensu stricto. It was also noted that the K values gradually decreased with drawdown, which further supports the previously described phenomenon of infilled joints in the rock mass. The pumping test results indicated that the karst poljes, along with the karstic rock mass below them, act as a barrier to groundwater flow; hence, they also protect the central island karst aquifer from southward seawater intrusion. The geology of the western boundary is clear and is represented by the VSE complex barrier. The existence of these barriers to seawater intrusion from the two sides is a geological precondition for the formation of such a high-quality aquifer on this relatively small karstic island [16]. For example, a similar pumping site in a karst polje in the central region of another remote island in southern Croatia, Lastovo, constantly yields brackish water; thus, a desalination plant had to be installed [15,69].

The results of the tracer test revealed apparent groundwater velocities of 0.18 cm/s (well BO-2) and 0.27 cm/s (well BO-5) (Figures 4 and 7; Table 2). Well BO-5 is situated in the tectonic valley in line with the dye-injection well (BO-6). Well BO-2 is a little outside of that line, which suggests that the groundwater velocity in the direction parallel to the main groundwater flow paths is the highest, whereas it is much lower perpendicular to the main flow paths (Figure 4, detail). This indicates a certain heterogeneity and, in particular, hydraulic anisotropy, which is typical for the Dinaric karst. As the central island karst aquifer is open to seawater intrusion from the north and the east (as mentioned, barriers exist from the western and southern sides), this emphasized anisotropy means that the eastern salinization direction is more dangerous due to a higher K in that direction (Figure 10).

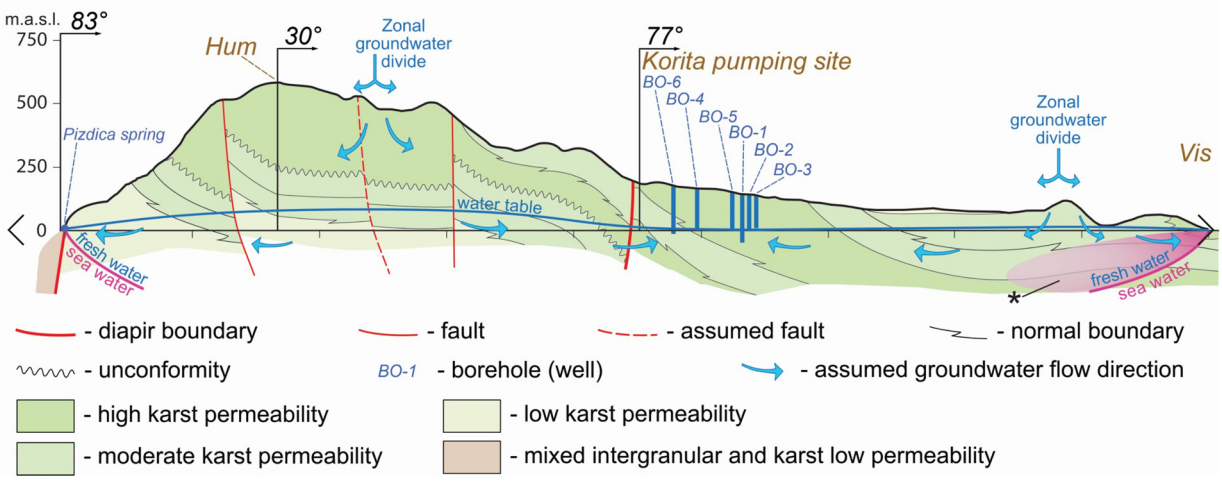

Figure 10. Schematic hydrogeological cross-section from the Pizdica spring, over the island's highest peak, and through the region of the Korita wells (BO-6 to BO-2) towards Vis town in the east. The legend and position of the cross-section are shown in Figure 4. * Indicates the most probable direction of the seawater wedge towards the Korita wells if the freshwater level drops in the future (either because of increased pumping rates or lower recharge due to climate change influences).

The tracer test also provided new insights regarding the delineation of catchments in the vicinity of the Korita wells and the Pizdica spring. During the first few weeks of sampling, samples were also taken from the BO-6 well to check the dye dispersion. The dye tracer was present at a high concentration and decreased slowly, thus implying that dispersion was very slow, and that groundwater flow predominantly occurred in rock mass

fractures and joints, and not via karst conduits [70]. This supports the assumption of the first phase of research, when the K calculations for the Korita wells suggested the presence of this type of aquifer, whereby karst voids and conduits are not mutually connected and do not act as typical Dinaric karst aquifers. The dye concentration curve (Figure 7) exhibits a local minimum that could either refer to (1) corrupted samples, (2) periodic heavy rainfall with fast infiltration components, or (3) an irregular pumping regime (which is most probable). Only during the first ten days following the dye injection did we arrange with the water supply company to use the two most distant wells (BO-1 and BO-2) continuously with a steady pumping rate. The dye was observed to have spread in a cloud-like manner all over the aquifer from injection well BO-6, whereby the groundwater flow was generally eastwards, following the main faults in the structural setting. Therefore, the presumption is that the apparent groundwater velocity in the main flow direction (approximately from west to east-northeast) is 0.27 cm/s (towards well BO-5). The velocity towards well BO-2 was 0.18 cm/s, which is a combination of the main direction velocity (0.27 cm/s) and a much lower velocity perpendicular to the main fault/groundwater flow direction. High precipitation at the tracer test beginning has highly disturbed the groundwater gradient between the BO-6 and pumped wells. According to rough data obtained from the water supply company, the gradient was approximately 0.004 at the beginning of the tracer test, but due to significant rainfall and infiltration in the next few days, levels were rising in the whole aquifer, including the two pumped wells. The natural groundwater gradient in this part of the aquifer is directed from the highest hills (Hum and others, close to Komiža Bay) towards the town of Vis (i.e., from west to east-northeast); however, it is ordinarily quite low and was highly disrupted by heavy rainfall during the first days of the tracer test. By neglecting the irregularities that are attributed to the pumping regime variations after the first 10 days, and/or possibly a human error, the curves in Figure 7 are quite regular and too elongated for typical karst aquifers. These facts suggest that there are no interconnected karst conduits and that most of the groundwater flow occurs within the rock mass. Accordingly, the tracer test validated the conclusions drawn from the reinterpretation of the old pumping test results in this area.

The fact that the dye injected into the BO-6 well did not appear at any of the monitored localities on the western coast of the island (Pizdica and Kamenice springs) proves that there is no groundwater flow from Korita toward the west. This means that the catchments of Korita and Pizdica are divided, and are not a single catchment, as previously hypothesized [16,38].

Another important aspect to consider is the amount of dye that was injected into the aquifer (i.e., only 0.4 kg). The maximum concentration of dye that reached the water supply wells was 5.77 µg/L, which is just below the level of visual detection. This optimal result was achieved owing to a detailed preparation that considered (i) the hydrological analyses and parameter calculations from previous research, (ii) the point of dye injection, and (iii) hydrometeorological forecasts. Had the dye been injected in a larger quantity, it would certainly have crossed the visual threshold, and water in the water supply system would have remained colored for a quite long time (as can be supposed from the elongated curves in Figure 7). Consequently, this situation was avoided given the timing being prior to the summer vacation season when the majority of tourists visit the island.

The hydrochemical data presented in Table 3 and Figure 8 suggest that the main direction of freshwater–seawater mixing is from the Pizdica spring towards the east. This direction is connected to some of the most important fault zones, but is fortunately localized in the southwestern area that is unprotected by the VSE complex barrier. The hydrochemical data fully corroborate the definition of the Korita and Pizdica catchment areas that were delineated on the basis of the tracer test and geological setting. For a more detailed analysis of the groundwater recharge and water circulation in the catchment area of other coastal springs in Komiža Bay, it would be necessary to undertake another tracer test and continuous hydrochemical monitoring. Although the data described here indicate the existence of a third catchment, which would include the springs at Gusarica and Kamenice

and the well at Dragevode, the data can only be considered representative for a specific minimum and maximum because no hydrochemical data were available for comparison.

In the central part of the island (i.e., Korita), water salinization was not recorded before the increase in pumping quantities during 2003–2007, while there are some indicators that suggest it has happened subsequently. Before the pumping rates increased (from 27 L/s up to 40 L/s), very low chloride concentrations in the Korita wells were considered to be a consequence of the tiny particles of seawater sprayed all over the island's surface by winds, which were then washed away during the rainy season to be infiltrated into the underlying aquifer. There are indications (Figure 9) that after 2007, a slight increase in the chloride concertation occurred during the dry season; however, this hypothesis would need to be explored more thoroughly once appropriate datasets are obtained.

Overall, it seems that mixing between freshwater and seawater is very limited during all seasons at all localities on Vis Island (Table 4). Two sets of samples showed significantly higher f_{sea}, namely, those from the spring at Pizdica and the borehole at Velo žalo, which is in accordance with their Na–Cl hydrochemical facies. These results also support the conclusions regarding the occurrence of seawater intrusion as a wedge under the discharge zone near Pizdica, as well as the hypothesis that chlorides in the samples from Korita mostly originate from wind-blown seawater spray that is washed out by rainwater. The possibility of a wedge-like seawater intrusion towards Korita (probably from the east, as hypothetically shown in Figure 10) represents a subject for further study. The phenomenon of additional chlorides from seawater spray can also be present in Velo žalo and Pizdica, which would explain why values are higher during the rainy season than in the summer. It could be a consequence of the fact that their (common) catchment is very steep below the island's highest peak, Hum, and oriented toward the predominant winds. This should also be more thoroughly studied in the future.

6. Conclusions

Based on previous and new data, a revised conceptual hydrogeological model of the groundwater system on Vis Island was conceived, as presented in the map and cross-section views in Figures 4 and 10. Practically no data for seawater intrusion in the Korita region (especially before 2007) corroborate the presumption of watertight (or very low permeability) deeper zones of rock mass at a few tens of meters below sea level. Quaternary sea-level changes in excess of 100 m caused much deeper karstification than would be expected according to the current sea level. On the other hand, there have been relatively low gradients and groundwater velocities during the last 5000 years, during which Vis has been an island (before that it was part of the mainland) [7,8]. These facts, combined with the lithological composition of dolomites that prevail in some parts of the inland area, have caused the infilling of tectonic and karst features, either by fine-grained material (dolomitic sandy material mixed with terra rossa) or by the calcification of voids.

The findings of this study collectively indicate that there is no freshwater lens on Vis Island, but rather a real karstic aquifer due to its favorable geological predispositions. Seawater penetrates the aquifer and forms a wedge under the freshwater, with the wedge length differing depending on the direction. The most significant zone of seawater intrusion is recorded on the western coast of the island, and is connected to the intersection area of a strong fault zone and the diapiric structure. Fortunately for the water supply, this intrusion is localized due to the barrier function of the VSE complex. According to all the available data, the wells in Korita may be at risk of seawater intrusion, mostly from the east or north. This wedge is quite irregular and penetrates the island much deeper in the main tectonic directions (i.e., main fault damage zones). On the other hand, if there is also a significant flux of fresh groundwater through these fault zones, then it is possible that the freshwater pressure maintains a balance with the seawater wedge. This presumption suggests that an early warning system for the Korita extraction site should be placed between Korita and the town of Vis (possibly also north of Korita), and its installation should be preceded by additional geophysical research, e.g., electrical tomography [71]. Such a system would be

more than advisable given the increasing irregularity in the precipitation regime, which is similar to globally observed climate change trends and their reflection on the Adriatic region [23,72]. Water balance calculations performed by Terzić [16] suggested that < 1% of the annually infiltrated water discharges from all registered spring localities and zones, whereas > 99% of the total discharge occurs via diffuse outflow zones in the northern and southern coast. These zones are composed of highly permeable limestones that extend in narrow coastal zones. Therefore, seawater forms a wedge underneath the freshwater aquifer; however, it does not spread under the entire island as a result of the relatively impervious base zone a few tens of meters below sea level. All of these facts support the assumption that additional groundwater quantities could be extracted, either by further increasing the pumping rates at Korita, or with the more long-term sustainable option of drilling new wells in a few prospective zones after further hydrogeological and geophysical investigations. This study also proposed SPZs for the public water supply system of Vis island, which encompassed the entire catchments of the Korita pumping site and Pizdica spring (Figure 11). These SPZs were subsequently approved by the local authorities, such that the protective measures are being implemented, which is of vital importance as the island currently has no alternative water supply option.

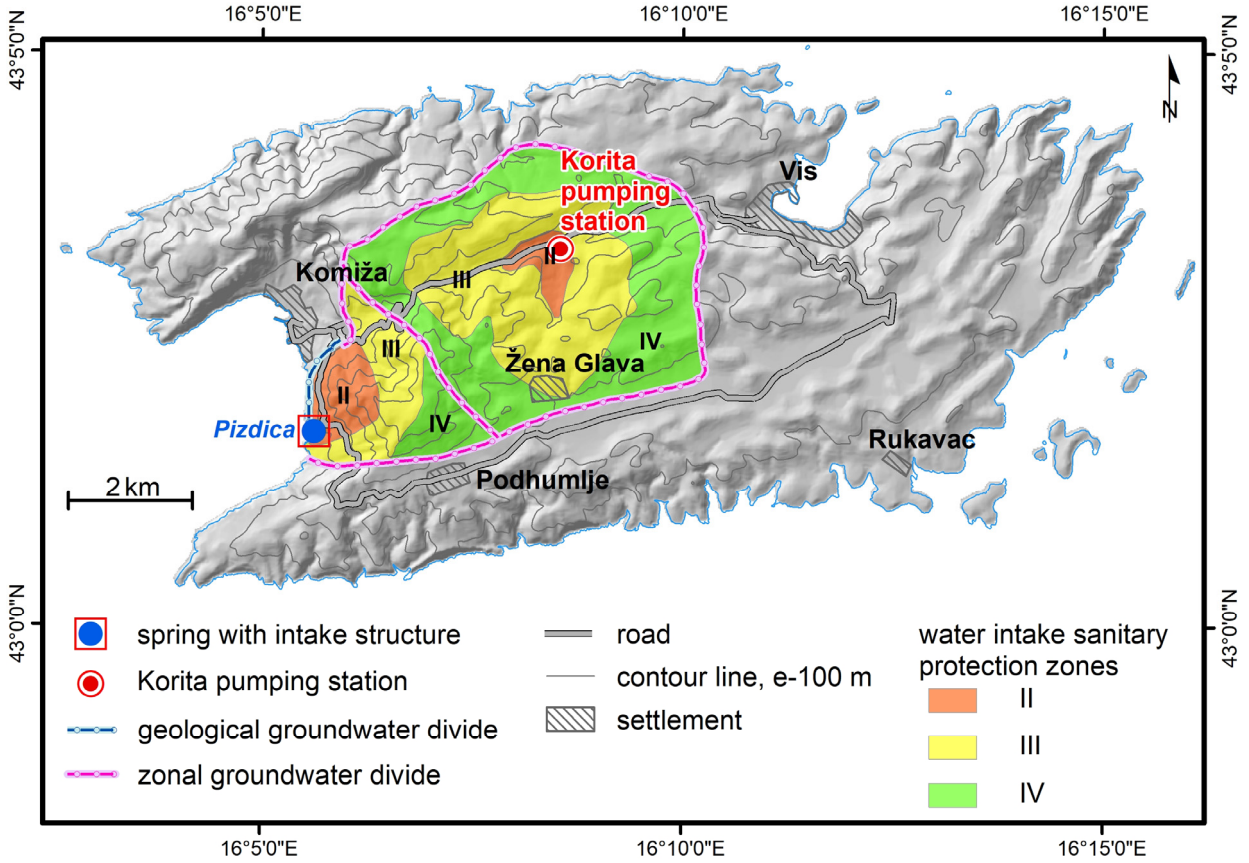

Figure 11. Sanitary protection zones on Vis Island.

Previous research hypothesized the existence of a single catchment area for Korita and Pizdica [16,38], whereby the presumed groundwater flow was from the central aquifer and the area around Korita towards Pizdica (except for the area influenced by the radius of the wells). On the other hand, the research and analyses in the present study, including the tracer test, provided an improved insight into the system and divided it into two catchments that are separated by a zonal groundwater divide (Figures 4 and 10). Moreover, the findings demonstrated that the main flow direction from Korita is eastwards, whereas it was previously considered to be towards Pizdica in the west. These findings have a paramount impact on the understanding of the hydrogeological relationships on Vis Island,

as well as strong implications for the protection of local water supply sources through SPZs. More detailed studies using hydrochemical and geophysical methods could lead to the delineation, and possibly utilization, of other separated catchments, which we have only postulated here on the basis of the geological and structural settings and basic hydrochemical data.

The groundwater resources of Vis Island are a very interesting research topic for karst hydrogeologists, and currently represent the only source of water supply for the island. Several questions remain unanswered following this study, and further research should aim to perform continuous monitoring using data loggers and regular sampling for hydrochemical analyses. In addition, monitoring and/or early warning system boreholes should be established to protect against seawater intrusion after further bulk hydrogeological and geophysical investigations.

Author Contributions: Conceptualization, J.T. and S.B.; methodology, J.T. and T.F.; software, T.F.; validation, J.T., S.B. and J.L.R.; formal analysis, J.T., S.B. and J.L.R.; investigation, J.T., T.F., S.B. and J.L.R.; resources, J.T.; data curation, J.T. and T.F.; writing—original draft, J.T.; preparation, M.P.; writing—review and editing, J.T., T.F., S.B., J.L.R. and M.P.; visualization, T.F.; supervision, J.T. All authors have read and agreed to the published version of the manuscript.

Funding: This research was partially funded and supported by Croatian Waters in two phases: during 1999/2000 and 2012.

Data Availability Statement: Not applicable.

Acknowledgments: The authors wish to express their gratitude to research investors, as well as to islanders who assisted with this research, especially to the water supply company on Vis: Vodovod i odvodnja otoka Visa. We express our special gratitude to our colleagues, Renato Buljan, Janislav Kapelj, and Sanja Kapelj, who were involved in previous research.

Conflicts of Interest: We hereby declare no real or perceived financial conflict of interest for any author as well as no other affiliations causing a conflict of interest. The funders had no role in the design of the study; in the collection, analyses, or interpretation of data; in the writing of the manuscript, or in the decision to publish the results.

References

1. Bakalowicz, M. Karst groundwater: A challenge for new resources. *Hydrogeol. J.* **2005**, *13*, 148–160. [CrossRef]
2. Ford, D.; Williams, P. *Karst Hydrogeology and Geomorphology*, 1st ed.; John Wiley and Sons Ltd.: New York, NY, USA, 2007. [CrossRef]
3. Goldscheider, N.; Drew, D. Methods in karst hydrogeology. In *IAH: International Contributions to Hydrogeology*; Taylor & Francis/Balkema: London, UK, 2007. [CrossRef]
4. Hartmann, A.; Goldscheider, N.; Wagener, T.; Lange, J.; Weiler, M. Karst water resources in a changing world: Review of hydrological modeling approaches. *Rev. Geophys.* **2014**, *52*, 218–242. [CrossRef]
5. Terzić, J.; Stroj, A.; Frangen, T. Hydrogeological investigation of karst system properties by common use of diverse methods: A case study of Lička Jesenica springs in Dinaric karst of Croatia. *Hydrol. Process.* **2012**, *26*, 3302–3311. [CrossRef]
6. Bonacci, O. Karst hydrogeology/hydrology of dinaric chain and isles. *Environ. Earth Sci.* **2015**, *74*, 37–55. [CrossRef]
7. Šegota, T. Razina mora i vertikalno gibanje dna Jadranskog mora od ris–virmskog interglacijala do danas [The sea level and vertical movements of the Adriatic Sea bottom since Ris-Würm glaciations till today]. *Geološki Vjesnik* **1982**, *35*, 93–109.
8. Surić, M. Submarine karst of Croatia—Evidence of former lower sea levels. *Acta Carsologica* **2002**, *31*, 89–98. [CrossRef]
9. Bakalowitz, M. Karst and karst groundwater resources in the Mediterranean. *Environ. Earth Sci.* **2015**, *74*, 5–14. [CrossRef]
10. Cappucci, S.; De Cassan, M.; Grillini, M.; Proposito, M. Multi-source water characterisation for water supply and management strategies on a small Mediterranean island. *Hydrogeol. J.* **2020**, *28*, 1155–1171. [CrossRef]
11. Babu, R.; Park, N.; Nam, B. Regional and well-scale indicators for assessing the sustainability of small island fresh groundwater lenses under future climate conditions. *Environ. Earth Sci.* **2020**, *79*, 47. [CrossRef]
12. Tiwari, A.K.; Pisciotta, A.; De Maio, M. Evaluation of groundwater salinization and pollution level on Favignana Island, Italy. *Environ. Pollut.* **2019**, *249*, 969–981. [CrossRef]
13. Frondini, F. Geochemistry of regional aquifer systems hosted by carbonate-evaporite formations in Umbria and southern Tuscany (central Italy). *Appl. Geochem.* **2008**, *23*, 2091–2104. [CrossRef]
14. Moral, F.; Cruz-Sanjulian, J.J.; Olias, M. Geochemical evolution of groundwater in the carbonate aquifers of Sierra de Segura (Betic Cordillera, southern Spain). *J. Hydrol.* **2008**, *360*, 281–296. [CrossRef]

15. Borović, S.; Terzić, J.; Pola, M. Groundwater quality on the Adriatic karst island of Mljet (Croatia) and its implications on water supply. *Geofluids* **2019**, *2019*, 14. [CrossRef]
16. Terzić, J. Hidrogeološki odnosi na krškim otocima–primjer otoka Visa [Hydrogeological relations on kart islands–the island of Vis case study]. *Min.-Geol.-Pet. Eng. Bull.* **2004**, *16*, 47–58.
17. Duplančić Leder, T.; Ujević, T.; Čala, M. Coastline lengths and areas of islands in the Croatian part of Adriatic Sea determined from the topographic maps at the scale of 1:25,000. *Geoadria* **2004**, *9*, 5–32. [CrossRef]
18. Crnolatac, I. Geologija otoka Visa [Geology of the island of Vis]. *Geološki Vjesn.* **1953**, *33*, 45–62.
19. Korbar, T.; Belak, M.; Fuček, L.; Husinec, A.; Oštrić, N.; Palenik, D.; Vlahović, I. *Basic Geological Map of the Republic of Croatia 1:50.Sheets Vis 3 and Biševo 1 with Part of the Sheet Vis 4 and Islands Sv Andrija, Brusnik, Jabuka and Palagruža*; Croatian Geological Survey: Zagreb, Croatia, 2012.
20. Šegota, T.; Filipčić, A. *Klimatologija za Geografe [Climatology for Geographers]*; Školska knjiga: Zagreb, Croatia, 1996.
21. Gajić-Čapka, M.; Zaninović, K. Climate of Croatia. In *Climate Atlas of Croatia 1961–1990, 1971–2000*; Zaninović, K., Gajić-Čapka, M., Perčec Tadić, M., Vučetić, M., Milković, J., Bajić, A., Cindrić, K., Cvitan, L., Katušin, Z., Kaučić, D., et al., Eds.; Meteorological and Hydrological Service of Croatia: Zagreb, Croatia, 2008.
22. Zaninović, K. Air temperature. In *Climate Atlas of Croatia 1961–1990, 1971–2000*; Zaninović, K., Gajić-Čapka, M., Perčec Tadić, M., Vučetić, M., Milković, J., Bajić, A., Cindrić, K., Cvitan, L., Katušin, Z., Kaučić, D., et al., Eds.; Meteorological and Hydrological Service of Croatia: Zagreb, Croatia, 2008.
23. Bonacci, O.; Patekar, M.; Pola, M.; Roje-Bonacci, T. Analyses of climate variations at four meteorological stations on remote islands in the Croatian part of the Adriatic Sea. *Atmosphere* **2020**, *11*, 1044. [CrossRef]
24. Tari, V. Evolution of the northern and western Dinarides: A tectonostratigraphic approach. In *European Geosciences Union: Stephan Mueller Special Publication Series. 1*; European Geosciences Union: Munich, Germany, 2002; pp. 223–236.
25. Prelogović, E.; Pribičević, B.; Ivković, Ž.; Dragičević, I.; Buljan, R.; Tomljenović, B. Recent structural fabric of the Dinarides and tectonically active zones important for petroleum-geological exploration in Croatia. *Naft. Explor. Prod. Process. Petrochem.* **2004**, *55*, 155–161.
26. Schmid, S.M.; Bernoulli, D.; Fügenschuh, B.; Matenco, L.; Schefer, S.; Schuster, R.; Ustaszewski, K. The Alpine-Carpathian-Dinaridic orogenic system: Correlation and evolution of tectonic units. *Swiss J. Geosci.* **2008**, *101*, 139–183. [CrossRef]
27. Vlahović, I.; Tišljar, J.; Velić, I.; Matičec, D. Evolution of the Adriatic Carbonate Platform: Palaeogeography, main events and depositional dynamics. *Palaeogeogr. Palaeoclimatol. Palaeoecol.* **2005**, *220*, 333–360. [CrossRef]
28. Korbar, T. Orogenic evolution of the External Dinarides in the NE Adriatic region: A model constrained by tectonostratigraphy of Upper Cretaceous to Paleogene carbonates. *Earth Sci. Rev.* **2009**, *96*, 296–312. [CrossRef]
29. Borović, I.; Marinčić, S.; Majcen, Ž. *Osnovna Geološka Karta, List Vis [Basic Geological Map, Vis Sheet]*; Savezni Geološki Institut: Belgrade, Yugoslavia, 1977.
30. Poljak, J. *Geološki i Hidrogeološki Izvještaj o Otoku Visu [Geological and Hydrogeological Report on Vis Island]*; Unpublished Report; Zavod za geološka istraživanja: Zagreb, Yugoslavia, 1953. (In Croatian)
31. Koch, G.; Belak, M. Evaporitic-carbonate deposits of Komiža diapiric structure (Island of Vis, Croatia): Their palynostratigraphy and sedimentological features. In Proceedings of the 22nd IAS Meeting of Sedimentology, Opatija, Croatia, 17–19 July 2003.
32. Palenik, D. Strukturni Sklop Otoka Visa Structural Frame of the Vis Island. Master's Thesis, Faculty of Science, University of Zagreb, Zagreb, Croatia, 2005.
33. Turc, L. Le bilan d'eau des sols, relation entre les précipitations, l'evaporation et l'écoulement [Ground water variations: Relations between precipitation, evaporation and runoff]. *Ann. Agron.* **1954**, *5*, 491–596.
34. De Breuck, W. *Hydrogeology of Salt Water Intrusion: A selection of SWIM Papers*; Verlag Heinz Heise GmbH & Co KG.: Hannover, Germany, 1991.
35. Motyka, J. A conceptual model of hydraulic networks in carbonate rocks, illustrated by examples from Poland. *Hydrogeol. J.* **1998**, *6*, 469–482. [CrossRef]
36. Urumović, K. Uvjeti prodora morske vode u krški vodonosnik pulskih zdenaca, [Conditions of a seawater intrusion into karst aquifer of Pula]. In Proceedings of the Second Croatian Geological Congress, Institute for Geological Research, Dubrovnik, Croatia, 17–20 May 2000.
37. Jones, I.C.; Banner, J.L. Estimating recharge thresholds in tropical karst island aquifers: Barbados, Puerto Rico and Guam. *J. Hydrol.* **2003**, *278*, 131–143. [CrossRef]
38. Kapelj, J.; Terzić, J.; Kapelj, S.; Dolić, M. Recent hydrogeologic study of the Vis Island. *Geologija* **2003**, *45*, 419–426. [CrossRef]
39. Vacher, H.L.; Quinn, T.M. Geology and hydrogeology of carbonate islands. In *Developments in Sedimentology*, 1st ed.; Vacher, H.L., Quinn, T.M., Eds.; Elsevier: Amsterdam, The Netherlands, 2004; Volume 54.
40. Winston, W.E.; Criss, R.E. Dynamic hydrologic and geochemical response in a perennial karst spring. *Water Resour. Res.* **2004**, *40*. [CrossRef]
41. Terzić, J. Hidrogeologija Jadranskih Krških Otoka [Hydrogeology of the Adriatic Karstic Islands]. Ph.D. Thesis, Faculty of Mining, Geology and Petroleum Engineering, University of Zagreb, Zagreb, Croatia, 2006.
42. Terzić, J.; Marković, T.; Pekaš, Ž. Influence of sea-water intrusion and agricultural production on the Blato Aquifer, Island of Korčula, Croatia. *Environ. Geol.* **2008**, *54*, 719–729. [CrossRef]

43. Terzić, J.; Peh, Z.; Marković, T. Hydrochemical properties of transition zone between fresh groundwater and seawater in karst environment of the Adriatic islands, Croatia. *Environ. Earth Sci.* **2010**, *59*, 1629–1642. [CrossRef]
44. Terzić, J.; Filipović, M.; Boljat, I.; Selak, A.; Lukač Reberski, J. Groundwater level and electrical conductivity datasets acquired within pumping tests on Ilovik in Croatia. *Data Br.* **2021**, *37*, 107180. [CrossRef]
45. Terzić, J.; Grgec, D.; Lukač Reberski, J.; Selak, A.; Boljat, I.; Filipović, M. Hydrogeological estimation of brackish groundwater lens on a small Dinaric karst island: Case study of Ilovik, Croatia. *Catena* **2021**, *204*, 105379. [CrossRef]
46. Ljubenkov, I. Water resources of the island of Korčula (Croatia): Availability and agricultural requirement. *J. Water Land Dev.* **2012**, *17*, 11–18. [CrossRef]
47. Viola, F.; Sapiano, M.; Schembri, M.; Brincat, C.; Lopez, A.; Toscano, A.; Diamadopoulos, E.; Charalambous, B.; Molle, B.; Zoumadakis, M.; et al. The state of water resources in major Mediterranean islands. *Water Resour.* **2014**, *41*, 639–648. [CrossRef]
48. Kourtis, I.M.; Kotsifakis, K.G.; Feloni, E.G.; Baltas, E.A. Sustainable water resources management in small Greek islands under changing climate. *Water* **2019**, *11*, 1694. [CrossRef]
49. Thiem, G. *Hydrologische Methoden [Hydrological Methods]*; J. M. Gebhardt: Leipzig, Germany, 1906. (In German)
50. Sauter, M. *Quantification and Forecasting of Regional Groundwater Flow and Transport in a Karst Aquifer (Gallusquelle, Malm, SW Germany)*; Tubinger Geowissenschaftliche Arbeiten: Tubingen, Germany, 1992; p. 151.
51. White, W.B. Karst hydrology: Recent developments and open questions. *Eng. Geol.* **2002**, *65*, 85–105. [CrossRef]
52. Milanović, P.T. *Karst Hydrogeology*; Water Resources Publications: Littleton, CO, USA, 1981.
53. Terzić, J.; Šumanovac, F.; Buljan, R. An assessment of hydrogeological parameters on the karstic island of Dugi otok, Croatia. *J. Hydrol.* **2007**, *343*, 29–42. [CrossRef]
54. Käss, W. *Tracing Technique in Geohydrology*; Balkema: Rotterdam, The Netherlands, 1998.
55. Benischke, R.; Goldscheider, N.; Smart, C. Tracer techniques. In *Methods in Karst Hydrogeology*; Goldscheider, N., Drew, D., Eds.; Taylor & Francis: London, UK, 2007.
56. Goldscheider, N.; Meiman, J.; Pronk, M.; Smart, C. Tracer tests in karst hydrogeology and speleology. *Int. J. Speleol.* **2008**, *37*, 27–40. [CrossRef]
57. Freeze, R.A.; Cherry, J.A. *Groundwater*; Prentice-Hall, Inc.: Englewood Cliffs, NJ, USA, 1979.
58. Piper, A.M. A graphic procedure in the geochemical interpretation of water analyses. *Eos Trans. Am. Geophys. Union* **1944**, *25*, 914–928. [CrossRef]
59. Yang, H.; Kagabu, M.; Okumura, A.; Shimada, J.; Shibata, T.; Pinti, D.L. Hydrogeochemical processes and long-term effects of sea-level rise in an uplifted atoll island of Minami-Daito, Japan. *J. Hydrol. Reg. Stud.* **2020**, *31*, 100716. [CrossRef]
60. Appelo, C.A.J.; Postma, D. *Geochemistry, Groundwater and Pollution*, 2nd ed.; A. A. Balkema: Leiden, The Netherlands, 2005.
61. Bahun, S. Geološka osnova zaštite podzemnih voda u kršu [Geological basis for water protection in karst]. *Geološki Vjesn.* **1989**, *42*, 201–211.
62. Pavičić, A.; Terzić, J.; Buljan, R. Micro zoning of terrain included in sanitary protection zones in karstic conditions. In Proceedings of the Second International Conference on Waters in Protected Areas, Croatian Water Pollution Control Society, Dubrovnik, Croatia, 24–28 April 2007.
63. Biondić, B.; Biondić, R.; Dukarić, F. Protection of karst aquifers in the Dinarides in Croatia. *Environ. Geol.* **1998**, *34*, 309–319. [CrossRef]
64. Ministry of Agriculture of Croatia. Dopune pravilnika o uvjetima za utvrđivanje zona sanitarne zaštite izvorišta [Additions to directives for conditions of determining the sanitary protection zones]. *Narodne Novine*. 2013. Available online: https://narodne-novine.nn.hr/clanci/sluzbeni/2013_04_47_910.html (accessed on 1 December 2021).
65. Ministry of Regional Development, Forestry and Water Management of Croatia. Pravilnik o uvjetima za utvrđivanje zona sanitarne zaštite izvorišta [Directives for conditions of determining the sanitary protection zones]. *Narodne Novine*. 2011. Available online: https://narodne-novine.nn.hr/clanci/sluzbeni/2011_06_66_1460.html (accessed on 1 December 2021).
66. Fritz, F.; Ramljak, T. Zaštitne zone izvorišta pitkih voda u kršu [Protection zones for potable water sources in karst]. *Građevinar* **1992**, *44*, 333–337.
67. Ghyben, W.B. Nota in verband met de voorgenomen putboring nabij Amsterdam [Notes on the probable results of proposed well drilling near Amsterdam]. *Tijdschr. Van Let K. Inst. Van Ing.* **1888**, *21*, 8–22.
68. Herzberg, A. Die Wasserversorgung einiger Nordseebader. *Wasserversorgung* **1901**, *44*, 815–819; discussion 842–844.
69. Buljan, R.; Marković, T.; Zelenika, M. Aquifer of the western part of Prgovo polje on the island of Lastovo. *Min. Geol. Pet. Eng. Bull.* **2006**, *18*, 15–27.
70. Bauer, S.; Liedl, R.; Sauter, M. Modeling of karst aquifer genesis: Influence of exchange flow. *Water Resour. Res.* **2003**, *39*, 1285. [CrossRef]
71. Bechtel, T.; Bosch, F.; Gurk, M. Geophysical methods in karst hydrogeology. In *Methods in Karst Hydrogeology*; Goldscheider, N., Drew, D., Eds.; Taylor and Francis/Balkema: London, UK, 2007.
72. Branković, Č.; Güttler, I.; Gajić-Čapka, M. Evaluating climate change at the Croatian Adriatic from observations and regional climate models' simulations. *Clim. Dyn.* **2013**, *41*, 2353–2373. [CrossRef]

DOI 10.7343/as-2022-557

ACQUE SOTTERRANEE
Italian Journal of Groundwater
journal homepage: https://www.acquesotterranee.net/

2022-AS40-557: 37 - 48

Multidisciplinary investigations of a karst reservoir for managed aquifer recharge applications on the island of Vis (Croatia)

Studio multidisciplinare per analizzare la ricarica in condizioni controllate dell'acquifero carsico dell'isola di Vis (Croazia)

Matko Patekar[a], Mihaela Bašić[a], Marco Pola[a] ✉, Ivan Kosović[a], Josip Terzić[a], Alessio Lucca[b], Silvia Mittempergher[c], Luigi Riccardo Berio[b], Staša Borović[a]

[a]Croatian Geological Survey, Sachsova 2, 10000 Zagreb, Croatia - ✉ email: *mpola@hgi-cgs.hr*
[b]University of Parma, Parma, Italy
[c]University of Modena and Reggio Emilia, Modena, Italy

ARTICLE INFO

Ricevuto/*Received*: 31 January 2022
Accettato/*Accepted*: 29 March 2022
Pubblicato online/*Published online*: 30 March 2022

Handling Editor:
Marco Rotiroti

Publication note:
This contribution has been selected from Flowpath 2021 congress held in Naples 1-3 December 2021

Citation:
Patekar M, Bašić M, Pola M, Kosović I, Terzić J, Lucca A, Mittempergher S, Berio LR, Borović S (2022) Multidisciplinary investigations of a karst reservoir for managed aquifer recharge applications on the island of Vis (Croatia). Acque Sotterranee - *Italian Journal of Groundwater*, 11(1), 37 - 48
https://doi.org/10.7343/as-2022-557

Correspondence to:
Marco Pola ✉
mpola@hgi-cgs.hr

Keywords: *groundwater management; managed aquifer recharge; karst aquifer; coastal aquifer; Vis island.*

Parole chiave: gestione delle acque sotterranee; ricarica delle falde in condizioni controllate; acquifero carsico; acquifero costiero; isola di Vis.

Riassunto

La ricarica dell'acquifero in condizioni controllate (MAR) è una metodologia attraverso la quale è possibile immagazzinare nel sottosuolo l'acqua superficiale in eccesso per una sua estrazione successiva o per scopi ambientali Questo approccio viene generalmente utilizzato in acquiferi non consolidati, mentre la sua applicazione in acquiferi carsici è scarsa. Questa ricerca presenta i primi risultati di uno studio di fattibilità di MAR nell'isola di Vis, una piccola isola carsica situata nel mare Adriatico. Condizioni geologiche ed idrogeologiche favorevoli permettono la formazione di una risorsa sotterranea idropotabile rendendo l'isola autonoma dal punto di vista idrico. L'acquifero carsico più importante, sfruttato nel campo pozzi di Korita, è protetto dall'ingressione di acqua marina da numerose barriere idrogeologiche. Tuttavia, il cambiamento climatico e l'elevata pressione antropica riconducibile all'intenso turismo nell'isola rappresentano una minaccia per la futura disponibilità di acqua potabile. In questo lavoro sono state condotte analisi multidisciplinari di campo ed in laboratorio per dettagliare l'assetto geologico ed idrogeologico dell'isola e le caratteristiche della sua risorsa idrica. Le analisi di campo comprendono il monitoraggio delle acque sotterranee ed il loro campionamento, indagini geofisiche (i.e., tomografia elettrica), e misure strutturali. Le analisi di laboratorio comprendono la misura dei cationi ed degli anioni principali e dell'attività di trizio. Nonostante la scarsa precipitazione durante il periodo di osservazione (settembre 2019 - dicembre 2020), la risorsa idrica nel campo pozzi di Korita ha mostrato parametri fisico-chimici stabili, una buona capacità di immagazzinamento ed una buona riserva a lungo termine. Le indagini geofisiche hanno evidenziato una struttura abbastanza omogenea delle rocce carbonatiche nel sottosuolo, mentre le analisi strutturali hanno indicato la presenza di fratture E-O aperte e carsificate che possono costituire delle vie di flusso preferenziale nell'acquifero carbonatico. L'approccio di MAR proposto in questo lavoro combina un bacino di accumulo e la ricarica diretta nell'acquifero mediante i pozzi esistenti. La risorsa idrica potenziale sarebbe costituita dall'acqua piovana e di ruscellamento raccolte mediante un bacino di accumulo in disuso situato a valle di un vecchio canale artificiale che scorreva attraverso la zona di Korita.

Abstract

Managed aquifer recharge (MAR) refers to a suite of methods by which excess surface water or non-conventional water is stored underground for subsequent recovery or environmental purposes. MAR solutions have been largely used in unconsolidated aquifers, while their application in karst aquifers is rare. This research presents the first results of a MAR viability study on the island of Vis, a small karstic island in the Adriatic Sea. Favorable geological and hydrogeological conditions enable the formation of karst aquifers, making the island autonomous in terms of water supply. The island's main aquifer, exploited in the Korita well field, is protected from seawater intrusion by several hydrogeological barriers. However, climate change and high seasonal pressures related to tourism pose a threat to the future availability of freshwater. Multidisciplinary field and laboratory investigations were carried out to detail the geological and hydrogeological setting of the island and its groundwater resource. Field analyses consisted of groundwater monitoring and sampling, geophysical investigations (i.e., electrical resistivity tomography), and structural measurements. Laboratory analyses included measurements of principal cations and anions and tritium activity. Despite low precipitation during the observation period (September 2019 - December 2020), the groundwater resource at the Korita site showed stable trends of physico-chemical parameters with a good storage potential and a long-term reserve. Geophysical investigations evidenced a relatively homogeneous sequence of the rock mass at a larger scale, while structural analyses indicated the occurrence of E-W karstified and open fractures that could represent a preferential flow path in the carbonate aquifer. A MAR solution for the Vis island was proposed combining an infiltration pond scheme with the direct injection of the accumulated waters into the aquifer using available wells. The potential water source could be represented by the runoff collected in an old artificial channel and the associated pond system in Korita.

Introduction

Sustainable management of groundwater resources in karstic aquifers is one of the key environmental challenges in the Mediterranean region (e.g., Cosgrove and Loucks 2015; García-Ruiz et al. 2011; Sapiano 2020). Karstic groundwater is one of the most important freshwater resource, and it is estimated that 10 to 25% of the global population depends on it (Ford and Williams 2007; Stevanović 2019). In the Mediterranean region, the percentage goes up to 50% (Hartmann et al. 2014), emphasizing its strategic importance and irreplaceability. The intensive karstification of the carbonate rock mass causes distinctive heterogeneity and anisotropy of aquifer's hydraulic properties posing a significant challenge for investigation, utilization, and management of groundwater resources (Worthington 2014). Climate change, overexploitation, improper land use or its modifications, and seawater intrusion are the most common drivers of groundwater resources' degradation (e.g., Giorgi 2006; Rosenzweig et al. 2007; Werner et al. 2013). In particular, the Mediterranean region is often regarded as a hot spot of climate change with a predicted temperature increase of 3.5-5.5 °C until 2100 (Bonacci et al. 2020; Branković et al. 2013) and an increase in precipitation variability with a negative influence on water balance (Aguilera and Murillo 2008; Touhami et al. 2015). The environmental challenges in the Mediterranean region are fostered by the rising anthropic pressure and the high population density with the local population (approximately 160 million people with approximately 10 million inhabitants in the islands; European Environment Agency 2015) drastically increasing during the tourist season (e.g., Leduc et al. 2017; Mongelli et al. 2019).

In Croatia, karstified carbonate rocks cover approximately half of the territory being the bedrock along the coast and its hinterland (HGI-CGS 2009; Velić and Vlahović 2009; Vlahović et al. 2005). The Croatian coast is one of the most indented coastlines in the world, consisting of 79 islands and 525 islets (Duplančić Leder et al. 2004). Merely a few of them have a completely autonomous water supply from karstic aquifers or freshwater lakes (e.g., Vis, Cres), whereas the majority are connected to the water supply system of the mainland. Furthermore, some islands have composite water supply solutions, such as small desalination plants for salinized water from brackish lakes (e.g., Borović et al. 2019). The most significant problem regarding the water supply on Croatian islands is represented by seawater intrusions into aquifers (e.g., Lukač Reberski et al. 2020; Plantak et al. 2021; Terzić et al. 2008). This problem is mostly inherent due to: (i) their small surface area resulting in small catchments and aquifers, (ii) intense fracturing and karstification with a karst base level below the present sea-level resulting in high permeability of the rock mass and preferential seawater intrusion through karstic conduits, and (iii) relatively low precipitation and high evapotranspiration. Anthropic pressures and overexploitation significantly add up to this problem (e.g., Alfrrah and Walraevens 2018; Gaaloul et al. 2012; Meybeck et al. 2003). Despite the relatively low population, the majority of Croatian islands experiences extreme seasonality in water demand due to intensive summer tourism, which coincides with the dry season. Efficient and integrated water management is needed to mitigate these problems increasing the groundwater quantity and improving its quality.

Vis, a small and remote island in the middle of the Adriatic Sea (Fig. 1), maintained an efficient and autonomous water supply system for decades. Currently, the system satisfies the freshwater demand of the local population, but occasional reductions can occur during the dry season due to very low precipitation and high water demand for tourism purposes. The need for alternative water management solutions yielded managed aquifer recharge (MAR) as an option for increasing the safety and resilience of the island's groundwater resources. MAR refers to a suite of methods by which excess surface water is intentionally stored underground for later recovery. MAR operations are generally done to mitigate declining groundwater tables, to improve water quality, or for other environmental benefits (Dillon et al. 2019; Fernández Escalante et al. 2020). On a global scale, MAR methods have been successfully used, but their application in the karstic environment is still marginal (e.g., Daher et al. 2011; Massaad 2000; Rolf 2017; Vanderzalm et al. 2002; Xanke 2017). The most common hydrogeological challenges for the implementation of MAR solutions in karst include: (i) poor knowledge of the aquifer geometry, (ii) high variability of hydraulic conductivity and porosity fields resulting in unpredictable flow paths, and (iii) complex geochemical water-rock interactions adding on the spatial complexity of karstic features.

Several comprehensive methodological approaches for assessing MAR viability were developed (e.g., Daher et al. 2011; DEEPWATER-CE 2020; Hayat et al. 2021; Lobo Ferreira and Leitão 2014; NRMMC-EPHC-NHMRC 2009; Rolf 2017; San-Sebastián-Sauto et al. 2018). The site characterization (e.g., climatological, morphological, geological, hydrogeological, and geochemical reconstructions) commonly represents the first phase of MAR solution planning. In this paper, we present the initial results of a multidisciplinary research to determine the MAR viability on the island of Vis. To detail the hydrogeological setting of the karstic aquifer and the physical and chemical characteristics of the groundwater, hydrogeological, geochemical, geophysical, and structural investigations were conducted. Firstly, the geological, hydrogeological, and climatological settings of the study area will be described. Then, an overview of the utilized data and methods will be provided, followed by the results and their interpretation in the context of the investigated topic.

Data and methods

Geographical setting and climate

The island of Vis is located in the central part of the Adriatic Sea (Fig. 1), approximately 50 and 120 km from the Croatian and Italian mainlands, respectively. The relief consists of three hilly terrains separated by two predominantly E-W valleys, locally hosting karst poljes. The highest peak is Hum

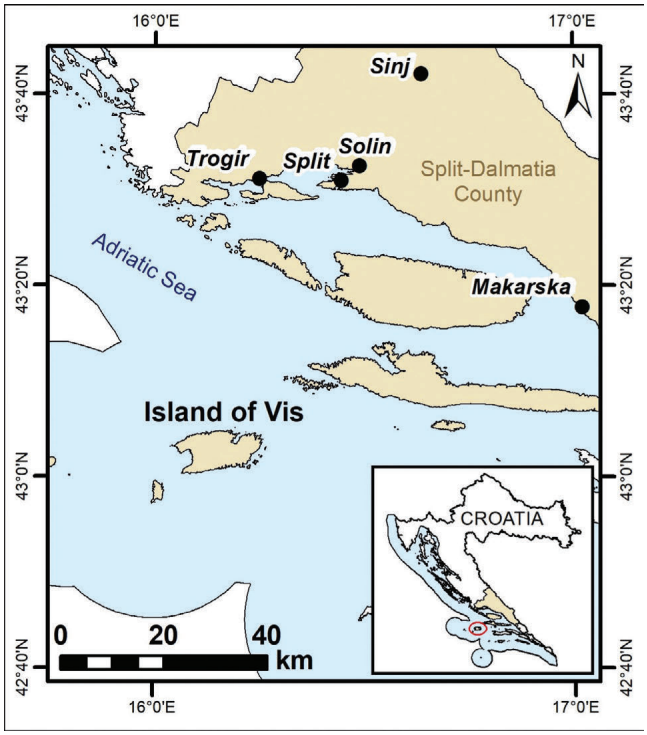

Fig. 1 - Location map of the study area.

Fig. 1 - Ubicazione dell'area di studio.

(587 m a.s.l.), located in the western part of the island. The local population consists of approximately 3,300 inhabitants mostly living in the cities of Vis and Komiža (Fig. 2). The island is well known in terms of summer tourism when the number of visitors surpasses the local population up to ten times.

The climate of the island can be classified as a Mediterranean climate with dry and hot summers (Filipčič 1998). Due to the island's position in the open sea, there is a strong maritime influence reflected in the mitigation of climate extremes and air temperature variations (Bonacci et al. 2020, 2021). In the period from 1991 to 2019, the mean annual air temperature was 17.1 °C and the mean annual precipitation was 775 mm. The precipitation is highly seasonal, with the peak in the colder part of the year (October-March). The evapotranspiration, calculated using Turc's method (Turc 1954), is approximately 65% resulting in annual effective precipitation of approximately 270 mm since surface runoff is negligible and only occurs during long-term rainfall or storms. Effective infiltration between 40 and 65% is common in the Dinaric karst (e.g., Bonacci 2001).

Geological and hydrogeological settings

The island of Vis belongs to the geotectonic unit of the External Dinarides, an area characterized by deep and irregular karstification. It exhibits a composite and peculiar structural fabric (Korbar et al. 2012) affecting its hydrogeological setting. The main lithological units are: (i) Cretaceous limestones and dolomites, (ii) the volcanic-sedimentary-evaporite (VSE) complex of Komiža bay (Middle to Upper Triassic) in the western part of the island, consisting of gypsum, dolomite-gypsum breccias, karst debris, andesites, volcanic agglomerates, siltites, marls, and tuffites, and (iii) Quaternary deposits, represented by the terra rossa cover in karst poljes, and locally colluvial deposits and aeolian sands.

Vis is crosscut by three main subvertical fault systems striking NE-SW to E-W (Fig. 2a). The NE-SW striking fault in the northern part of the island (Oključna fault) and the E-W striking fault in the S (Podšpilje-Rukavac fault) constitute the northern and southern boundaries of the Komiža diapir (VSE complex), and both diverge towards the E defining a radial pattern. The fault system with the strongest morphological expression and associated with the most productive wells (Korita well field) is the Komiža-Vis fault system, striking approximately N70°. Overall, the onshore structure of Vis is an open anticline with an axial plane striking E-W and hinge dipping towards the E. The anticline is bounded to the N and S by the Oključna and Podšpilje-Rukavac faults, respectively.

Terzić (2004) and Terzić et al. (2022) provided a detailed description of the hydrogeological setting of the Vis island and assessed its freshwater resources. The main conclusions were:

- the most significant water-bearing hydrostratigraphic units are represented by moderate permeability laminated and well-bedded limestones with dolomitic beds/interbeds and by high permeability limestones (Fig. 2a). Conversely, low permeability units are: (i) well-bedded dolomites, and (ii) the VSE complex. Locally, low permeability terra rossa sediments from karst poljes infill the underlying rock mass, decreasing its hydraulic conductivity;
- the transmissivity in the Korita well field is from 9×10^{-4} to 2.3×10^{-3} m^2/s, with the results of pumping tests pointing to a homogeneous flow through a densely fractured rock mass rather than conduit flow;
- tracer test evidenced two distinctive catchments (Korita and Pizdica), with the zonal groundwater divide following the relief E of the Komiža bay and including the Hum ridge (Fig. 2b). The precipitation infiltrates and flows east- and westward from the groundwater divide through the moderate to high permeability carbonates. In the E, the groundwater forms the water resource exploited in Korita, which is also partially recharged by the precipitation from the relief in the vicinity of Vis city. In the W, the groundwater flow is stopped by the low permeability VSE complex and it is locally discharged along the coast (Pizdica spring). Small scale catchments develop along the northern and southern coasts resulting in diffused discharges to sea through highly karstified limestones, with the periodical occurrence of vruljas (submerged springs);
- the two most significant hydrogeological barriers that prevent seawater intrusions into the Korita aquifer are represented by the low permeability VSE complex from the W, and by rock mass with reduced permeability below karst poljes in the S. Therefore, the highest risk of seawater intrusion is from the E, along the Komiža-Vis fault zone. Conversely, the Pizdica water resource and

the small scale water resources along the coast are prone to seawater intrusion. The mixing ratio with seawater strongly depends on the permeability of the rock mass.

The Vis water supply system consists of five wells (BO1 to BO5) drilled in the Korita well field, two wells (K1 and B1) in the Komiža hinterland, and the Pizdica spring (Fig. 2). The maximum pumping capacity at Korita is 42 l/s, and the groundwater is pumped from the approximate depth of 110 to 140 m. Groundwater levels vary between 10-20 m a.s.l. depending on the well location and pumping quantity (Terzić et al. 2022). Groundwater quality is excellent since hydrogeological barriers protect it from seawater intrusion. However, the Komiža-Vis fault and its high permeable damage zone could represent a potential seawater flow path posing a great risk for resource management. The wells and the Pizdica spring in the western part of the island provide a total of approximately 5 l/s. Their water quality is variable and mostly depends on the different interactions with the seawater and the bedrock.

Approximately 450,000 m^3 of freshwater is abstracted annually with a variable flow rate depending on the high tourist season. During high season, a fivefold increase in demand exerts stresses on freshwater resources and several reductions for consumers occurred in the last two decades.

Numerous less productive springs and wells on the island are not utilized for drinking water supply. Despite their low yield, they were investigated and sampled since they could represent a possible local water resource during droughts or high exploitation periods (Fig. 2a).

Hydrogeological and hydrochemical investigations

Hydrogeological and geochemical investigations were conducted monthly from September 2019 to December 2020 and consisted of in-situ monitoring and groundwater sampling. Groundwater samples were taken from wells and springs (Fig. 2a) and stored in 200 mL pre-rinsed polyethylene bottles that prevent evaporation and were kept refrigerated at 16 °C. Samples were taken from: (i) deep wells BO2, BO5, K1, B1, DP1, and V1, (ii) shallow dug wells AB (Austrijski bunar) and DRV (Dragevode), and (iii) springs Gusarica, Kamenica, and Pizdica. Electrical conductivity (EC), pH, dissolved oxygen content, and water temperature were measured in-situ using a WTW multi-parameter probe (Multi 3630 IDS SET G; WTW 2021). Laboratory investigations were performed in the Hydrochemical Laboratory of the Department of Hydrogeology and Engineering Geology at the Croatian Geological Survey in Zagreb, Croatia. Principal ion composition (Cl^-, SO_4^{2-}, NO_3^-, Ca_2^+, Mg_2^+, Na^+, K^+) was

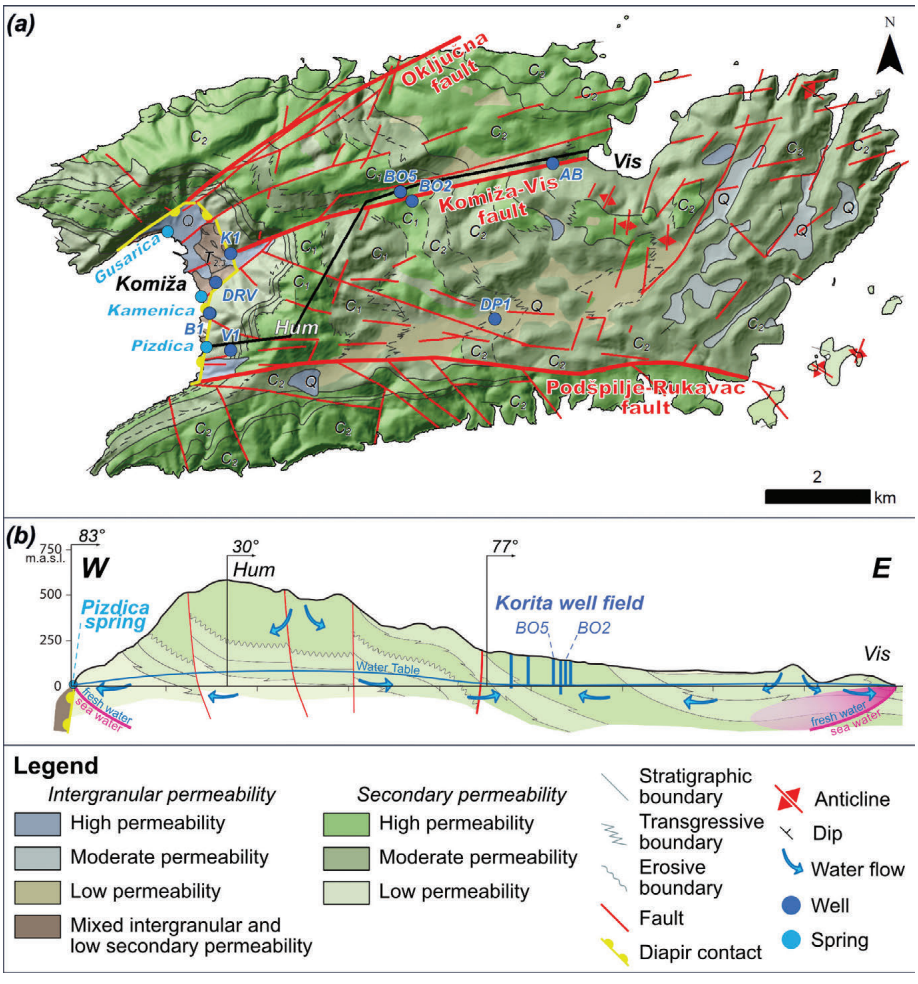

Fig. 2 - Hydrogeological map of the island of Vis with sampling locations (a) and schematic hydrogeological cross-section (b). The age of the lithostratigraphic units is also reported ($T_{2,3}$: Middle to Upper Triassic; C_1: Lower Cretaceous; C_2: Upper Cretaceous; Q: Quaternary). (modified after Korbar et al. 2012 and Terzić et al. 2022)

Fig. 2 - Carta idrogeologica dell'isola di Vis con pozzi e sorgenti campionati in questo lavoro (a) e sezione idrogeologica schematica (b). La carta idrogeologica riporta anche l'età delle unità litostratigrafiche ($T_{2,3}$: Triassico medio – superiore; C_1: Cretaceo inferiore; C_2: Cretaceo superiore; Q: Quaternario). (modificato da Korbar et al. 2012 e Terzić et al. 2022).

analyzed by ion chromatography on DIONEX ICS-6000 DP (Thermo Scientific 2018). The concentration of bicarbonate ions was determined in-situ by volumetric titration (HACH digital titrator) with 1.6 N H_2SO_4 to pH 4.5. Furthermore, the Laboratory for Low-level Radioactivities of Ruđer Bošković Institute in Zagreb conducted the determination of ^3H activity concentration by the method of electrolytic enrichment using the liquid scintillation counter Quantulus 1220 (Krajcar Bronić et al. 2020).

Electrical resistivity tomography (ERT)

Electrical resistivity tomography (ERT) survey was conducted in June 2020 to assess the soil-rock interface and the rock mass quality and to delineate the depth of the groundwater table. A 2D-ERT was carried out using the POLARES 2.0 electrical imaging system (P.A.S.I. s.r.l 2022), which uses a sinusoidal alternate current of adjustable frequency. This system was connected to 32 stainless steel electrodes, which were laid out in a straight line with a constant spacing of 10 m via a multi-core cable. Surveys were conducted using the Wenner–Schlumberger array at a frequency of 1.79 Hz and a maximum phase of 20° between the voltage signal and the current signal. During the field measurements, the frequency was lowered until the number of incorrect measurements was below 10%. The RES2DINV resistivity inversion software (Loke 2011) was used to automatically invert the apparent resistivity data from the field into two-dimensional resistivity subsurface models.

Structural-geological investigations

Since fluid flow in carbonate aquifers is generally dominated by fractures and karstic conduits, it is fundamental to study the geometrical attributes of fractures. High-resolution structural measurements, including orientation, kinematics, and crosscutting relationships, were performed. Orientations of deformation structures were plotted using the Daisy 3 software (Salvini 2004) in stereographic projections (Wulff lower hemisphere stereonet).

Results

Hydrogeological and hydrochemical investigations

Hydrochemical facies of the groundwater enable the determination of the relationship between the chemical properties of water, rock lithology, and local groundwater flow. The chemical composition of the groundwater is graphically represented on the Piper diagram (Fig. 3).

The sampling period was characterized by low rainfall, with the cumulative precipitation being 824 mm from September 2019 to December 2020 and a peak of 200 mm in December 2020. Despite the prolonged dry season and the decline in water levels, the principal ion composition showed relative stability at the analyzed wells and springs (Fig. 3). The groundwater in BO2, BO5, DRV, DP1, B1, and K1 showed a Ca-HCO_3 hydrochemical facies, which is the most common chemical footprint of groundwater in carbonate aquifers. Increasing chlorides at BO2 and BO5 were observed when the wells were pumped at maximum capacity. At the coastal well B1, increased chlorides were caused by the mixing of freshwater and seawater. Coastal springs Kamenica and Gusarica displayed a mixture of Ca-HCO_3 and mixed (Ca-Mg-Cl-SO_4) types due to the increasing SO_4 content resulting from the dissolution of gypsum in the VSE complex. The shallow coastal well AB had mixed (Ca-Mg-Cl-SO_4) hydrofacies with high chloride as a result of seawater

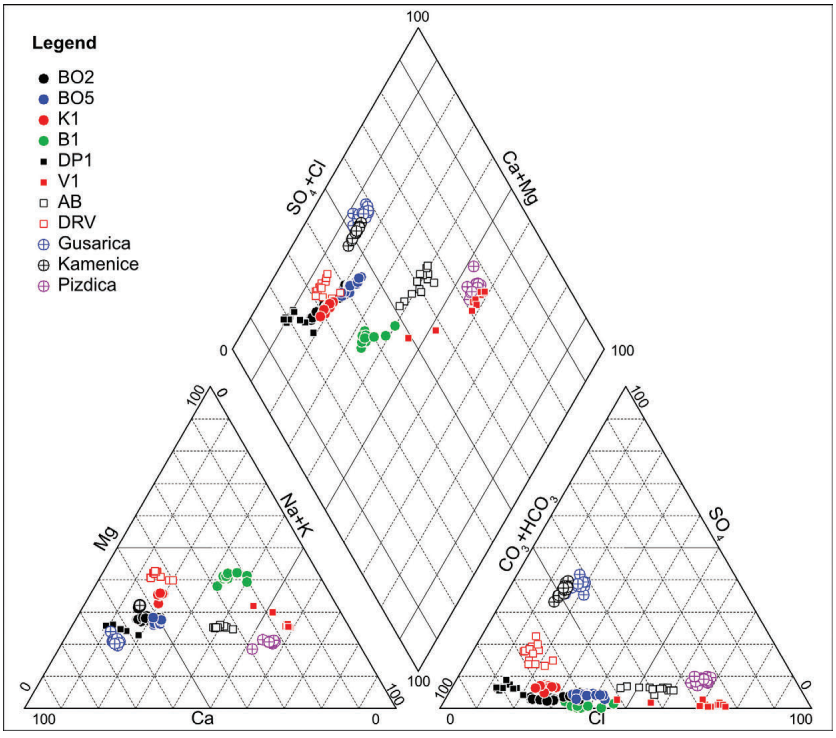

Fig. 3 - Piper diagram of groundwater samples from the island of Vis (September 2019 - December 2020).

Fig. 3 - Diagramma di Piper delle acque sotterranee campionate nell'isola di Vis (settembre 2019 - dicembre 2020).

interaction. V1 well and Pizdica spring displayed Na-Cl facies due to their proximity to the sea and significant mixing of freshwater with seawater. Despite their hydrochemical facies, these waters show relatively high Mg and HCO_3 contents pointing to a water-rock interaction with dolomites.

Time series of in-situ measurements of electrical conductivity, groundwater temperature, and pH in BO2, BO5, K1, and B1 wells and Pizdica (Fig. 4) were further investigated since they are the main water supply sites and have the highest potential for MAR implementation due to existing infrastructure.

EC values displayed relatively stable trends throughout the analyzed period with different amplitudes (Fig. 4a). Peak values occurred in August and September, however, seasonal oscillations were dampened by the prolonged dry season and very low recharge of the aquifer. Despite their vicinity, different EC values in BO2 and BO5 reflect different depths of their well screens, with BO5 being 15 m deeper, as well as variations in pumping rates. Despite a discontinuous time series due to pump malfunctions or intermittent usage, K1 and B1 showed static EC values. Similarly, EC values were mostly static at the brackish spring of Pizdica. The spring was used mostly during the summer season, but a significant increase in EC values was not detected due to the buffer effect of the spring accumulation pond and the relatively low pumping rate (Qmax=3.3 l/s).

Groundwater temperature varies throughout the year following the air temperature (Fig. 4b), with higher values in summer and lower values in winter. Such oscillations were not observed in Pizdica except for a slight temperature increase in August and October 2020. Mean groundwater temperatures are in concordance with the mean annual air temperature on the island of Vis, which varies between 16 °C and 18 °C. The differences in temperatures are caused by variations in catchment size, elevation, recharge/discharge dynamics, and the depths of the saturated zone. Due to the low precipitation in the analyzed period, its effect on the groundwater temperature can be neglected.

The groundwater pH was neutral to weak alkaline (Fig. 4c). BO2, BO5, K1, and Pizdica had similar values and amplitudes, while B1 had higher base values as well as amplitude.

Analyses of ^3H activity were performed on samples from BO2, Pizdica, and K1 during the hydrological minimum of September 2020. The results (in TU) were 1.68 ± 0.72, 2.3 ± 1.0, and 2.3 ± 1.1 for BO2, K1, and Pizdica, respectively. These waters can be classified as a mixture of sub-modern and modern water (0.8-4 TU; Motzer 2007). The lower TU in BO2 possibly indicates a shift towards older groundwater reflecting the exploitation of a deeper resource.

Electrical resistivity tomography (ERT)

ERT survey was conducted in the karst polje Dol, as it represents the lower part of Korita catchment where subsurface and groundwater data are rather scarce or missing. The profile (Fig. 5) was 320 m long and its western-most part is located 1.3 km NE from BO2 (Fig. 2a).

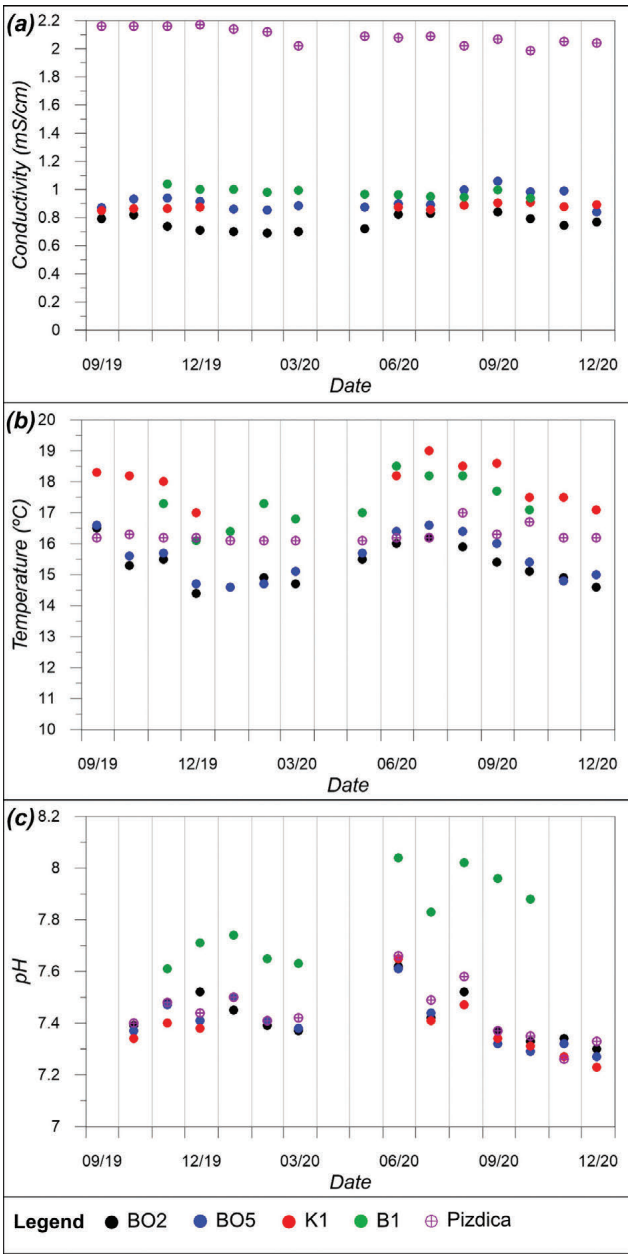

Fig. 4 - . Time series of (a) electrical conductivity, (b) groundwater temperature, and (c) pH. Some data are missing due to the random well closure and to the COVID-19 lockdown in April 2020.

Fig. 4 - Serie temporali della (a) conducibilità elettrica, (b) temperatura, e (c) pH delle acque sotterranee. La mancanza di alcuni dati è riconducile a malfunzionamenti temporanei delle pompe installate nei pozzi ed al lock-down causato dalla pandemia di COVID-19 (aprile 2020).

The results showed a low resistivity zone (15-110 Ωm) interpreted as topsoil (i.e., terra rossa) above a high resistivity bedrock. Clayey materials tend to hold more moisture and have a higher concentration of ions that conduct electricity, resulting in resistivity lower than 100 Ωm (Telford et al. 1990). The distribution of higher and lower resistivity zones in the topsoil coincides with agricultural activities. In particular, the lowest values (15-50 Ωm) were observed in correspondence with a vineyard where an irrigation system is installed. The resistivity increased with depth. The high

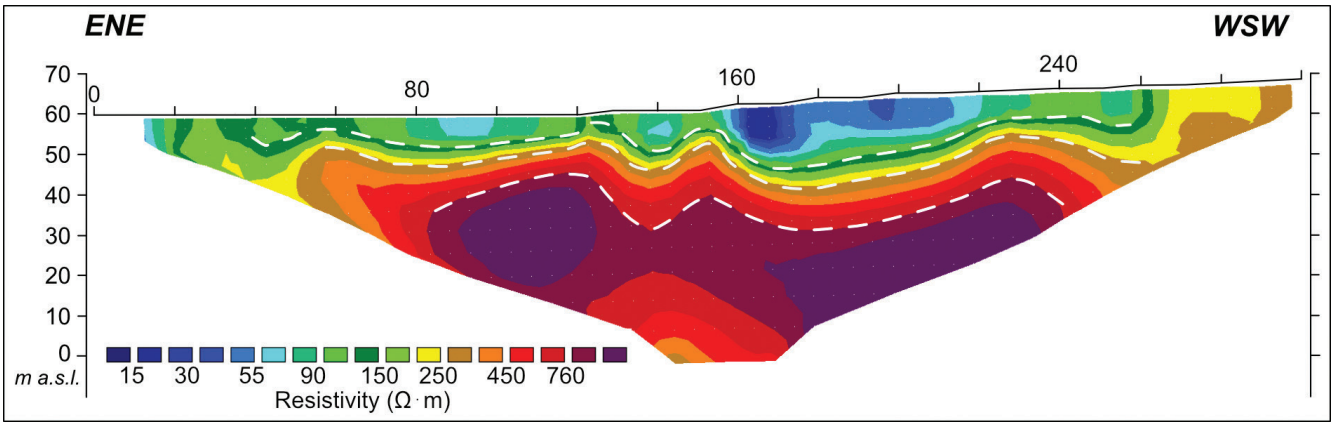

Fig. 5 - ERT profile in Dol polje. Interfaces between the topsoil (low resistivity), lower and upper weathering zones (moderate resistivity), and compact carbonates (high resistivity) are highlighted by white dashed lines.

Fig. 5 - Profilo geoelettrico effettuato nel polje di Dol. L'interfaccia fra il suolo (bassa resistività), la zona di degradazione meteorica (resistività moderata), e l'ammasso roccioso compatto (resistività elevata) è marcata dalla linea bianca tratteggiata.

resistivity bedrock was divided in an upper weathering zone (110-250 Ωm), where open discontinuities with weathered walls are infilled with clay and rock fragments. Values of electrical resistivity between 250-700 Ωm were interpreted as the lower weathering zone, where discontinuities have small apertures and moderate to negligible infilling. Resistivity values higher than 700 Ωm were interpreted as compact carbonates. Carbonates show a significantly higher resistivity than clayey soil because of lower porosity. In the middle section of the profile, at a depth of 0-20 m a.s.l., an anomaly with a resistivity of 300-500 Ωm was observed, indicating a potential groundwater target.

Structural-geological investigations

Structural-geological investigations were performed in 15 sites along the Komiža-Vis road and around the Korita well field, where the Komiža-Vis fault system is observed in tectonized Cretaceous carbonates (Fig. 6).

The collected dataset was dominated by high-angle (mostly >60°) deformation structures, namely faults, fractures, veins, and stylolites. In sites 3 to 15 along the Komiža-Vis fault (Fig. 6), the deformation pattern is constituted by a set of sinistral strike-slip fault planes striking roughly N70°, i.e. subparallel to the fault system, and associated with NE-SW veins and roughly NW-SE striking pressure solution planes, coherent with sinistral shear sense. A subsidiary set of sinistral, N40° striking fault planes, splaying from the E-W striking fault planes, was in turn associated with N-S veins. Moving away from the Komiža-Vis fault zone towards the S (sites 8 and 14), fault planes and associated veins were organized in two orthogonal sets: N100°-110° and N10°-20°. Fault cores of pluridecametric fault segments are composed of chaotic breccias infiltrated by terra rossa, while minor faults splay in their damage zones showing crackle breccia pockets and abundant striae and clear to reddish calcite slickenlines. The same type of calcite occurs in the described vein sets. Fractures, which include both joints and other deformation elements overprinted by abundant meteoric dissolution, were found in all the aforementioned orientations.

Sites 1 and 2 are hosted in the dolostones close to the Komiža diapir contact and showed slightly different deformation structures. Site 1 shows a principal sinistral strike-slip fault plane, striking N80°, and associated veins. This fault plane was abutted by mutually crosscutting dextral NE-SW, sinistral NW-SE fault planes, and N-S cleavage planes. Fault cores of principal faults in dolostones were characterized by intense cataclasis and dolomite cementation, which occurs also in the associated veins and constitutes slickenlines of the subsidiary fault planes. Site 2 showed bedding dipping 45° to the ENE and slickenlines indicating extensional, sinistral, and dextral kinematics. Here, four fault sets were observed: (i) N-S bedding-orthogonal extensional faults, (ii) high angle, N70° striking, mostly sinistral faults, (iii) subvertical NW-SE trending, sinistral faults, and (iv) NE-SW faults and fractures, filled by terra rossa. In this latter area, complex transtensional kinematics are the result of the interaction of the diapir contact and the Komiža-Vis fault.

Discussion and conclusions

The present study describes a multidisciplinary approach (i.e., hydrogeology, geochemistry, geophysics, structural geology) for the assessment of the Managed Aquifer Recharge (MAR) potential on the island of Vis. A detailed characterization of the pilot site is a common prerequisite in several workflows for MAR implementation (e.g., Daher et al. 2011; DEEPWATER-CE 2020; Lobo Ferreira and Leitão 2014; NRMMC-EPHC-NHMRC 2009; Rolf 2017; San-Sebastián-Sauto et al. 2018).

Hydrogeological and hydrochemical analyses were used to establish trends and dynamics of the groundwater resource. The water exploited in the Korita well field displayed long-term stability (i.e., ion composition, EC, pH) despite very low precipitation during the monitoring time, with a slight increase in chloride and EC in the warmer period (Figs. 3 and 4). These variations suggested relatively large groundwater reserves with a good resilience towards seasonal over-pumping

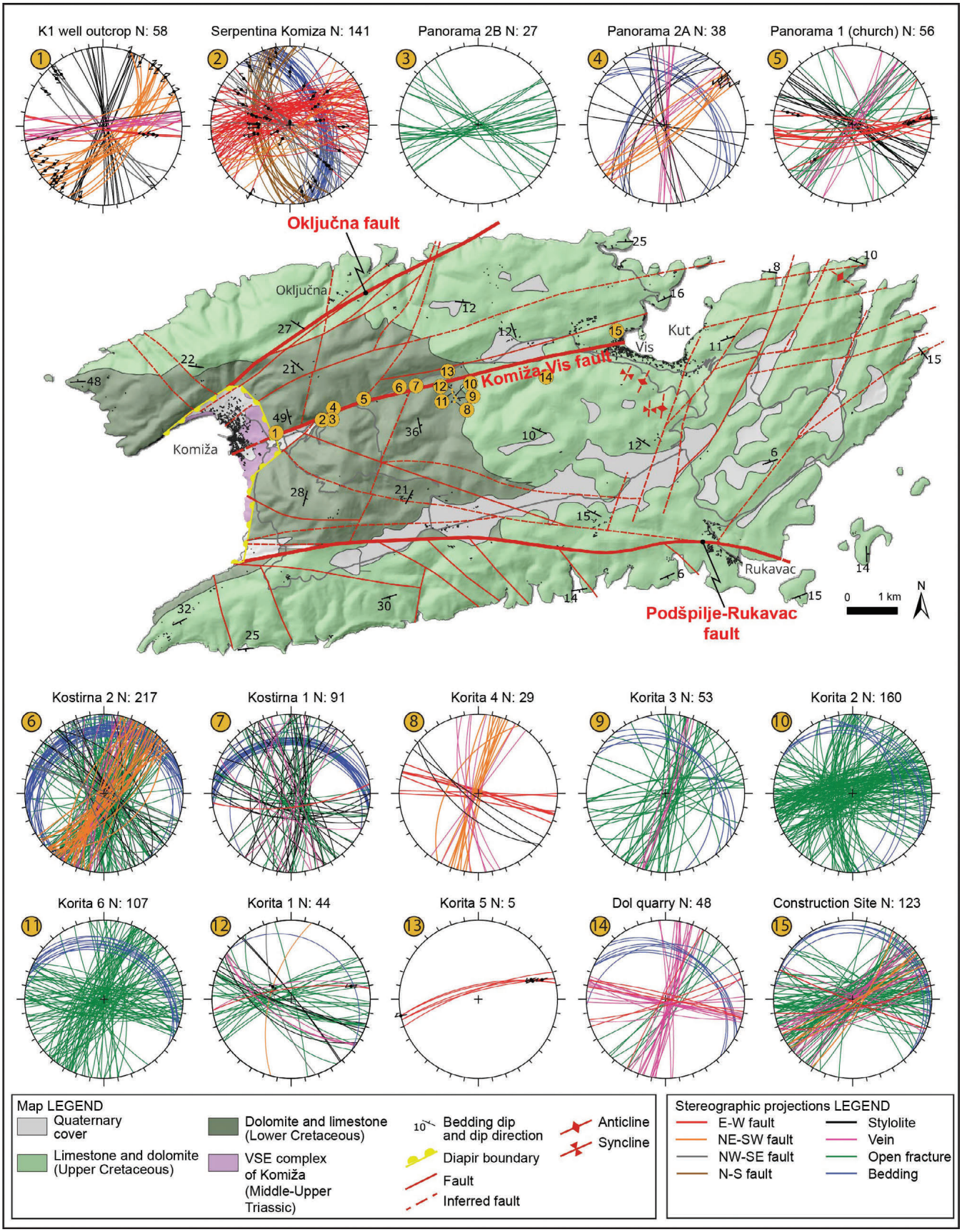

Fig. 6 - Simplified geological map of the island of Vis after Korbar et al. (2012). Structural measurement sites are in orange and numbered 1-15. Deformation structures are plotted in stereographic projections lower hemisphere Wulff nets (Daisy 3 software; Salvini 2004).

Fig. 6 - Schema geologico dell'Isola di Vis, semplificato a partire da Korbar et al. (2012). I siti delle stazioni strutturali sono rappresentati in arancione e numerati da 1 a 15. Le strutture deformative sono rappresentate come proiezioni stereografiche sul reticolo di Wulff (Daisy 3 software; Salvini 2004).

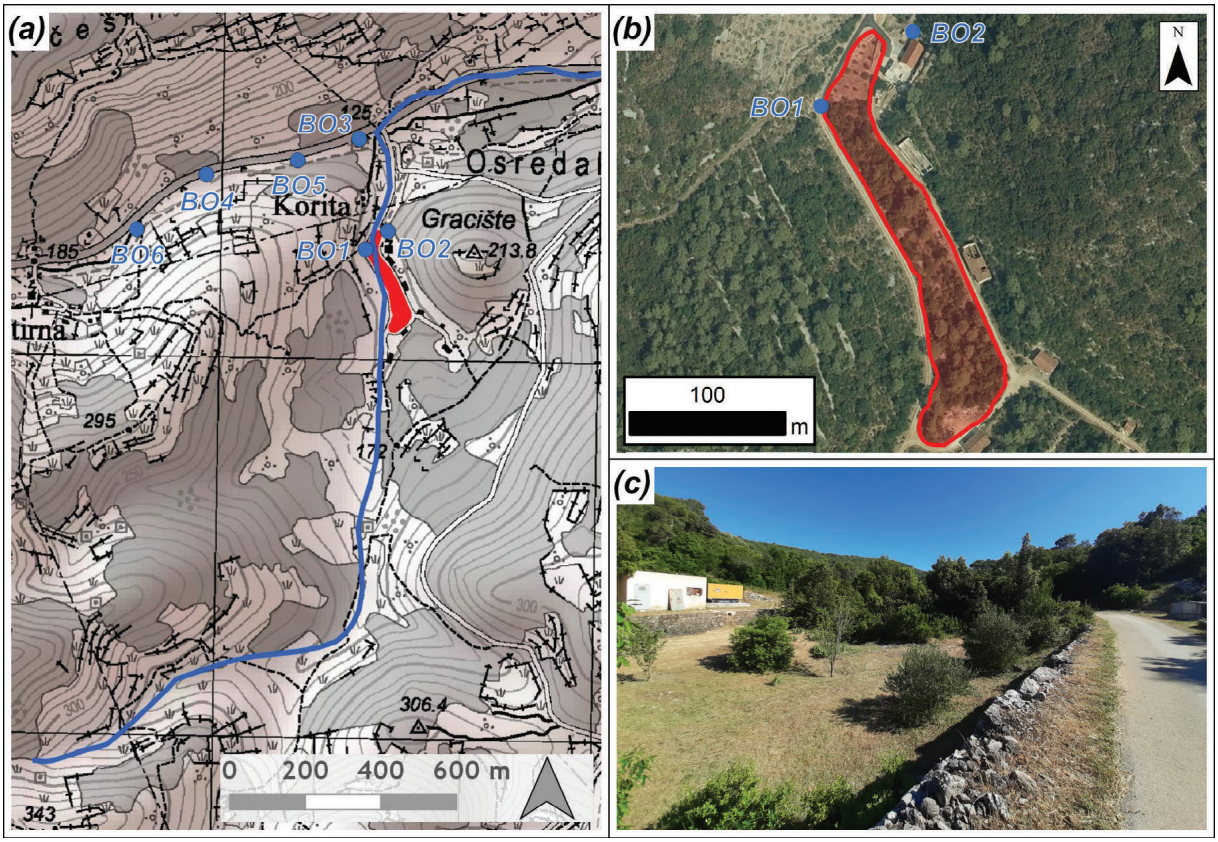

Fig. 7 -(a) Proposed location of the accumulation structure in Korita (red) in relation to the abandoned channel (blue line) and Korita wells (blue dots), (b) aerial view of the infiltration pond, (c) current situation of the structure. The base map (a) and the ortoimage (b) were taken from the Geoportal Državne geodetske uprave portal (https://geoportal.dgu.hr/).

Fig. 7 - (a) Ubicazione del bacino di accumulo nell'area di Korita (poligono rosso) in relazione al canale di deflusso abbandonato (linea blu) e ai pozzi (cerchi blu), (b) ortofoto dell'area di Korita, e (c) situazione attuale del bacino di accumulo. La mappa (a) e l'ortofoto sono tratte dal portale Geoportal Državne geodetske uprave portal (https://geoportal.dgu.hr/).

and dry seasons. This result was corroborated by the analyses of ^{3}H activity, pointing to a mixture of sub-modern and modern waters.

The Korita aquifer is protected from seawater intrusions and has excellent water quality, making it the most suitable and safe for MAR implementation. A sufficient storage capacity was evidenced by the high transmissivity values (Terzić et al. 2022) that also suggested a homogenous groundwater flow through a densely fractured, "porous-like" aquifer. These characteristics are favorable since they allow a diffuse infiltration without a quick discharge toward the sea through large karstic conduits. In particular, the E-W fractures represent a preferential path for water infiltration and flow. This set of fractures is characterized by larger aperture and terra rossa infilling suggesting a transtensional regime that promotes their opening.

From the point of the groundwater quality, the highest uncertainty is related to the differences in the chemical composition of the infiltrated water and the groundwater as well as the water-rock interactions, which can change the groundwater chemical status (Ringleb et al. 2016; Xanke 2017). In particular, the infiltration of slightly acidic water results in increased $CaCO_3$ dissolution leading to increased karstification. The physico-chemical parameters of rainwater on the island of Vis were not investigated, but literature data are available. Beysens et al. (2010) reported high variations in rainwater pH and EC, with mean values of 6.4 and 132 µS/cm, respectively, while Skevin-Sovic et al. (2012) reported precipitation pH values from 3.94 to 8.06, showing that acid rain could occur. These parameters could be favorable since pH higher than 5.5 and low $CaCO_3$ content were recommended for MAR solution in karstic aquifers (e.g., Rolf 2017).

Despite the groundwater resource quality and the hydrogeological characteristics of the aquifer, MAR implementation has to account for the subsurface geometry. Geophysical investigations (i.e., ERT survey) in the vicinity of Korita highlighted a relatively homogeneous sequence of the rock mass below an approximately 10 m thick Quaternary cover. These data could contribute to a more detailed construction plan for the MAR solution (e.g., removal of the topsoil), decreasing the design risks.

A tentative project of a MAR solution on Vis could be the revitalization of an old artificial channel and the associated pond system used to evacuate storm and flood waters from hilly areas of Hum and Korita towards the E and its conversion into an accumulation structure (Fig. 7).

The possible conceptual design of the infiltration pond at Korita should include: (i) the revitalization of the abandoned

channel and pond system, (ii) the construction of an accumulation dam at its lowest point, and (iii) the topsoil removal enhancing the natural infiltration. The volume of the proposed pond is approximately 25,000 m^3 (Fig. 7b). Generally, surface recharge methods are preferred in karst since the epikarst zone acts as a buffer for slow, delayed, and diffuse water infiltration (Daher et al. 2011), promoting the degradation of pollutants and reducing the risk of contamination. Considering the specific climatological, geological, and hydrogeological conditions of the Korita site, the major constraints for a surface recharge could be: (i) differential infiltration rates, (ii) clogging, (iii) high evaporation, and (iv) algae and plankton blooms. Spatially differential infiltration rates could be caused by the heterogeneity of the epikarst zone. The presence of sinkholes or karstic conduits could cause the rapid inflow of the source water, while epikarst with significant soil infill (i.e., clayey terra rossa) could hinder the infiltration. Furthermore, the infiltration rate could be diminished by mechanical (fine particles) or biological (algae) clogging, affecting the quality of the source water as well. High evaporation, variable climate conditions (prolonged dry periods), and climate change (extreme meteorological events) could affect the availability of the source water.

The construction of an infiltration ditch or gallery in the pond could mitigate some of these quality and quantity issues. This structure could surpass the epikarst zone avoiding uncontrolled infiltration or prolonged water stagnation that could promote clogging and algal bloom. It could be combined with pre-treatment systems that could improve the quality of the source water. Considering the existing infrastructure of the Korita well field, one of the nearby wells could be used for injecting the water accumulated in the pond using a combined pond-aquifer storage and recovery approach. Although direct injection into the phreatic zone should be avoided due to possible degradation of groundwater quality and unwanted water-rock interaction (Daher et al. 2011), the obtained results indicate that this method could be suitable for the Korita aquifer.

However, the current major threat for the Korita water resource is represented by the possible seawater intrusion through the highly permeable damage zone of the Komiža-Vis fault. This problem could be aggravated by increasing pumping rates and sea-level rise. The MAR solution could increase the hydraulic gradient in the Korita aquifer mitigating the possible seawater inflow. Furthermore, it could be accompanied by monitoring piezometers located downstream of the Korita well field. The monitoring network could be used to: (i) evaluate the efficiency of the MAR system, (ii) monitor the quality of the groundwater, and (iii) establish an early warning system for the seawater intrusion.

The most significant constraint for MAR implementation on the Vis island is represented by the current legislation that does not allow the development of MAR solutions, especially in drinking water protection zones. This issue requires detailed and site-specific research, which could promote MAR solutions as a safe and sustainable approach for increasing the groundwater quality and quantity, and the sensibilization and collaboration with key stakeholders and decision-makers.

Acknowledgments

This research was carried out within the framework of the INTERREG-CE project DEEPWATER-CE, funded by the European Regional Development Fund (ERDF). The authors would like to thank Maja Briški for performing hydrochemical analyses and Vlatko Brčič for detailing the geological setting of the Vis island. The authors are very grateful to the Vis Water Supply Company and the director, Mr. Marko Plenča, for granting access to water supply infrastructure on the island of Vis. The authors would also like to express gratitude to the Reviewers and Editor, whose suggestions improved the quality of this paper.

Competing interest

The authors declare no competing interest.

Author contributions

Data collection by all authors; data analyses by Patekar M., Kosović I., Lucca A.; manuscript conceptualization by Patekar M., Pola M., Terzić J., Borović S.; writing original draft by Patekar M., Bašić M., Pola M., Kosović I., Lucca A., Mittempergher S., Berio L.; graphical editing by Bašić M., Pola M., Mittempergher S., Berio L.; review of the final draft by all authors.

Additional information

Supplementary information is available for this paper at https://doi.org/10.7343/as-2022-557

Reprint and permission information are available writing to acquesotterranee@anipapozzi.it

REFERENCES

Aguilera H, Murillo JM (2008) The effect of possible climate change on natural groundwater recharge based on a simple model: A study of four karstic aquifers in SE Spain. Environmental Geology 57:963-974. doi:10.1007/s00254-008-1381-2

Alfarrah N, Walraevens K (2018) Groundwater Overexploitation and Seawater Intrusion in Coastal Areas of Arid and Semi-Arid Regions. Water 10:143. doi:10.3390/w10020143

Beysens D, Lekouch I, Muselli M, Mileta M, Milimouk-Melnytchouk I, Sojat V (2010) Physical and chemical properties of dew and rain water in the Dalmatian coast, Croatia. 5th International Conference on Fog, Fog Collection and Dew. Münster, Germany. Available from: https://meetingorganizer.copernicus.org/FOGDEW2010/FOGDEW2010-24-5.pdf - last accessed 25/02/2022

Bonacci O (2001) Monthly and annual effective infiltration coefficients in Dinaric karst: example of the Gradole karst spring catchment. Hydrological Sciences Journal 46:287-299. doi:10.1080/02626660109492822

Bonacci O, Bonacci D, Patekar M, Pola M (2021) Increasing Trends in Air and Sea Surface Temperature in the Central Adriatic Sea (Croatia). Journal of Marine Science and Engineering 9:358. doi:10.3390/jmse9040358

Bonacci O, Patekar M, Pola M, Roje-Bonacci T (2020) Analyses of Climate Variations at Four Meteorological Stations on Remote Islands in the Croatian Part of the Adriatic Sea. Atmosphere 11:1044. doi:10.3390/atmos11101044

Borović S, Terzić J, Pola M (2019) Groundwater Quality on the Adriatic Karst Island of Mljet (Croatia) and Its Implications on Water Supply. Geofluids 2019:5142712. doi:10.1155/2019/5142712

Branković Č, Güttler I, Gajić-Čapka M (2013) Evaluating climate change at the Croatian Adriatic from observations and regional climate models' simulations. Climate Dynamics 41: 2353-2373. doi:10.1007/s00382-012-1646-z

Cosgrove WJ, Loucks DP (2015) Water management: Current and future challenges and research directions. Water Resources Research 51: 4823-4839. doi:10.1002/2014WR016869

Daher W, Pistre S, Kneppers A, Bakalowicz M, Najem W (2011) Karst and artificial recharge: Theoretical and practical problems; a preliminary approach to artificial recharge assessment. Journal of Hydrology 408: 189-202. doi:10.1016/j.jhydrol.2011.07.017.

DEEPWATER-CE (2020) Transnational Decision Support Toolbox For Designating Potential MAR Locations In Central Europe. Available from: https://www.interreg-central.eu/Content.Node/2020-09-07-Handbook-Deliverable-D.T2.4.3-final.pdf - last accessed 10/02/2022.

Dillon P, Stuyfzand P, Grischek T et al. (2019) Sixty years of global progress in managed aquifer recharge. Hydrogeology Journal, 27: 1-30. doi:10.1007/s10040-018-1841-z

Duplančić Leder T, Ujević T, Čala M (2004) Coastline lengths and areas of islands in the Croatian part of the Adriatic Sea determined from the topographic maps at the scale of 1:25000. Geoadria 9: 5-32. doi:10.15291/geoadria.127

European Environment Agency (2015) Mediterranean Sea region briefing - The European environment - state and outlook 2015. Available from: https://www.eea.europa.eu/soer/2015/countries/mediterranean - last accessed 18/02/2022.

Fernández Escalante, E, Henao Casas JD, Vidal Medeiros AM, San Sebastiàn Sauto J (2020) Regulations and guidelines on water quality requirements for Managed Aquifer Recharge. International comparison. Acque Sotterranee - Italian Journal of Groundwater, 9:7-22. doi:10.7343/as-2020-462

Filipčić A (1998) Klimatska regionalizacija Hrvatske po W. Köppenu za standardno razdoblje 1961.-1990. u odnosu na razdoblje 1931.-1960. (Climatic regionalization of Croatia according to W. Köppen for the standard period 1961-1990 in relation to the period 1931-1960) Acta Geographica Croatica 33:7-14.

Ford D, Williams P (2007) Karst Hydrogeology and Geomorphology. John Wiley & Sons Ltd., Chichester, UK. doi:10.1002/9781118684986

Gaaloul N, Pliakas F, Kallioras A, Schuth C, Marinos P (2012) Simulation of Seawater Intrusion in Coastal Aquifers: Forty Five'Years exploitation in an Eastern Coast Aquifer in NE Tunisia. The Open Hydrology Journal 6:31-44. doi:10.2174/1874378101206010031

García-Ruiz JM, López-Moreno JI, Vicente-Serrano SM, Lasanta–Martínez T, Beguería S (2011) Mediterranean water resources in a global change scenario. Earth-Science Reviews 105:121-139. doi:10.1016/j.earscirev.2011.01.006

Giorgi F (2006) Climate change hot-spots. Geophysical Research Letters 33:L08707. doi:10.1029/2006GL025734

Hartmann A, Goldscheider N, Wagener T, Lange J, Weiler M (2014) Karst water resources in a changing world: Review of hydrological modeling approaches. Review of Geophysics 52:218-242. doi:10.1002/2013RG000443

Hayat S, Szabó Z, Tóth Á, Mádl-Szőnyi J (2021) MAR site suitability mapping for arid–semiarid regions by remote data and combined approach: A case study from Balochistan, Pakistan. Acque Sotterranee - Italian Journal of Groundwater 10:17–28. doi:10.7343/as-2021-505

HGI-CGS (2009) Geological Map of the Republic of Croatia at the Scale 1:300 000. Department of Geology, Croatian Geological Survey: Zagreb, Croatia.

Korbar T, Belak M, Fuček L, Husinec A, Oštrić N, Palenik D, Vlahović I (2012) Basic geological map of the Republic of Croatia 1:50.000. Sheets Vis 3 and Biševo 1 with part of the sheet Vis 4 and islands Sv Andrija, Brusnik, Jabuka and Palagruža. Croatian Geological Survey, Zagreb, Croatia.

Krajcar Bronić I, Barešić J, Sironić A, Lovrenčić Mikelić I, Borković D, Horvatinčić N, Kovač Z (2020) Isotope Composition of Precipitation, Groundwater, and Surface and Lake Waters from the Plitvice Lakes, Croatia. Water 12:2414. doi:10.3390/w12092414

Leduc C, Pulido-Bosch A, Remini B (2017) Anthropization of groundwater resources in the Mediterranean region: processes and challenges. Hydrogeology Journal 25:1529-1547. doi:10.1007/s10040-017-1572-6

Lobo Ferreira JP, Leitão TE (2014) Demonstrating managed aquifer recharge as a solution for climate change adaptation: results from Gabardine project and asemwaterNet coordination action in the Algarve region (Portugal). Acque Sotterranee, Italian Journal of Groundwater 3: 15-22. doi:10.7343/AS-080-14-0106

Loke M (2011) Electrical resistivity surveys and data interpretation. In: Gupta H (ed.) Encyclopedia of Solid Earth Geophysics, Second Edition. Springer: Dordrecht, The Netherlands.

Lukač Reberski J, Rubinić J, Terzić J, Radišić M (2020) Climate Change Impacts on Groundwater Resources in the Coastal Karstic Adriatic Area: A Case Study from the Dinaric Karst. Natural Resources Research 29:1975–1988. doi:10.1007/s11053-019-09558-6

Massaad B (2000) Salt Water Intrusion in the Hadeth Aquifer: Groundwater Rehabilitation Techniques, Expert Group Meeting on Implications of Groundwater Rehabilitation Fro Water Resources Protection and Conservation." ESCWA, Beirut.

Meybeck M, Vorosmarty C, Schultze R, Becker A (2003) Conclusions: Scaling Relative Responses of Terrestrial Aquatic Systems to Global Changes. In: Kabat P, Claussen M, Dirmeyer P A, Gash J H C et al. (eds.) Vegetation, Water, Humans and the Climate. Springer: Berlin/Heidelberg, Germany.

Mongelli G, Argyraki A, Lorenzo MLG, Shammout MW, Paternoster M, Simeone V (2019) Groundwater Quality in the Mediterranean Region. Geofluids 2019:7269304. doi:10.1155/2019/7269304

Motzer W (2007) Tritium age dating of groundwater. In: Hydro visions, 16(2). Groundwater Resources Association of California, USA. Available from: https://www.grac.org/media/files/files/388022b0/Summer_2007.pdf - last accessed 24/02/2022

Natural Resource Management Ministerial Council (NRMMC), Environment Protection and Heritage Council (EPHC), National Health and Medical Research Council (NHMRC) (2009) Australian Guidelines for Water Recycling, Managing Health and Environmental Risks, Volume 2C – Managed Aquifer Recharge. Available from: https://www.waterquality.gov.au/sites/default/files/documents/water-recycling-guidelines-mar-24.pdf - last accessed 23/03/2022

PASI s.r.l. (2022) Electrical imaging system in alternate current POLARES32. Available from: https://www.pasisrl.it/Documenti/POLARES_32_EN_lq.pdf - last accessed 25/03/2022

Plantak L, Biondić R, Meaški H, Težak D (2021) Hydrochemical Indicators Analysis of Seawater Intrusion in Coastal Karstic Aquifers on the Example of the Bokanjac-Poličnik Catchment Area in Zadar, Croatia. Applied Sciences 11:11681. doi:10.3390/app112411681

Ringleb J, Sallwey J, Stefan C (2016) Assessment of Managed Aquifer Recharge through Modeling-A Review. Water 8:579. doi:10.3390/w8120579

Rolf L (2017) Assessing the Site Suitability of Managed Aquifer Recharge (MAR) Projects in Karst Aquifers in Lebanon, Master's Thesis, Utrecht University, Utrecht.

Rosenzweig C, Casassa G, Karoly D J, Imeson A, Liu C, Menzel A, Rawlins S, Root TL, Seguin B, Tryjanowski P, Hanson CE (2007) Assessment of observed changes and responses in natural and managed systems. In: Parry M L, Canziani OF, Palutikof JP, van der Linden PJ (eds.) Climate Change 2007: Impacts, Adaptation and Vulnerability. Contribution of Working Group II to the Fourth Assessment Report of the Intergovernmental Panel on Climate Change. Cambridge University Press, UK.

Salvini F (2004) Daisy 3: The Structural Data Integrated System Analyzer. Software

San-Sebastián-Sauto J, Fernández-Escalante E, Calero-Gil R, Carvalho T, Rodríguez-Escales P (2018) Characterization and benchmarking of seven managed aquifer recharge systems in south-western Europe. Sustainable Water Resources Management 4:193-215 doi:10.1007/s40899-018-0232-x

Sapiano M (2020) Integrated Water Resources Management in the Maltese Islands. Acque Sotterranee - Italian Journal of Groundwater 9:25-32. doi:10.7343/as-2020-477

Skevin-Sovic J, Djuricic V, Kosanovic C (2012) Major ions wet deposition and trends during the last decade on the eastern Adriatic coast. WIT Transactions on Ecology and the Environment 157:339-349. doi:10.2495/AIR120301.

Stevanović Z (2019) Karst waters in potable water supply: a global scale overview. Environmental Earth Sciences 78:662. doi:10.1007/s12665-019-8670-9

Telford WM, Geldart LP, Sheriff RE (1990) Applied geophysics. Cambridge University Press, New York, USA.

Terzić J (2004) Hydrogeological relations on karstified islands - Vis island case study. Mining-Geology-Petroleum Bulletin 16:47-58.

Terzić J, Marković T, Pekaš V (2008) Influence of sea-water intrusion and agricultural production on the Blato Aquifer, Island of Korčula, Croatia. Environmental Earth Sciences 54:719-729. doi:10.1007/s00254-007-0841-4

Terzić J, Frangen T, Borović S, Lukač Reberski J, Patekar M (2022) Hydrogeological Assessment and Modified Conceptual Model of a Dinaric Karst Island Aquifer. Water 14:404. doi:10.3390/w14030404

Thermo Scientific (2018) Dionex ICS-6000 Ion Chromatography System Operator's Manual. Thermo Fisher Scientific Inc., USA. Available from: https://www.thermofisher.com/document-connect/document-connect.html?url=https%3A%2F%2Fassets.thermofisher.com%2FTFS-Assets%2FCMD%2Fmanuals%2Fman-22181-97002-ics-6000-man2218197002-en.pdf – last accessed 25/03/2022

Touhami I, Chirino E, Andreu JM, Sánchez JR, Moutahir H, Bellot J (2015) Assessment of climate change impacts on soil water balance and aquifer recharge in a semiarid region in south east Spain. Journal of Hydrology 527:619-629. doi:10.1016/j.jhydrol.2015.05.012

Turc L (1954) Le bilan d'eau des sols: relation entre les precipitations, l'evaporation et l'ecoulment (Soil water balance: relationship between precipitation, evaporation and runoff). Troisiesme journees de l'hydraulique a Alger 3-1:36-44

Vanderzalm J, Le Gal La Salle C, Hutson JL, Dillon P (2002) Water quality changes during aquifer storage and recovery Bolivar, South Australia. In: Vanderzalm J, Sidhu J, Bekele E, Ying G-G, Pavelic P et al (eds.) Management of Aquifer Recharge for Sustainability. CRC Press, London, UK.

Velić I, Vlahović I (2009) Explanatory Notes of the Geological Map of the Republic of Croatia in 1:300.000 Scale. Department of Geology, Croatian Geological Survey: Zagreb, Croatia.

Vlahović I, Tišljar J, Velić I (2005) Evolution of the Adriatic Carbonate Platform: Palaeogeography, main events and depositional dynamics. Palaeogeography Palaeoclimatology Palaeoecology 220:333-360. doi:10.1016/j.palaeo.2005.01.011

Werner AD, Bakker M, Post VEA, Vandenbohede A, Lu C, Ataie-Ashtiani B, Simmon CT, Barry DA (2013) Seawater intrusion processes, investigation and management: Recent advances and future challenges. Advances in Water Resources 51:3-26. doi:10.1016/j.advwatres.2012.03.004.

Worthington S (2014) Characteristics of channel networks in unconfined carbonate aquifers. Geological Society of America Bulletin 127:759-769. doi:10.1130/B31098.1

WTW (2021) Multi 3630 IDS Operating Manual. Xylem Analytics Germany GmbH. Available at: https://www.xylemanalytics.com/File%20Library/Resource%20Library/WTW/01%20Manuals/ba77170e05_3630_Multi.pdf - last accessed 25/03/2022

Xanke J (2017) Managed aquifer recharge into a karst groundwater system at the Wala reservoir, Jordan, doctoral dissertation, Faculty of Civil Engineering, Geo and Environmental Sciences of the Karlsruhe Institute of Technology (KIT), Karlsruhe, Germany.